Eliminating error in the chemical abundance scale for extragalactic HII regions

López-Sánchez, Dopita, Kewley, Zahid, Nicholls & Scharwächter 2012
MNRAS, in press, arXiv:1203.5021

Ángel R. López-Sánchez
Australian Astronomical Observatory / Macquarie University

Mapping Oxygen in the Universe – Pto Cruz – Tenerife – 16 May 2012

Oxygen abundance is a key parameter in galaxy evolution

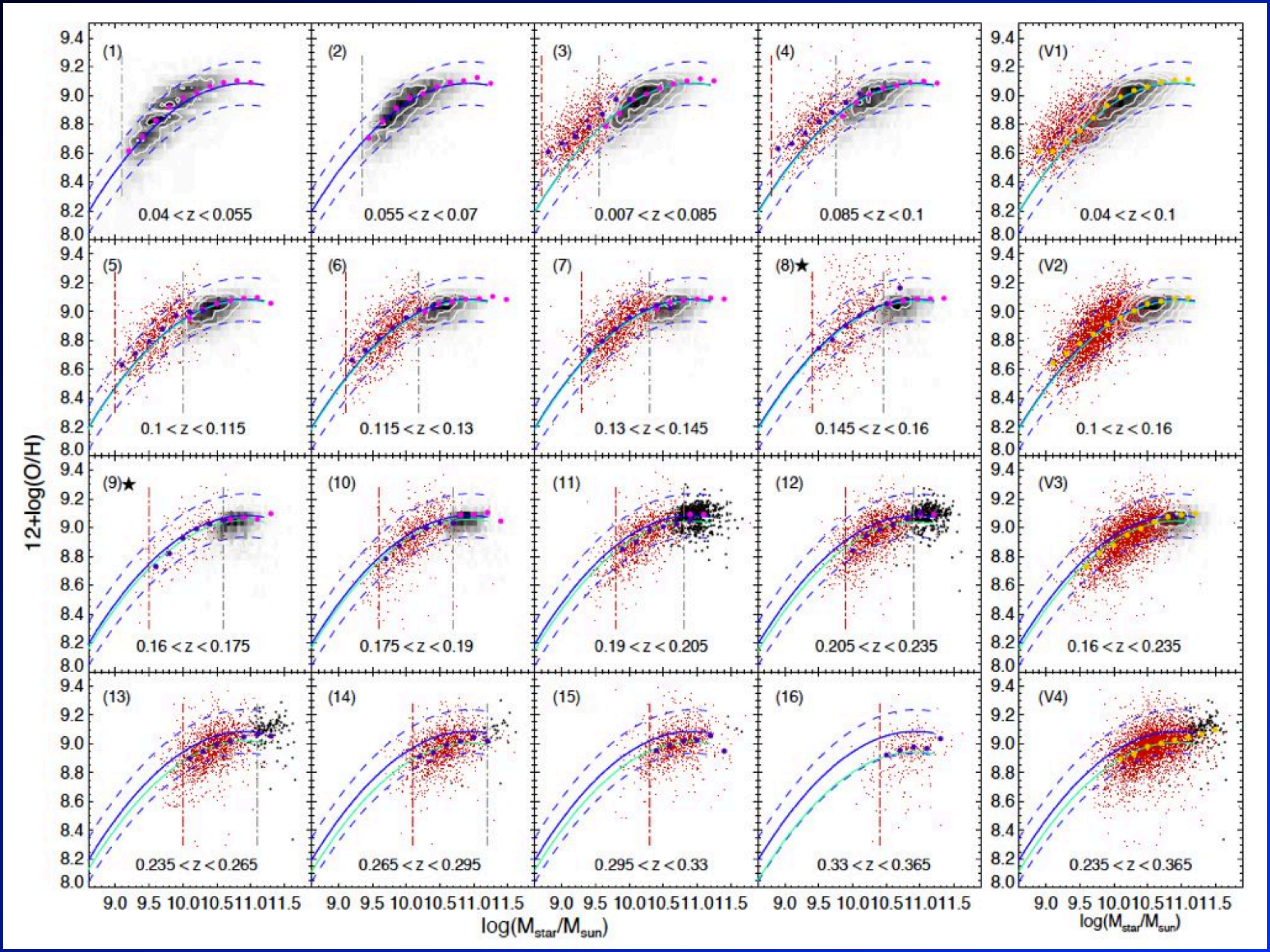

Lara-López et al. 2010a, A&A, 519, 31 (SDSS), Lara-López et al. 2012, in progress (SDSS+GAMA)

Stellar Mass = f (oxygen abundance and SFR)

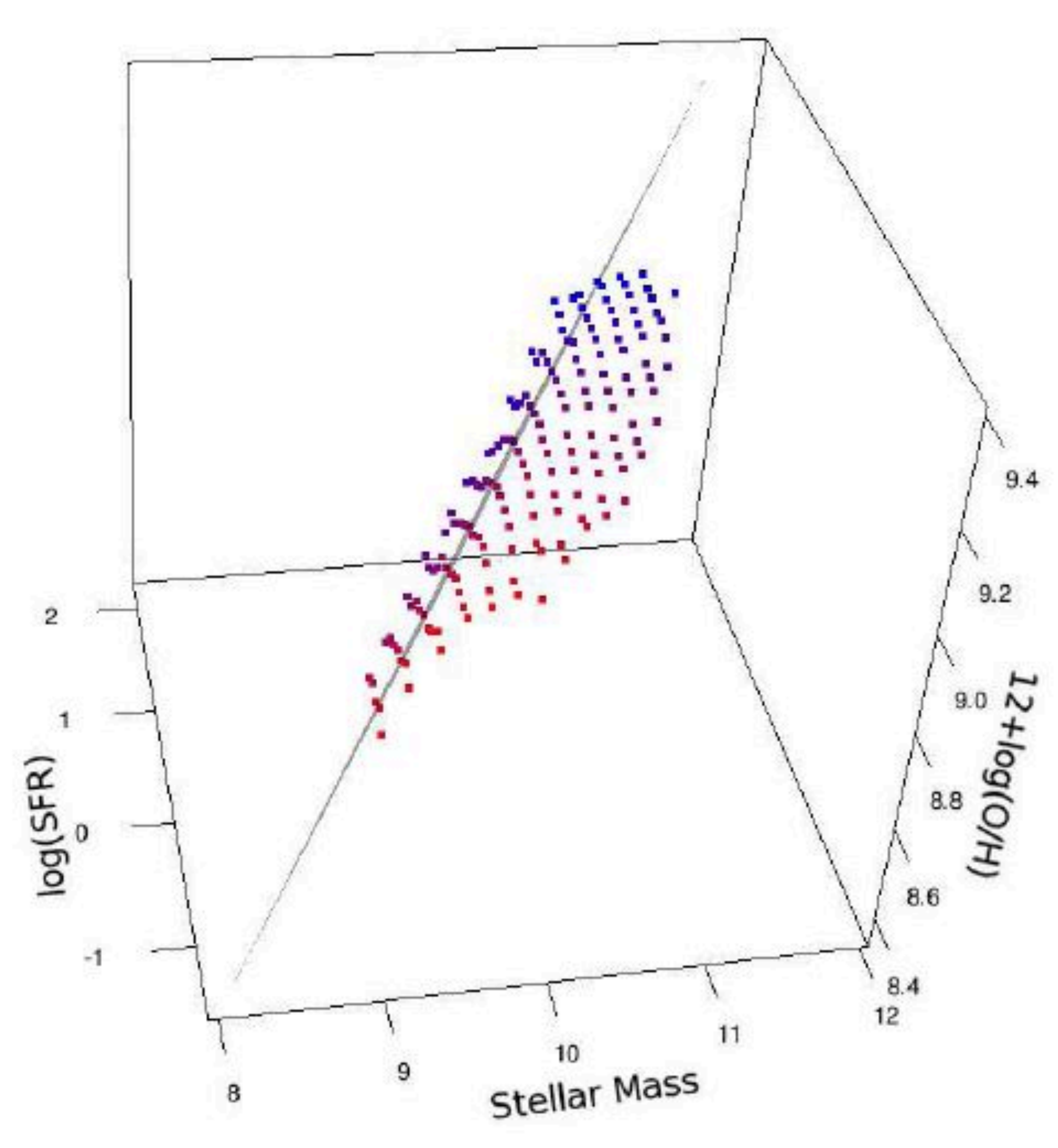

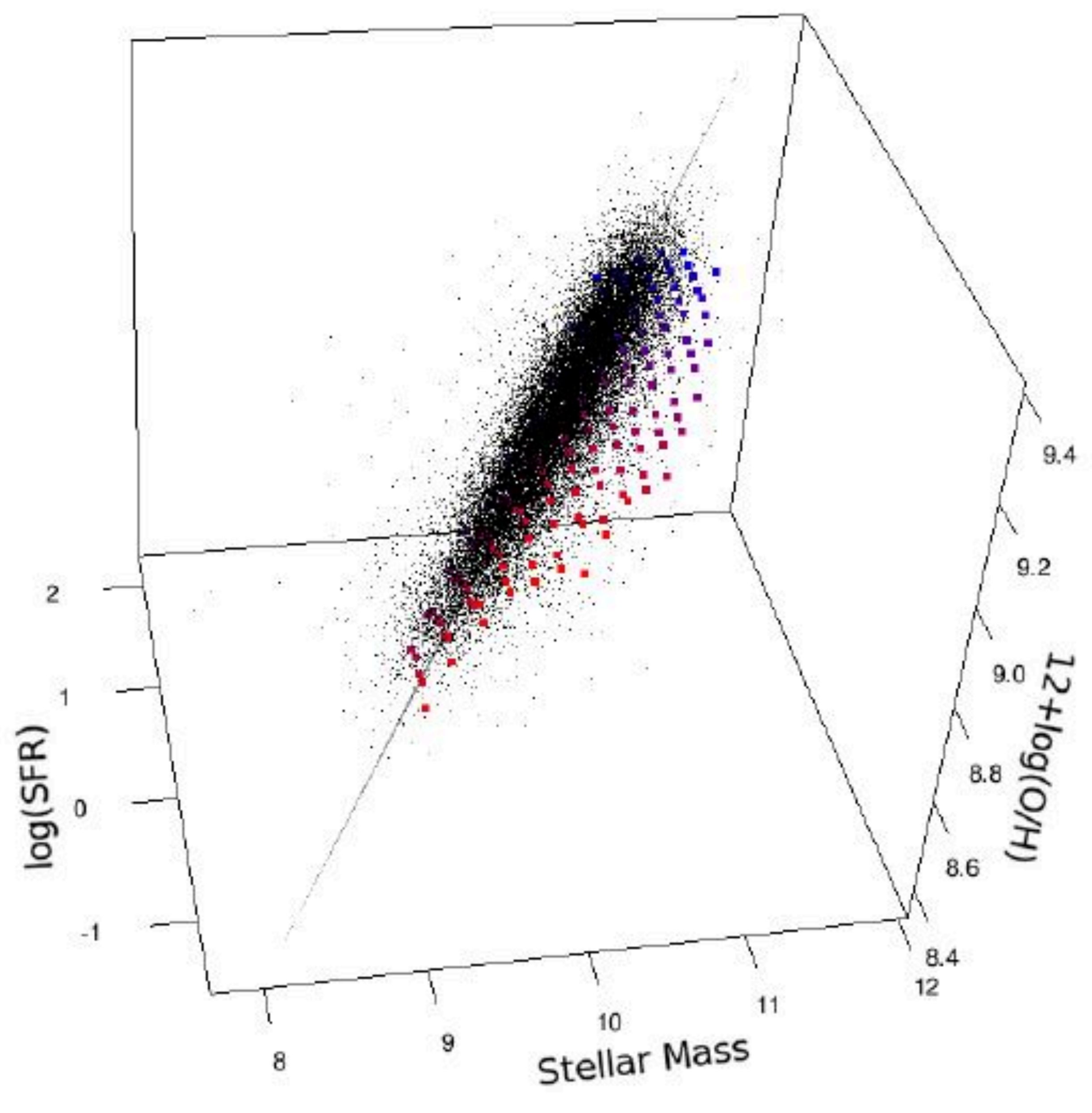

- Lara-López et al. 2010b, A&A, 521, 53L ***"Fundamental Plane"***
- *Mannucci et al. (2010), O/H = f (M_{star} , SFR)*
- Lara-López, López-Sánchez & Hopkins, 2012, ApJ, in rev (SDSS): **PCA analysis**
- Lara-López et al. 2012 in prep (SDSS+GAMA)

Oxygen abundance: a key parameter to galaxy evolution models

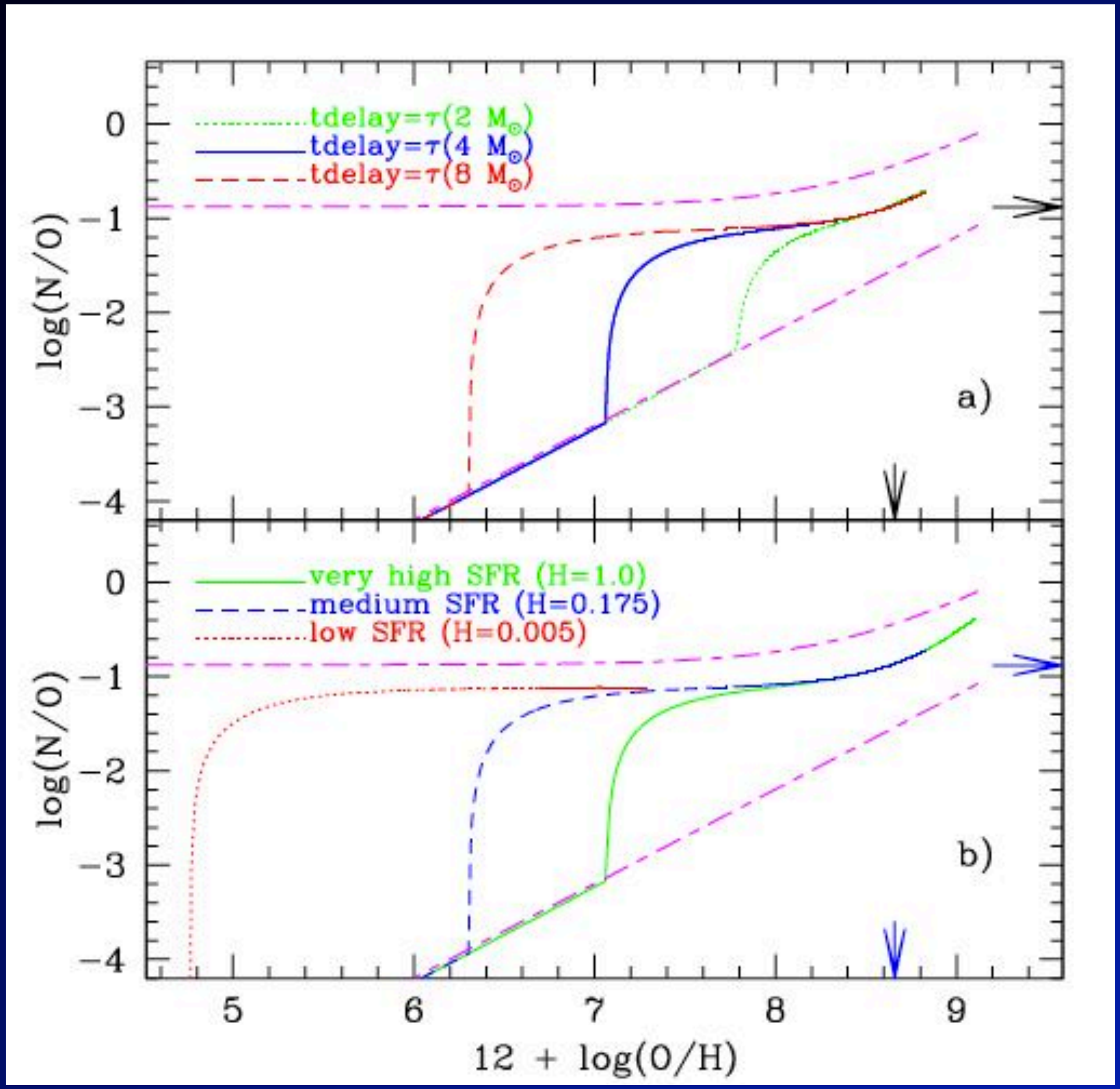

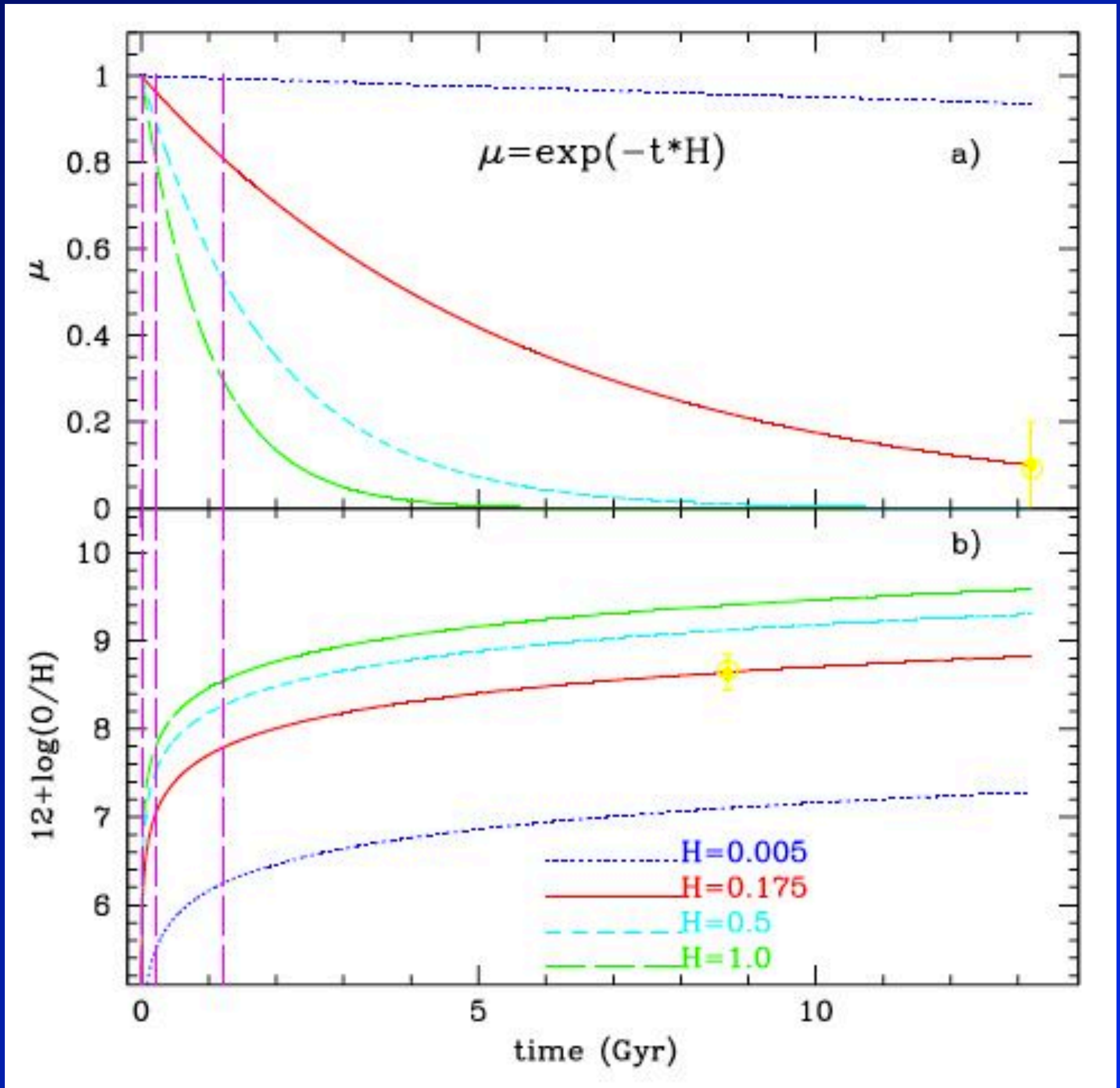

Evolution of N/O vs. O/H

a) Stars with **different masses ejecting NP**

b) 4Mo stars ejecting NP but where **SF occurs with different efficiencies**

Evolution of the gas fraction and O/H for different SF efficiencies

(Mollá et al. 2005, Mollá & Gavilán 2008; Martín-Majón et al. 2008, 2012)

Oxygen abundance: a key parameter to galaxy evolution models

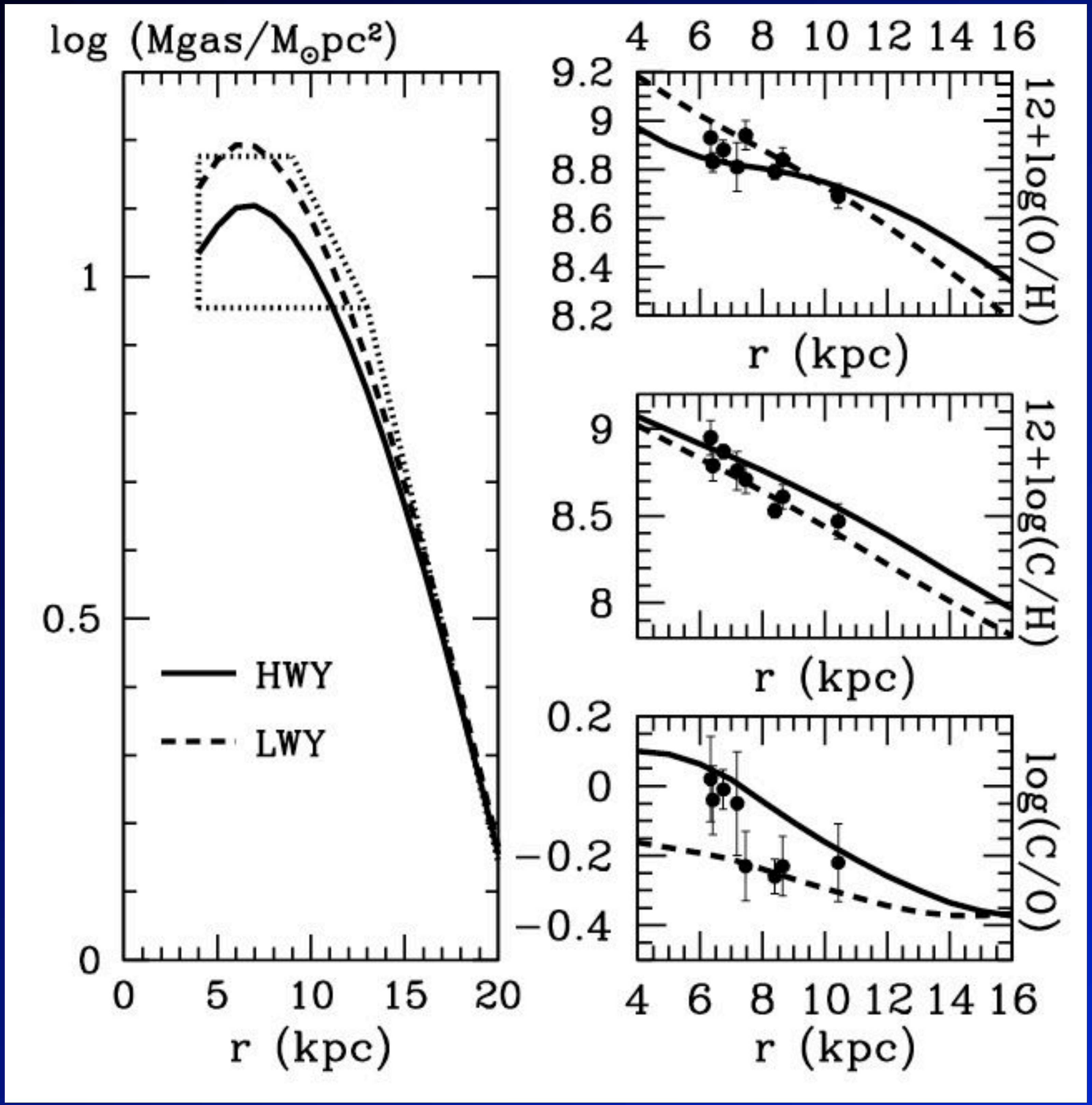

Carigi & Peimbert 2008, 2011

Present-day radial distribution of gas surface mass density and ISM abundance ratios + **predictions given by chemical evolution models** for the Galactic disc at the present time.

"To test stellar yields it is necessary to have good absolute abundances values of stars and HII regions"

Data points from
García-Rojas & Esteban 2007

Oxygen abundance and the distance scale

- Cepheids and O/H abundance: Scowcroft et al. 2009 MNRAS, 396, 1287, Urbaneja, Kudritzki et al. 2009, Bresolin et al. 2011

  "***It is necessary an ABSOLUTE O/H to get a proper distance to galaxies***" and measurements of Hubble constant comes from there! ***cif. Miguel Urbaneja***

- SN Ia and the expanding Universe (Mollá et al. 2012, submitted)
  - The **metallicity** of the **SN Ia** progenitor may play an important role in the estimation of its **maximum absolute luminosity**
  - The luminosities assigned to SN Ia with **over-solar** (sub-solar) **metallicities** result **smaller** (higher) than those obtained from the standard calibration for a same value of ΔM.

$$\Delta M_V(Z) = -2.5\log\left(1 - 0.075\frac{Z}{Z_\odot}\right) - 0.0846\ \mathrm{mag},$$

$$\Delta M_V(Z) = -2.5\log\left[1 - 0.18\frac{Z}{Z_\odot}\left(1 - 0.10\frac{Z}{Z_\odot}\right)\right] - 0.191\ \mathrm{mag}$$

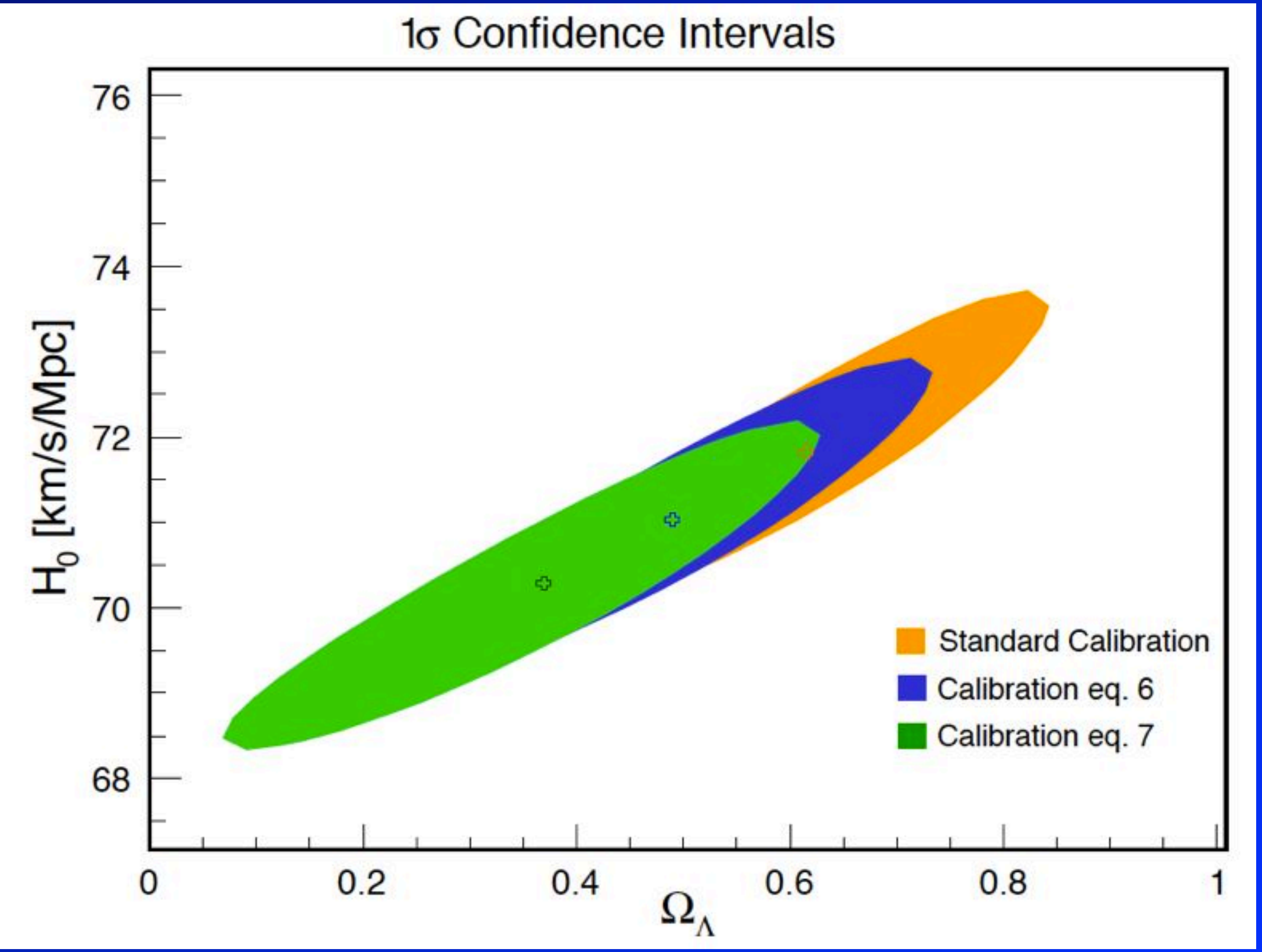

How do we estimate the gas-phase abundances?

We use the emission lines observed in the integrated spectrum of a galaxy. The majority of these lines are **collisionally excited lines** (CEL) of metallic elements (O, N, S, Ne, Ar, Cl, Fe ...). Also Recombination Lines (RL) of H and He.

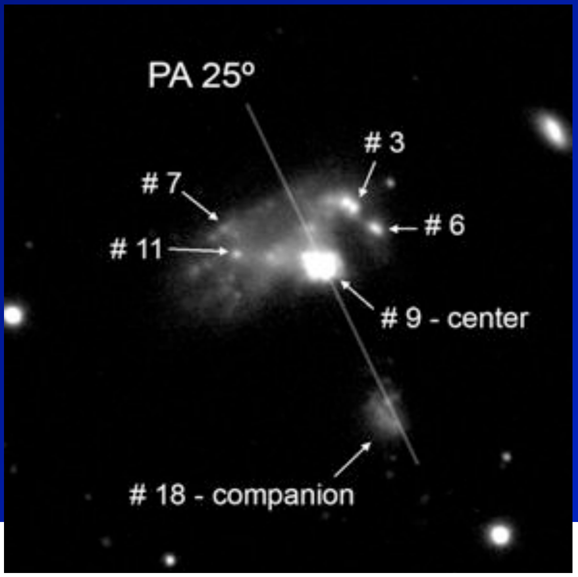

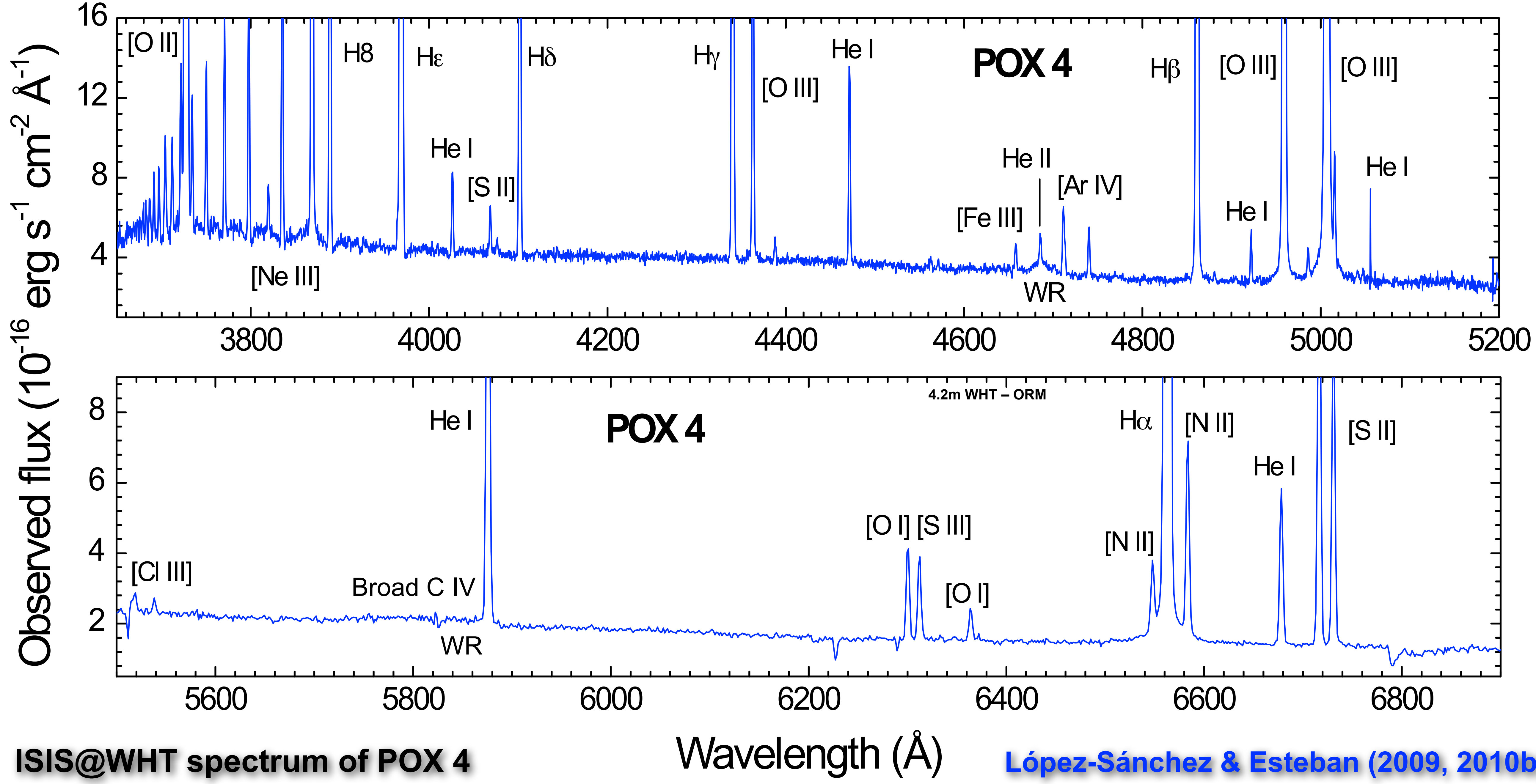

ISIS@WHT spectrum of POX 4

López-Sánchez & Esteban (2009, 2010b)

Methods to derive the oxygen abundance of the ionized gas

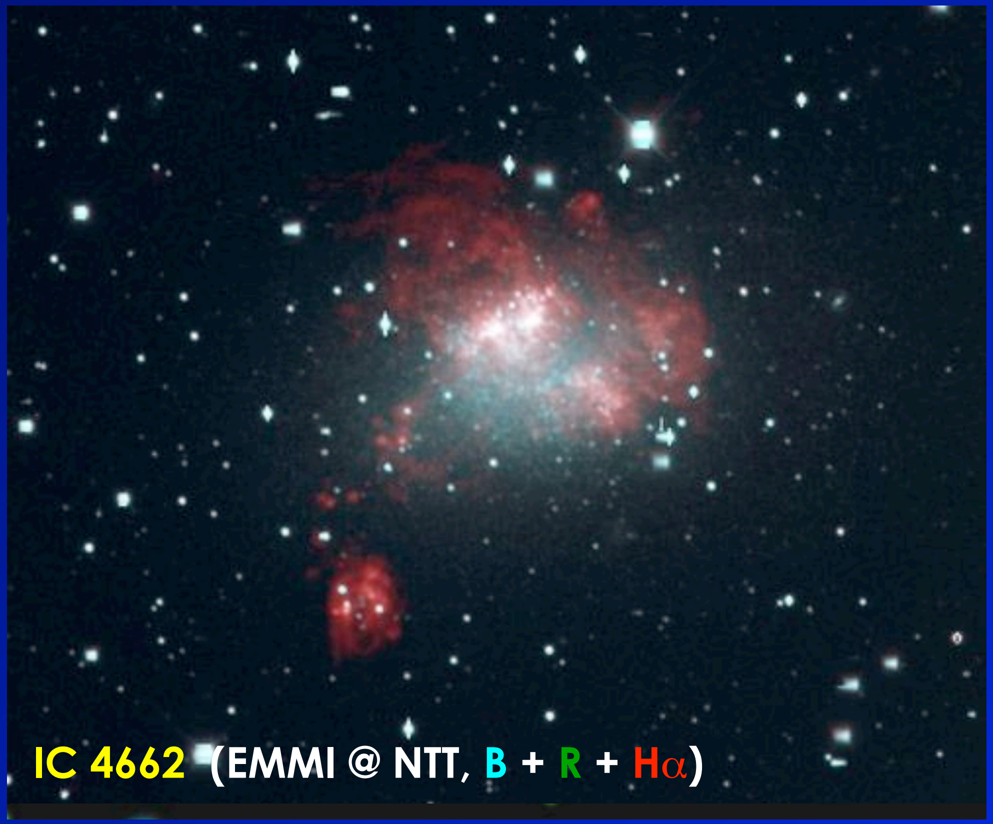

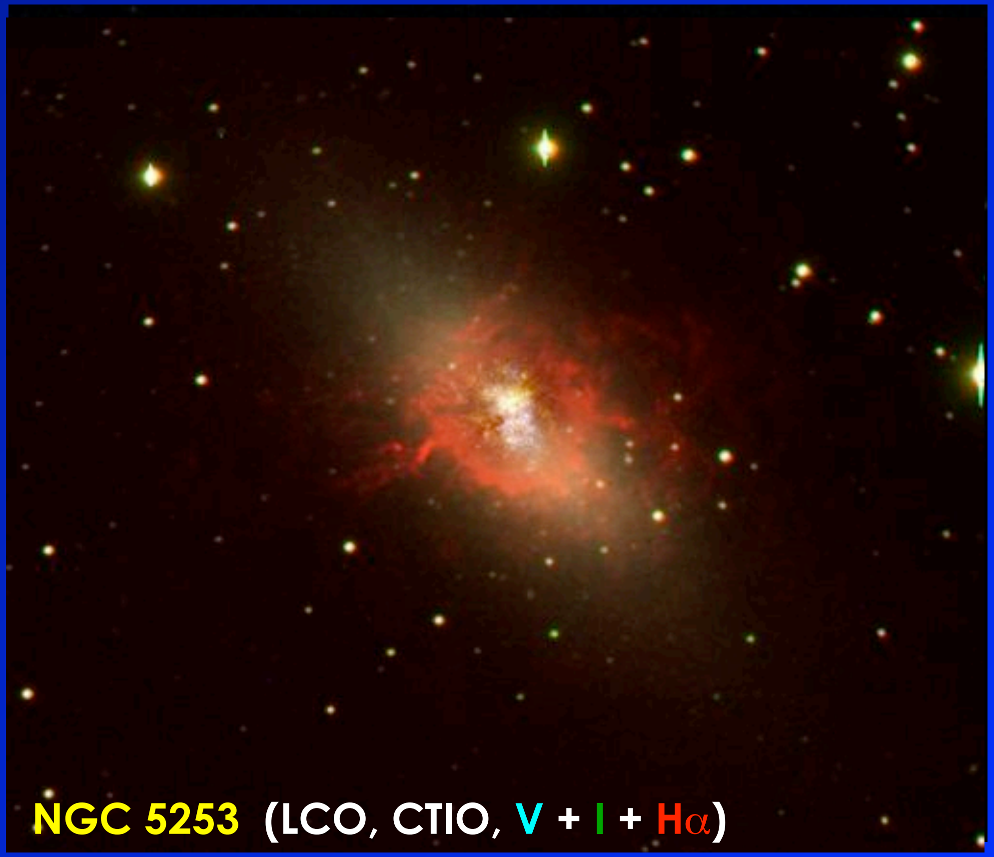

Ángel R. López-Sánchez

Methods to derive the oxygen abundance of the ionized gas

1. **Direct Method**
   - **There is a DIRECT estimation of the electron temperature**
   - **Observations and measurement of the faint auroral lines, e.g., [O III] λ4363.**
   - We then apply **Statistical Mechanics equations** and solve them for each **ion using CELs**

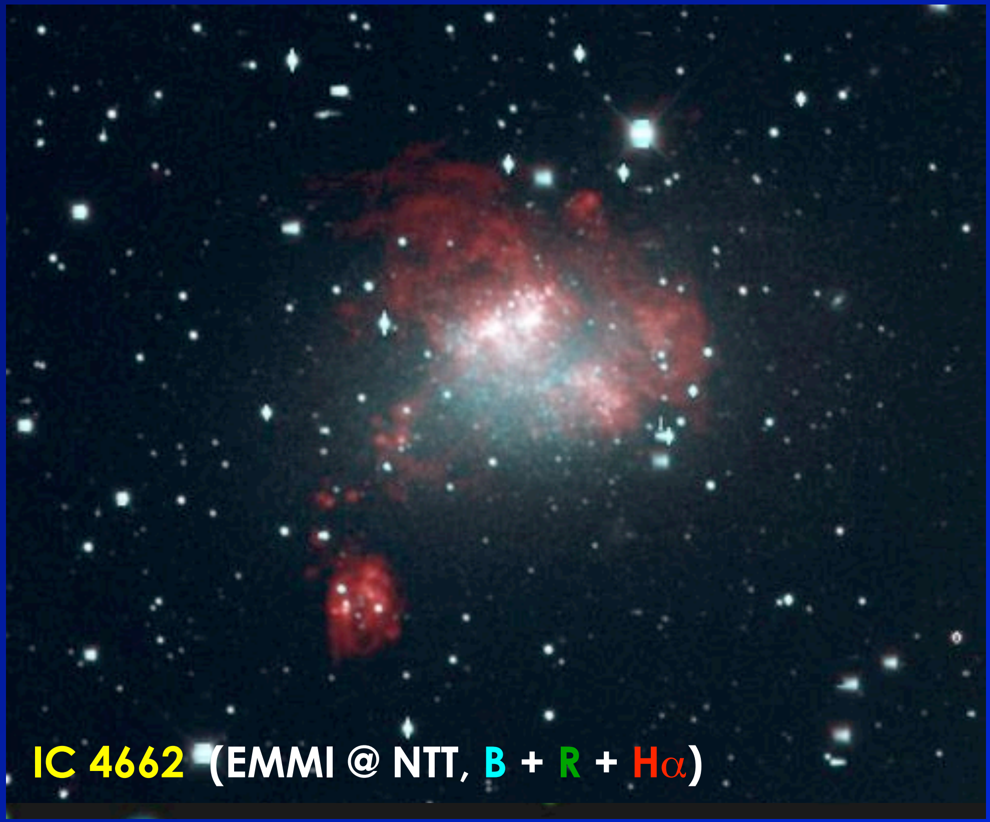

IC 4662 (EMMI @ NTT, B + R + Hα)

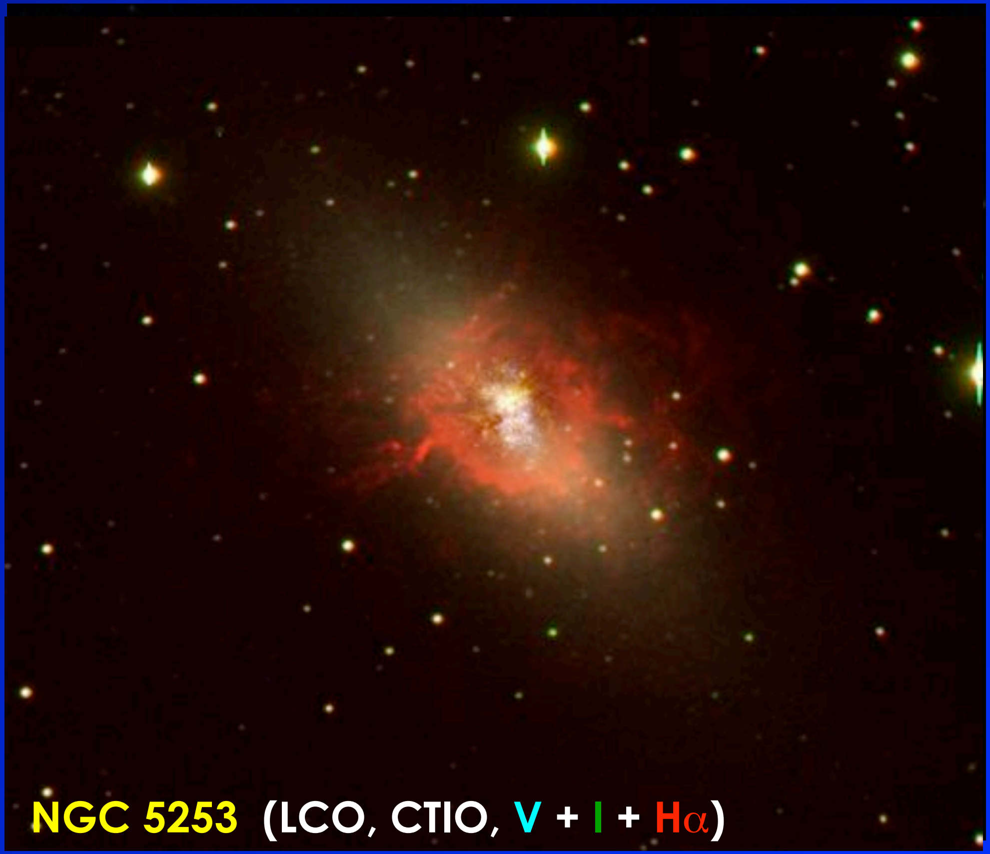

NGC 5253 (LCO, CTIO, V + I + Hα)

Methods to derive the oxygen abundance of the ionized gas

1. **Direct Method**
   - **There is a DIRECT estimation of the electron temperature**
   - **Observations and measurement of the faint auroral lines, e.g., [O III] λ4363.**
   - We then apply **Statistical Mechanics equations** and solve them for each **ion using CELs**
2. **Strong-line methods**
   a. Calibrations of the **bright emission lines** using objects for which the Te is known (e.g., Pilyugin method, Pagel & Pettini 2004)
   b. Use calibrations based on **photoionization models** (Kewley & Dopita 2002, Tremonti+ 2004)

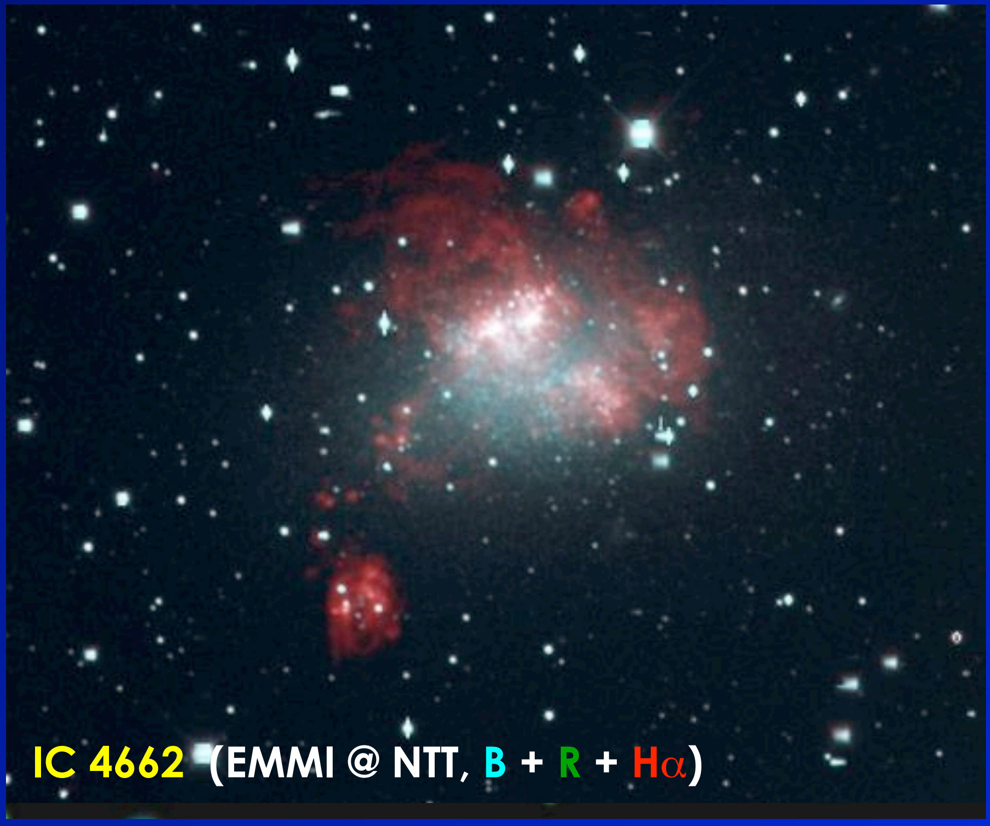

IC 4662 (EMMI @ NTT, B + R + Hα)

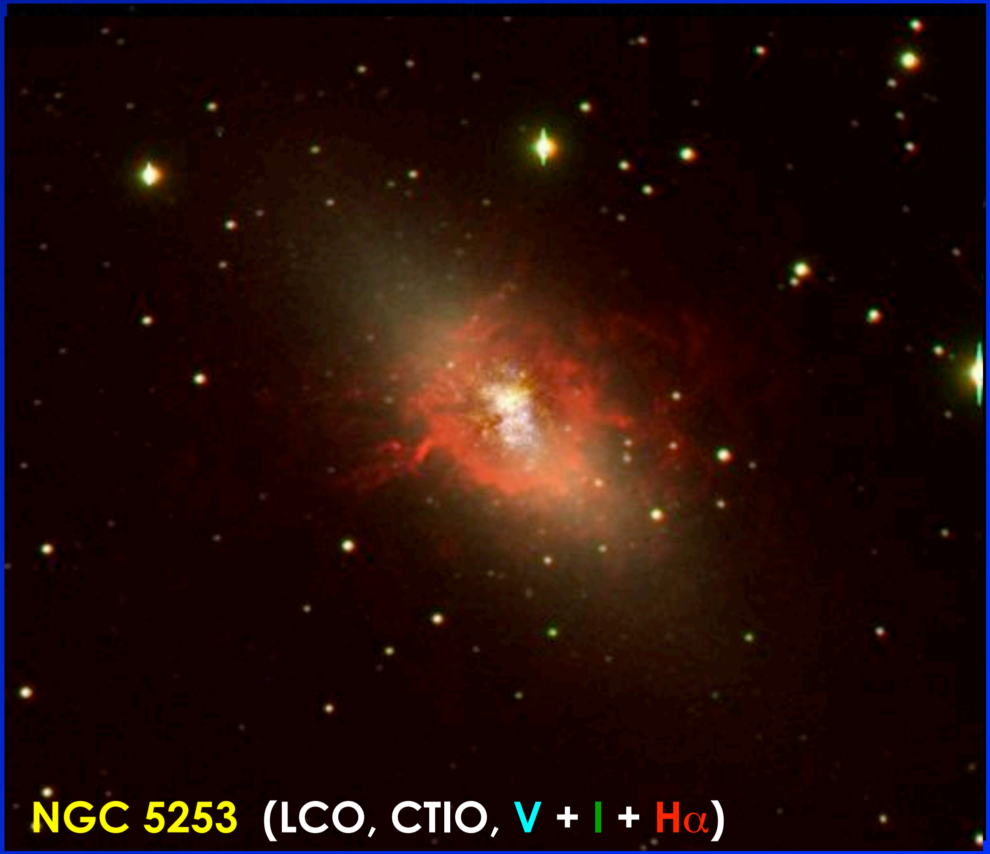

NGC 5253 (LCO, CTIO, V + I + Hα)

Methods to derive the oxygen abundance of the ionized gas

1. **Direct Method**
   - **There is a DIRECT estimation of the electron temperature**
   - **Observations and measurement of the faint auroral lines, e.g., [O III] λ4363.**
   - We then apply **Statistical Mechanics equations** and solve them for each **ion using CELs**
2. **Strong-line methods**
   a. Calibrations of the **bright emission lines** using objects for which the Te is known (e.g., Pilyugin method, Pagel & Pettini 2004)
   b. Use calibrations based on **photoionization models** (Kewley & Dopita 2002, Tremonti+ 2004)
3. **Tailored photoionization models**
   - E.g., Castellanos et al. 2002; Garnett et al. 2004, Morisset et al. 2005, Pérez-Montero et al. 2010, Dors et al. 2011

IC 4662 (EMMI @ NTT, B + R + Hα)

NGC 5253 (LCO, CTIO, V + I + Hα)

Methods to derive the oxygen abundance of the ionized gas

1. **Direct Method**
   - **There is a DIRECT estimation of the electron temperature**
   - **Observations and measurement of the faint auroral lines, e.g., [O III] λ4363.**
   - We then apply **Statistical Mechanics equations** and solve them for each **ion using CELs**
2. **Strong-line methods**
   a. Calibrations of the **bright emission lines** using objects for which the Te is known (e.g., Pilyugin method, Pagel & Pettini 2004)
   b. Use calibrations based on **photoionization models** (Kewley & Dopita 2002, Tremonti+ 2004)
3. **Tailored photoionization models**
   - E.g., Castellanos et al. 2002; Garnett et al. 2004, Morisset et al. 2005, Pérez-Montero et al. 2010, Dors et al. 2011
4. Using **Recombination Lines** of metallic elements (but they are ~1000 times fainter than CEL!!!)
   - E.g., Peimbert +1993, 2007, Esteban + 1998, 2005, 2006, 2009 García-Rojas + 2006, 2007, López-Sánchez et al. 2007).
   - Advantage: they depend very weakly on Te

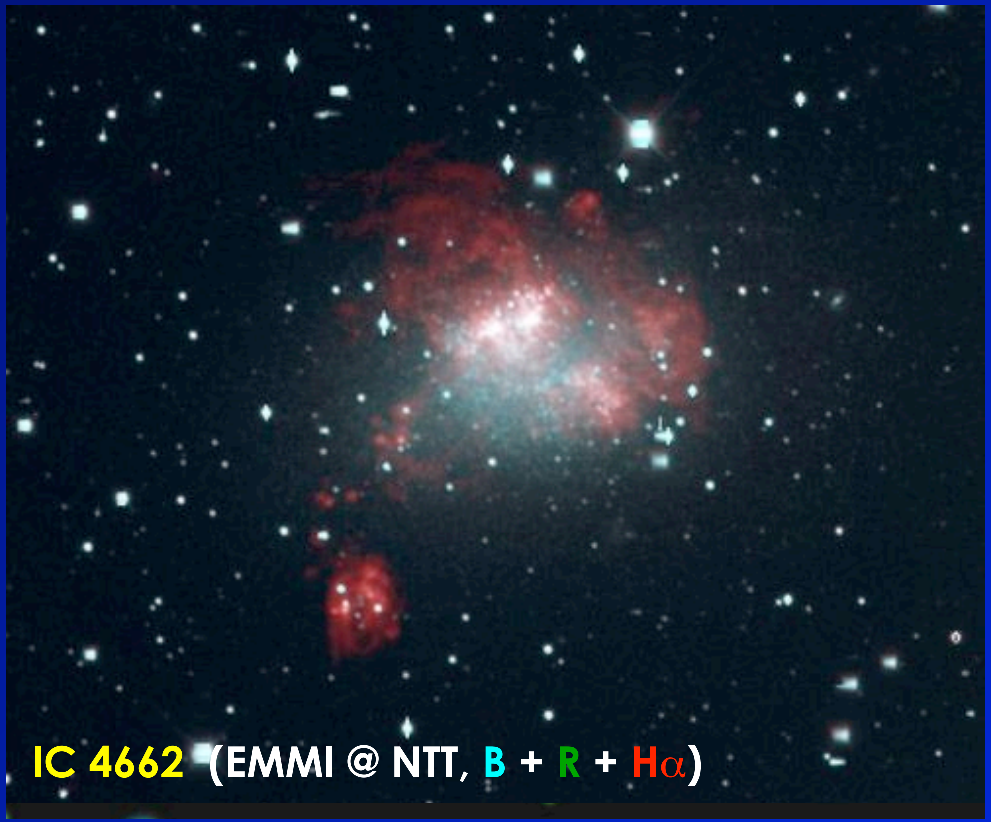

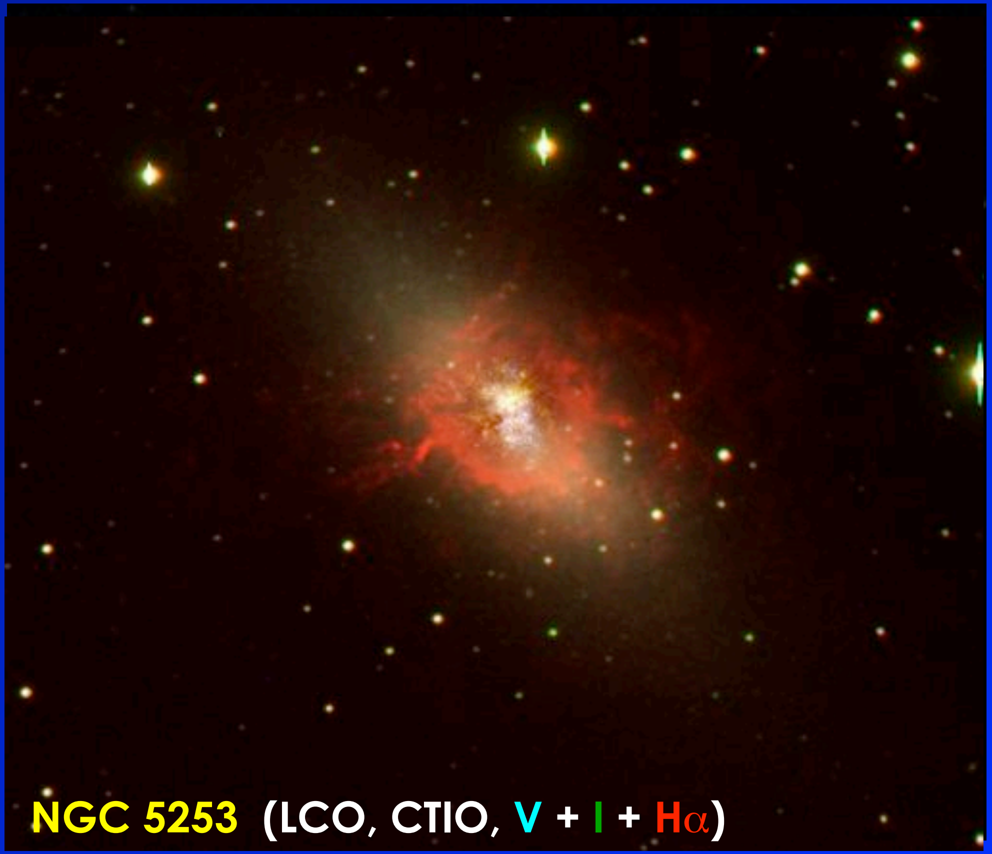

Oxygen Recombination Lines

- Deep and high-resolution spectra are needed to measure RLs.
  - Esteban+ 2004, 2005, 2006, 2009
  - García-Rojas+ 04,05,06,07

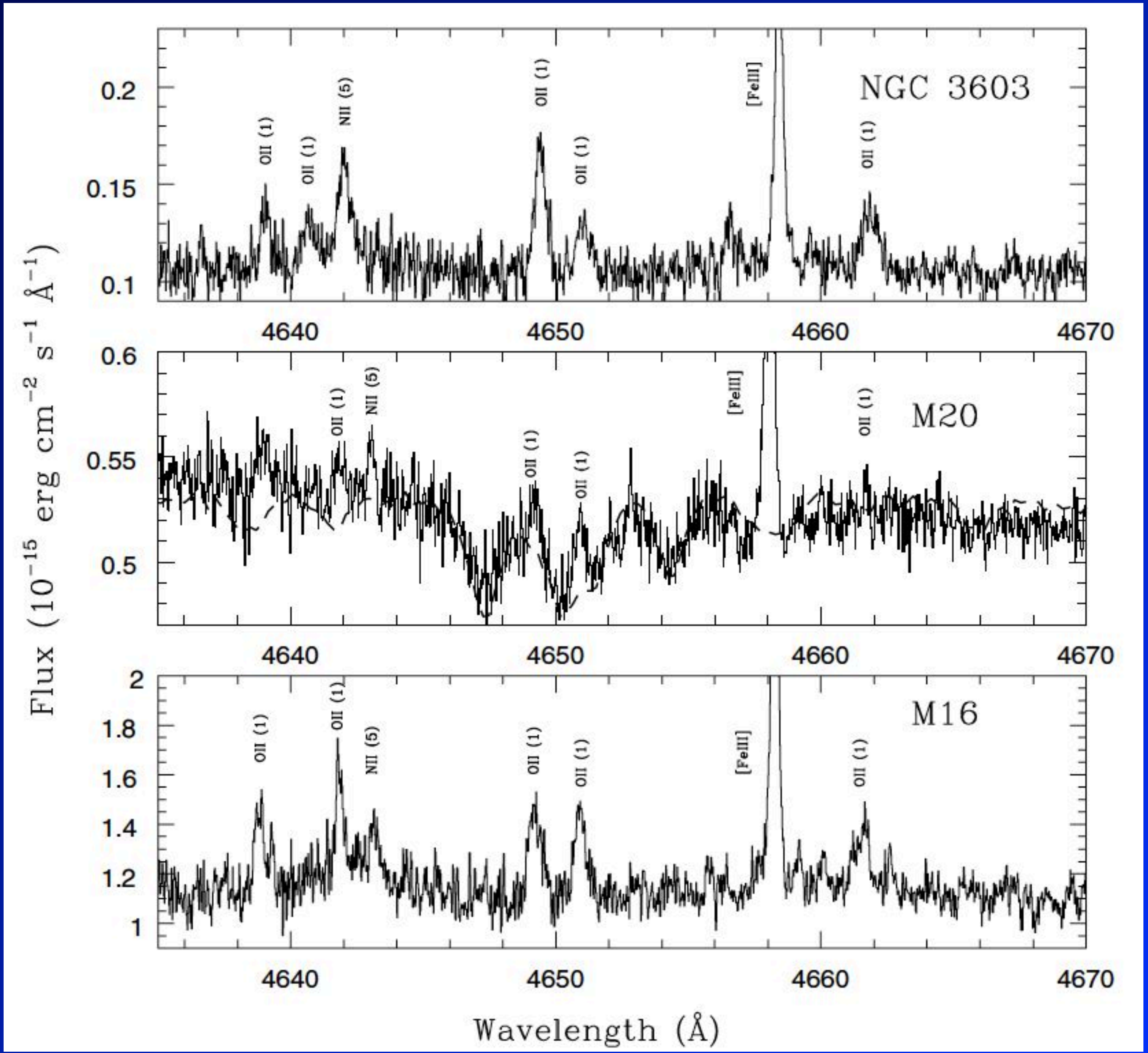

García-Rojas & Esteban 2007, ApJ, 670, 457 **- VLT UVES data - O II $\lambda\lambda$4550**

Oxygen Recombination Lines

- Deep and high-resolution spectra are needed to measure RLs.
  - Esteban+ 2004, 2005, 2006, 2009
  - García-Rojas+ 04,05,06,07
- **Abundance Discrepancy Problem** in both HII regions (Esteban+, García-Rojas+, Peimbert 2003, Mesa-Delgado+09) and PNe (Liu+00, Tsamis+05)
- **ADF = 0.26 ± 0.09** independent of the properties of HII regions
- Temperature fluctuations / inhomogeneities?
  - Peimbert 1967, Peimbert & Peimbert 2009
- **See also** López-Sánchez et al. 2007, Peimbert et al. 2007, Rodríguez & Delgado-Inglada (2011), Peña-Guerrero et al. 2012a,b...
  - + dust depletion ~0.08 - 0.12 dex
- **Rodríguez & García-Rojas (2010)**
  - Errors in the recomb. coef of O II RLs ?

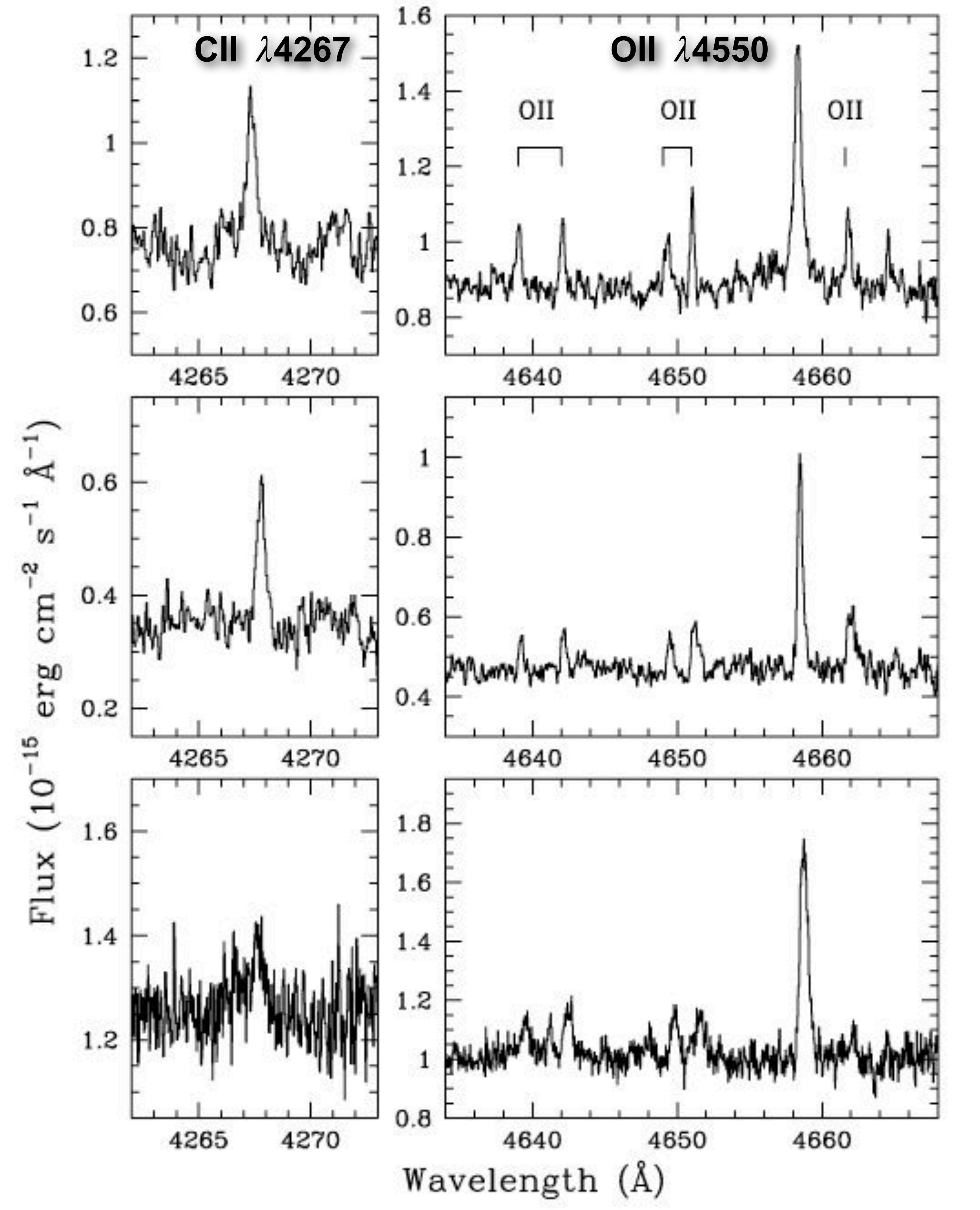

Esteban et al. 2009, ApJ, 700, 654 - Keck I HRES data

Oxygen Recombination Lines

- Deep and high-resolution spectra are needed to measure RLs.
  - Esteban+ 2004, 2005, 2006, 2009
  - García-Rojas+ 04,05,06,07
- Abundance Discrepancy Problem in both HII regions (Esteban+, García-Rojas+, Peimbert 2003, Mesa-Delgado+09) and PNe (Liu+00, Tsamis+05)
- ADF = 0.26 ± 0.09 independent of the properties of HII regions
- Temperature fluctuations / inhomogeneities?
  - Peimbert 1967, Peimbert & Peimbert 2009
- See also López-Sánchez et al. 2007, Peimbert et al. 2007, Rodríguez & Delgado-Inglada (2011), Peña-Guerrero et al. 2012a,b...
  - + dust depletion ~0.08 - 0.12 dex
- Rodríguez & García-Rojas (2010)
  - Errors in the recomb. coef of O II RLs ?
- RL-based abundances agree with stellar abundances (Simón-Díaz 2010; Simón-Díaz & Stasinska 2011)
  - But not Temperature fluctuations?
- O/H derived from BA supergiants (Firnstein & Przybilla 2012) and early B stars (Nieva & Przybilla 2012) agree VERY well with O/H derived using RL in Galactic HII regions (Esteban et al. 2005)

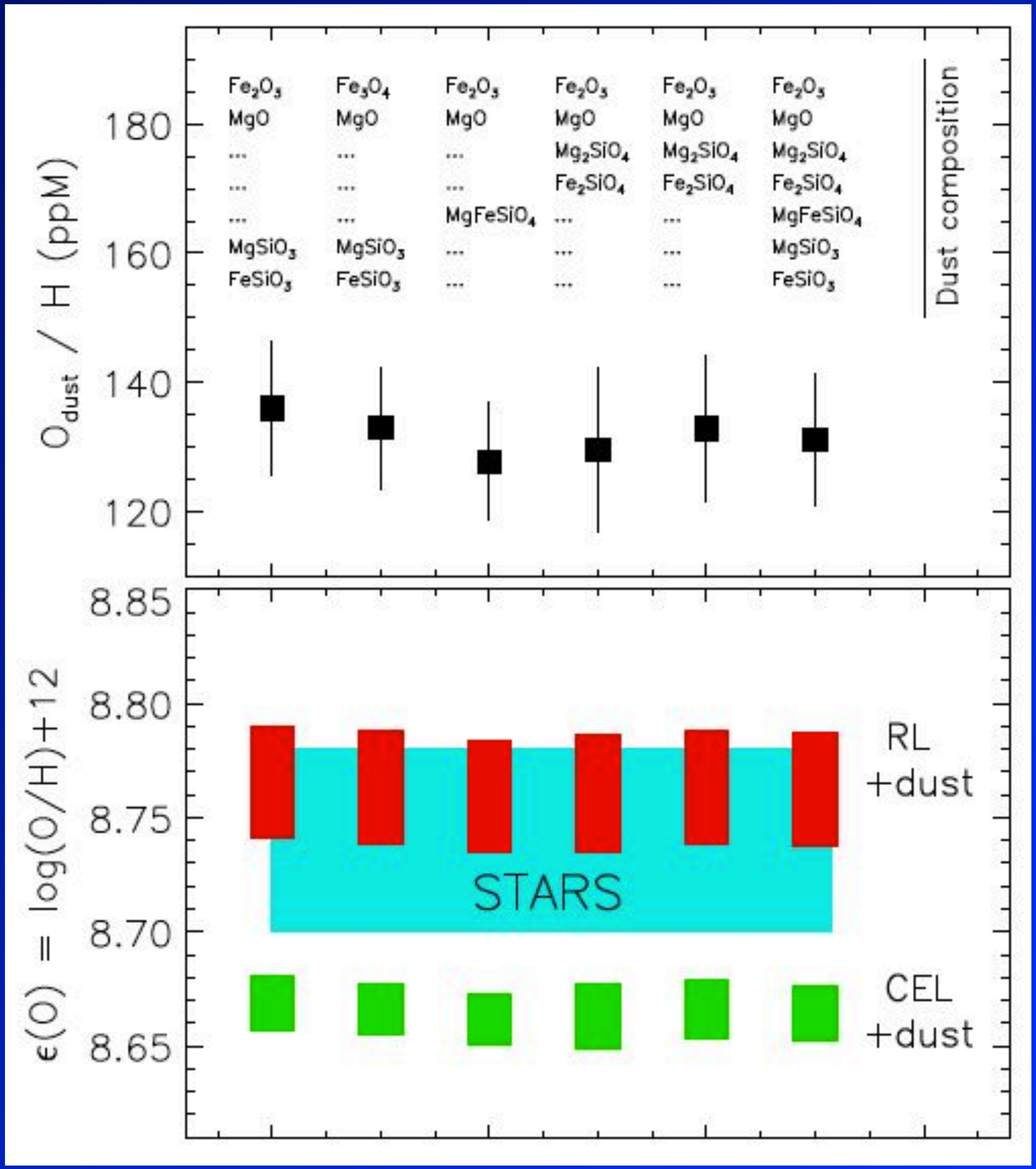

Simón-Díaz & Stasinska 2011, A&A, 526, 48

- RL abundances fit best Galactic gradients (Esteban et al. 2005; Carigi & Peimbert 2008, 2011)

The direct method: using electron temperatures of the ionized gas

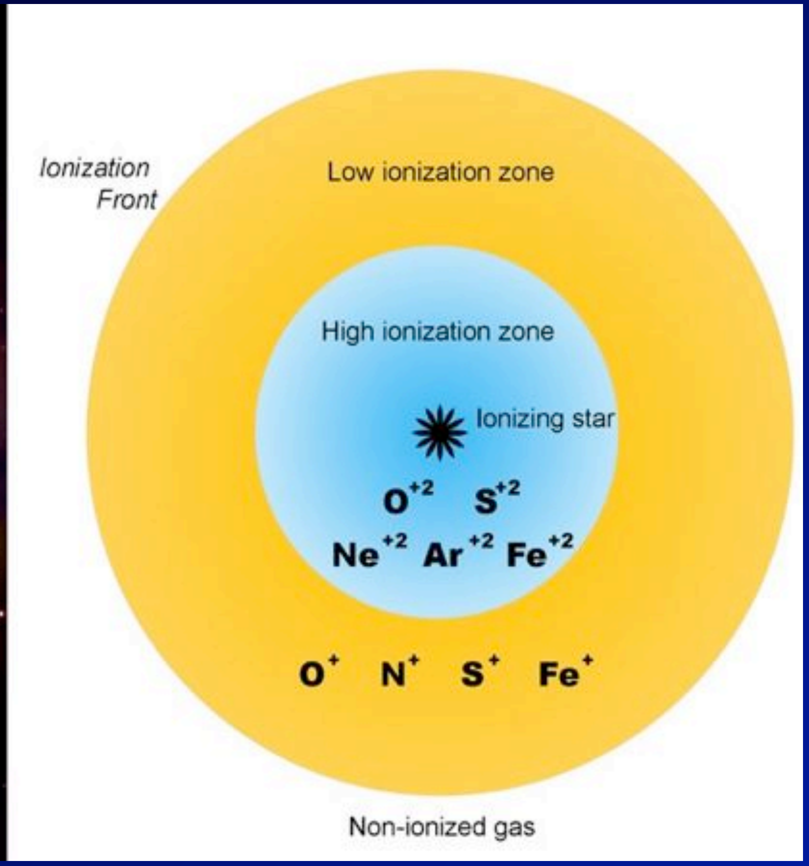

- **Auroral lines** (e.g., [O III] λ4363) **are detected**
- **A two-zone approximation:**
  - **HIGH Te**: using [O III] ratio → **T [O III]**

$$\frac{I(\lambda4959)+I(\lambda5007)}{I(\lambda4363)}=\frac{8.32\exp\left(\frac{3.29\times10^4}{T_e}\right)}{1+4.5\times10^{-4}\frac{n_e}{T_e^{1/2}}}.$$

  - **LOW Te**: using [O II] or [N II] ratio → **T [O II]**

$$\frac{I(\lambda6548)+I(\lambda6583)}{I(\lambda5755)}=\frac{7.53\exp\left(\frac{2.50\times10^4}{T_e}\right)}{1+2.7\times10^{-3}\frac{n_e}{T_e^{1/2}}}.$$

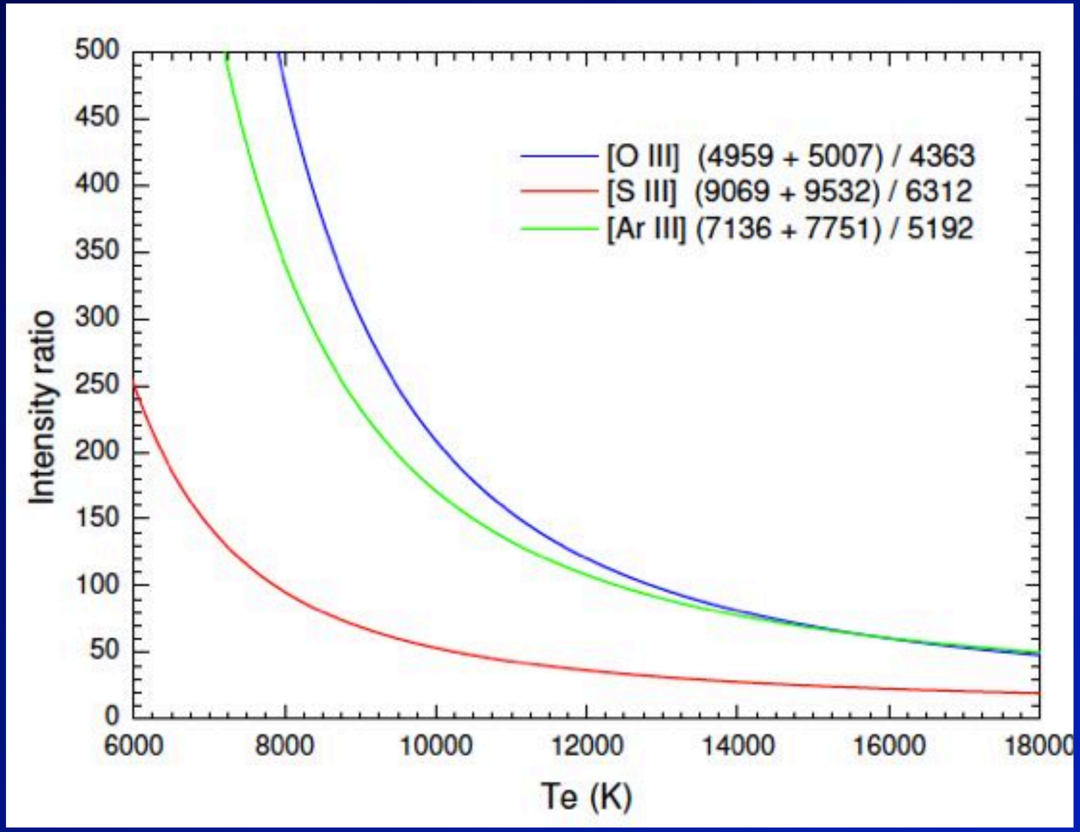

  - Sometimes, **T [O III] → T [O II]** **e.g. using Garnett (1992):**

$$T_e(\text{O II})=0.7\times T_e(\text{O III})+3000,$$

- Use package NEBULAR in IRAF (task "ionic") added by Shaw & Dufour (1995), which uses a 5-level atom (Robertis et al. 1987) to solve the **Statistical Equilibrium Equations for** Te and Ne. Atomic data are updated periodically.
- Derive **ionic abundance** for each ion.
- Add all ionic abundances to derive the **TOTAL abundance** of each element, many times **an ICF factor** must be used.

Mónica Rodríguez talk, Osterbrock (1989), Osterbrock & Ferland (2006), López-Sánchez PhD (2006)

Example: Ionized gas in Wolf-Rayet galaxies

Galaxy	T_e (a)	T_e High [K]	T_e Low [K]	n_e [cm^{-3}]	$c(H\beta)$	W_{abs} [Å]	$-W(H\beta)$ [Å]
HCG 31 AC	D	9400 ± 600	10 800 ± 300	210 ± 70	0.09 ± 0.03	2.0	91.1 ± 2.1
HCG 31 B	D	11 500 ± 700	12 000 ± 400	<100	0.28 ± 0.08	2.0	12.9 ± 0.5
HCG 31 E	D	11 100 ± 1000	11 800 ± 600	<100	0.11 ± 0.05	2.0	21.1 ± 1.1
HCG 31 F1	D	12 600 ± 1100	12 600 ± 700	<100	0.32 ± 0.06	2.0	218 ± 13
HCG 31 F2	D	12 300 ± 1300	12 400 ± 800	<100	0.14 ± 0.05	2.0	256 ± 30
HCG 31 G	D	11 600 ± 700	12 000 ± 400	<100	0.09 ± 0.05	2.0	37.0 ± 1.6
Mkn 1087	EC	7100 ± 1000	8000 ± 1000	220 ± 50	0.17 ± 0.02	1.7 ± 0.2	22.3 ± 0.9
Mkn 1087 N	EC	10 900 ± 1000	10 600 ± 1000	115 ± 50	0.17 ± 0.02	0.2 ± 0.1	25.0 ± 1.7
Haro 15 C	EC	9500 ± 800	9600 ± 600	<100	0.11 ± 0.03	2.4 ± 0.4	16.4 ± 1.1
Haro 15 A	D	12 850 ± 700	12 000 ± 500	<100	0.33 ± 0.03	1.3 ± 0.3	75.7 ± 4.2
Mkn 1199	D	5400 ± 700	6800 ± 600	300 ± 100	0.30 ± 0.03	1.8 ± 0.4	21.4 ± 1.3
Mkn 1199 NE	EC	8450 ± 800	8900 ± 600	<100	0.16 ± 0.03	0.6 ± 0.3	20.2 ± 2.3
Mkn 5	D	12 450 ± 650	11 700 ± 450	<100	0.17 ± 0.02	0.8 ± 0.2	75 ± 5
IRAS 08208+2816	D	10 100 ± 700	10 100 ± 500	<100	0.11 ± 0.02	3.2 ± 0.1	80 ± 5
IRAS 08339+6517	EC	8700 ± 1000	9100 ± 1000	100	0.22 ± 0.02	1.8 ± 0.2	19.0 ± 0.8
IRAS 08339+6517c	EC	9050 ± 1000	9300 ± 1000	100	0.18 ± 0.03	1.5 ± 0.2	7.5 ± 0.2
POX 4	D	14 000 ± 500	12 800 ± 400	250 ± 80	0.08 ± 0.01	2.0 ± 0.1	200 ± 9
POX 4 Comp	EC	12 400 ± 1000	11 700 ± 700	<100	0.06 ± 0.03	1.4 ± 0.3	12 ± 4
UM 420	D	13 200 ± 600	12 200 ± 500	140 ± 80	0.09 ± 0.01	2.0 ± 0.1	169 ± 10
SBS 0926+606 A	D	13 600 ± 700	12 500 ± 500	<100	0.12 ± 0.03	0.7 ± 0.1	125 ± 6
SBS 0926+606 B	EC	11 500 ± 1000	11 000 ± 800	<100	0.18 ± 0.04	1.0 ± 0.3	18 ± 3
SBS 0948+532	D	13 100 ± 600	12 200 ± 400	250 ± 80	0.35 ± 0.03	0.3 ± 0.1	213 ± 11
SBS 1054+365	D	13 700 ± 900	12 600 ± 700	<100	0.02 ± 0.02	0.8 ± 0.1	89 ± 7
SBS 1054+365 b	EC	11 800 ± 1100	11 300 ± 900	300 ± 200	0.03 ± 0.03	0.3 ± 0.1	8 ± 3
SBS 1211+540	D	17 100 ± 600	15 000 ± 400	320 ± 50	0.12 ± 0.01	1.3 ± 0.1	135 ± 10
SBS 1319+579 A	D	13 400 ± 500	12 400 ± 400	<100	0.03 ± 0.01	0.0 ± 0.1	285 ± 14
SBS 1319+579 B	D	11 900 ± 800	11 300 ± 600	<100	0.11 ± 0.03	0.4 ± 0.1	42 ± 4
SBS 1319+579 C	D	11 500 ± 600	11 050 ± 400	<100	0.02 ± 0.02	0.2 ± 0.1	94 ± 6
SBS 1415+579 C	D	16 400 ± 600	14 500 ± 400	<100	0.01 ± 0.02	0.8 ± 0.1	222 ± 11
SBS 1415+579 A	D	15 500 ± 700	13 850 ± 500	<100	0.15 ± 0.03	1.0 ± 0.2	130 ± 8
III Zw 107 A	D	10 900 ± 900	10 500 ± 800	200 ± 60	0.68 ± 0.04	2.0 ± 0.3	44 ± 2
Tol 9	D	7600 ± 1000	8300 ± 700	180 ± 60	0.50 ± 0.05	7.5 ± 0.8	33 ± 2
Tol 1457-262 A	D	14 000 ± 700	12 500 ± 600	200 ± 80	0.57 ± 0.03	1.4 ± 0.2	101 ± 6
Tol 1457-262 B	D	15 200 ± 900	14 200 ± 700	<100	0.00 ± 0.05	0.0 ± 0.1	82 ± 7
Tol 1457-262 C	D	13 400 ± 1100	12 400 ± 1000	200 ± 100	0.15 ± 0.02	0.7 ± 0.1	92 ± 9
ESO 566-8	D	8700 ± 900	9100 ± 800	300 ± 100	0.49 ± 0.03	1.3 ± 0.1	95 ± 7
ESO 566-7	EC	7900 ± 1000	8500 ± 900	100 ± 50	0.23 ± 0.05	2.7 ± 0.2	13 ± 2
NGC 5253 A	D	12 100 ± 260	11 170 ± 520	580 ± 110	0.23 ± 0.02	1.3 ± 0.1	234 ± 5
NGC 5253 B	D	12 030 ± 260	11 250 ± 490	610 ± 100	0.38 ± 0.03	1.7 ± 0.1	254 ± 5
NGC 5253 C	D	10 810 ± 230	10 530 ± 470	370 ± 80	0.25 ± 0.03	0.8 ± 0.1	94 ± 3
NGC 5253 D	D	11 160 ± 510	10 350 ± 650	230 ± 70	0.10 ± 0.02	0.6 ± 0.1	39 ± 2

Notes. [a] In this column we indicate if T_e was computed using the direct method (D) or via empirical calibrations (EC).

Deep MULTIWAVELENGTH analysis of 20 strong star-forming systems

31 regions with a direct estimation of 12+log (O/H)

In many cases, using SEVERAL auroral lines

López-Sánchez 2006, PhD

López-Sánchez & Esteban 2009, A&A, 508, 615

López-Sánchez & Esteban 2010b, A&A, 517, 85

Example: Ionized gas in Wolf-Rayet galaxies

Galaxy	T_e^a	12+log(O/H)	log $\frac{O^{++}}{O^{+}}$	log(N/O)	log(S/O)	log(Ne/O)	log(Ar/O)	log(Fe/O)
HCG 31 AC	D	8.22 ± 0.05	1.51 ± 0.12	−1.12 ± 0.08	...	−0.93 ± 0.12	...	−2.12 ± 0.21
HCG 31 B	D	8.14 ± 0.08	0.63 ± 0.09	−1.39 ± 0.10	−1.67 ± 0.14	−0.42 ± 0.13	...	−1.87 ± 0.32
HCG 31 E	D	8.13 ± 0.09	1.00 ± 0.11	−1.26 ± 0.12	−1.58 ± 0.15	−0.42 ± 0.14	...	−1.77 ± 0.32
HCG 31 F1	D	8.07 ± 0.06	3.72 ± 0.32	−1.27 ± 0.11	−1.69 ± 0.15	−0.80 ± 0.17	...	−1.9:
HCG 31 F2	D	8.03 ± 0.10	2.19 ± 0.21	−1.43 ± 0.16	−1.67 ± 0.18	−0.76 ± 0.20	...	...
HCG 31 G	D	8.15 ± 0.07	1.15 ± 0.11	−1.31 ± 0.10	−1.67 ± 0.22	−0.56 ± 0.14	...	−2.0:
Mkn 1087	EC	8.57 ± 0.10	0.55 ± 0.18	−0.81 ± 0.12	−1.78 ± 0.16	−0.45 ± 0.17	...	...
Mkn 1087 N	EC	8.23 ± 0.10	0.99 ± 0.25	−1.46 ± 0.15	...	−0.52 ± 0.19	...	...
Haro 15 C	EC	8.37 ± 0.10	−0.23 ± 0.16	−1.03 ± 0.15	−1.71 ± 0.18	−0.65 ± 0.18	...	−2.2:
Haro 15 A	D	8.10 ± 0.06	0.66 ± 0.10	−1.35 ± 0.11	−1.89 ± 0.15	−0.68 ± 0.12	...	−1.6:
Mkn 1199	D	8.75 ± 0.12	−0.36 ± 0.16	−0.62 ± 0.10	−1.54 ± 0.14	−0.58 ± 0.17	...	−1.86 ± 0.26
Mkn 1199 NE	EC	8.46 ± 0.13	−0.19 ± 0.09	−1.20 ± 0.11	−1.54 ± 0.17	−0.65 ± 0.18	...	...
Mkn 5	D	8.07 ± 0.04	0.25 ± 0.08	−1.38 ± 0.07	−1.62 ± 0.11	−0.80 ± 0.13	−2.31 ± 0.12	−1.96 ± 0.18
IRAS 08208+2816	D	8.33 ± 0.08	0.43 ± 0.12	−0.89 ± 0.11	−1.64 ± 0.16	−0.67 ± 0.13	−2.51 ± 0.15	−1.95 ± 0.17
IRAS 08339+6517	EC	8.45 ± 0.10	0.53 ± 0.16	−0.94 ± 0.14	...	−0.45 ± 0.18	...	...
IRAS 08339+6517c	EC	8.38 ± 0.10	0.81 ± 0.21	−1.13 ± 0.17	...	−0.55:	...	...
POX 4	D	8.03 ± 0.04	0.74 ± 0.06	−1.54 ± 0.06	−1.80 ± 0.10	−0.78 ± 0.10	...	−2.17 ± 0.11
POX 4c	EC	8.03 ± 0.14	−0.30 ± 0.22	−1.60 ± 0.20	...	-0.60:	...	...
UM 420	D	7.95 ± 0.05	0.00 ± 0.08	−1.11 ± 0.07	−1.66 ± 0.13	−0.71 ± 0.13	...	−2.16 ± 0.13
SBS 0926+606 A	D	7.94 ± 0.08	0.42 ± 0.12	−1.45 ± 0.09	−1.60 ± 0.13	...	−2.34 ± 0.13	−1.99 ± 0.16
SBS 0926+606 B	EC	8.15 ± 0.16	0.21 ± 0.14	−1.35 ± 0.12	...	...	...	...
SBS 0948+532	D	8.03 ± 0.05	0.61 ± 0.08	−1.42 ± 0.08	−1.69 ± 0.14	−0.73 ± 0.12	...	−1.78 ± 0.10
SBS 1054+365	D	8.00 ± 0.07	0.70 ± 0.11	−1.41 ± 0.08	−1.79 ± 0.15	−0.67 ± 0.11	−2.29 ± 0.14	...
SBS 1054+365 b	EC	8.13 ± 0.16	−0.35 ± 0.20	−1.47 ± 0.20	...	...	...	...
SBS 1211+540	D	7.65 ± 0.04	0.69 ± 0.07	−1.62 ± 0.10	−1.47 ± 0.14	−0.75 ± 0.10	...	...
SBS 1319+579 A	D	8.05 ± 0.06	0.77 ± 0.12	−1.53 ± 0.10	−1.76 ± 0.10	...	−2.41 ± 0.11	...
SBS 1319+579 B	D	8.12 ± 0.10	0.16 ± 0.19	−1.49 ± 0.12	−1.76 ± 0.14	...	...	...
SBS 1319+579 C	D	8.15 ± 0.07	0.18 ± 0.13	−1.38 ± 0.10	−1.60 ± 0.11	...	...	−2.3:
SBS 1415+437 C	D	7.58 ± 0.05	0.35 ± 0.08	−1.57 ± 0.08	−1.62 ± 0.12	...	−2.31 ± 0.13	−1.91 ± 0.13
SBS 1415+437 A	D	7.61 ± 0.06	0.42 ± 0.14	−1.57 ± 0.09	−1.72 ± 0.14	...	...	−1.9:
III Zw 107 A	D	8.23 ± 0.09	0.12 ± 0.14	−1.16 ± 0.10	−1.82 ± 0.15	−0.73 ± 0.15	−2.46 ± 0.13	−2.3:
Tol 9	D	8.57 ± 0.10	0.16 ± 0.17	−0.81 ± 0.11	−1.62 ± 0.12	−0.72 ± 0.14	−2.55 ± 0.15	−2.1:
Tol 1457-262 A	D	8.05 ± 0.07	0.27 ± 0.11	−1.57 ± 0.11	−1.88 ± 0.13	−0.88 ± 0.18	−2.50 ± 0.13	−2.2:
Tol 1457-262 B	D	7.88 ± 0.07	0.43 ± 0.11	−1.61 ± 0.12	−1.72 ± 0.18	−0.88 ± 0.20	−2.44 ± 0.18	−1.90 ± 0.22
Tol 1457-262 C	D	8.06 ± 0.11	0.14 ± 0.16	−1.59 ± 0.16	...	−0.84 ± 0.22	−2.45 ± 0.20	...
ESO 566-8	D	8.46 ± 0.11	−0.19 ± 0.17	−0.76 ± 0.12	...	−0.56 ± 0.19	−2.17 ± 0.19	−2.5:
ESO 566-7	EC	8.50 ± 0.16	−0.57 ± 0.22	−0.82 ± 0.16	...	...	−2.49 ± 0.25	...
NGC 5253 A	D	8.18 ± 0.04	2.88 ± 0.18	−0.91 ± 0.07	−1.58 ± 0.08	−0.71 ± 0.08	−2.19 ± 0.07	−2.10 ± 0.12
NGC 5253 B	D	8.19 ± 0.04	3.09 ± 0.14	−1.02 ± 0.07	−1.60 ± 0.08	−0.70 ± 0.08	−2.21 ± 0.07	−2.18 ± 0.11
NGC 5253 C	D	8.28 ± 0.04	1.95 ± 0.13	−1.50 ± 0.08	−1.69 ± 0.09	−0.74 ± 0.08	−2.30 ± 0.08	−2.46 ± 0.14
NGC 5253 D	D	8.31 ± 0.07	0.56 ± 0.14	−1.49 ± 0.10	−1.74 ± 0.13	−0.70 ± 0.15	−2.30 ± 0.13	−2.25 ± 0.16

López-Sánchez & Esteban 2010b A&A, 517, 85

Example: Evolution of the N/O ratio with the O/H in WR galaxies

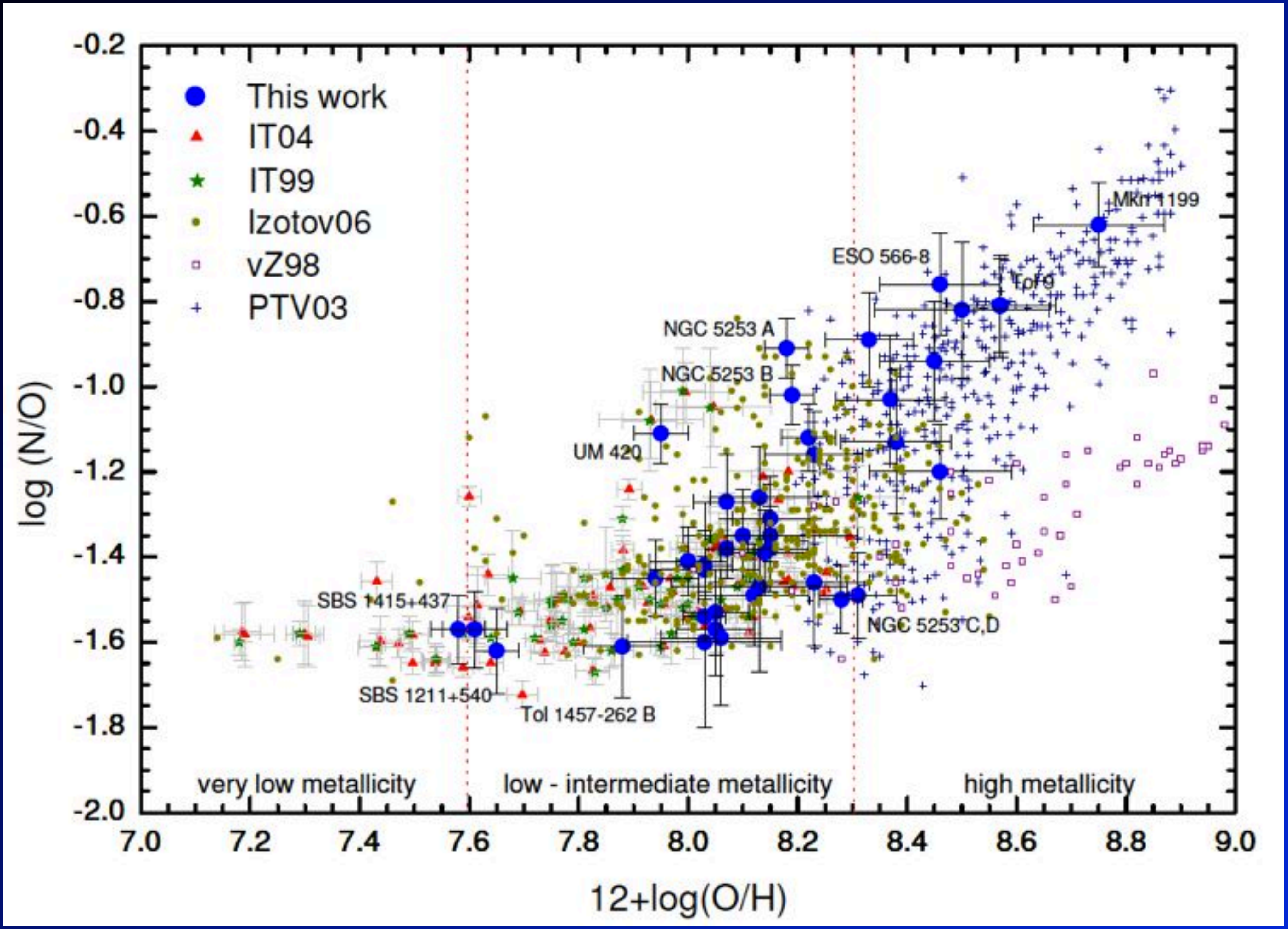

- Constant for 12+log O/H < 7.6
  Primary production
  Izotov & Thuan (1999)
  However see
  Henry et al. 2000,
  Pilyugin et al. 2003,
  Mollá et al. 2006,
  Berg et al. 2012
- Dispersion for 7.6 < 12+log O/H < 8.3
  Delay in N production & loss via galactic winds
  (e.g. Kobulnicky & Skillman 1999)
- Increases for 12+log O/H > 8.3
  Metalicity-dependence of N in both massive and intermediate-mass stars
  Secondary production
  (e.g. Pilyugin et al. 2003)

López-Sánchez & Esteban, 2010b, A&A, 517, 85

Kobulnicky et al. 1997; Izotov et al 2006; Pérez-Montero & Contini 2009

Example: Evolution of the N/O ratio with the O/H in WR galaxies

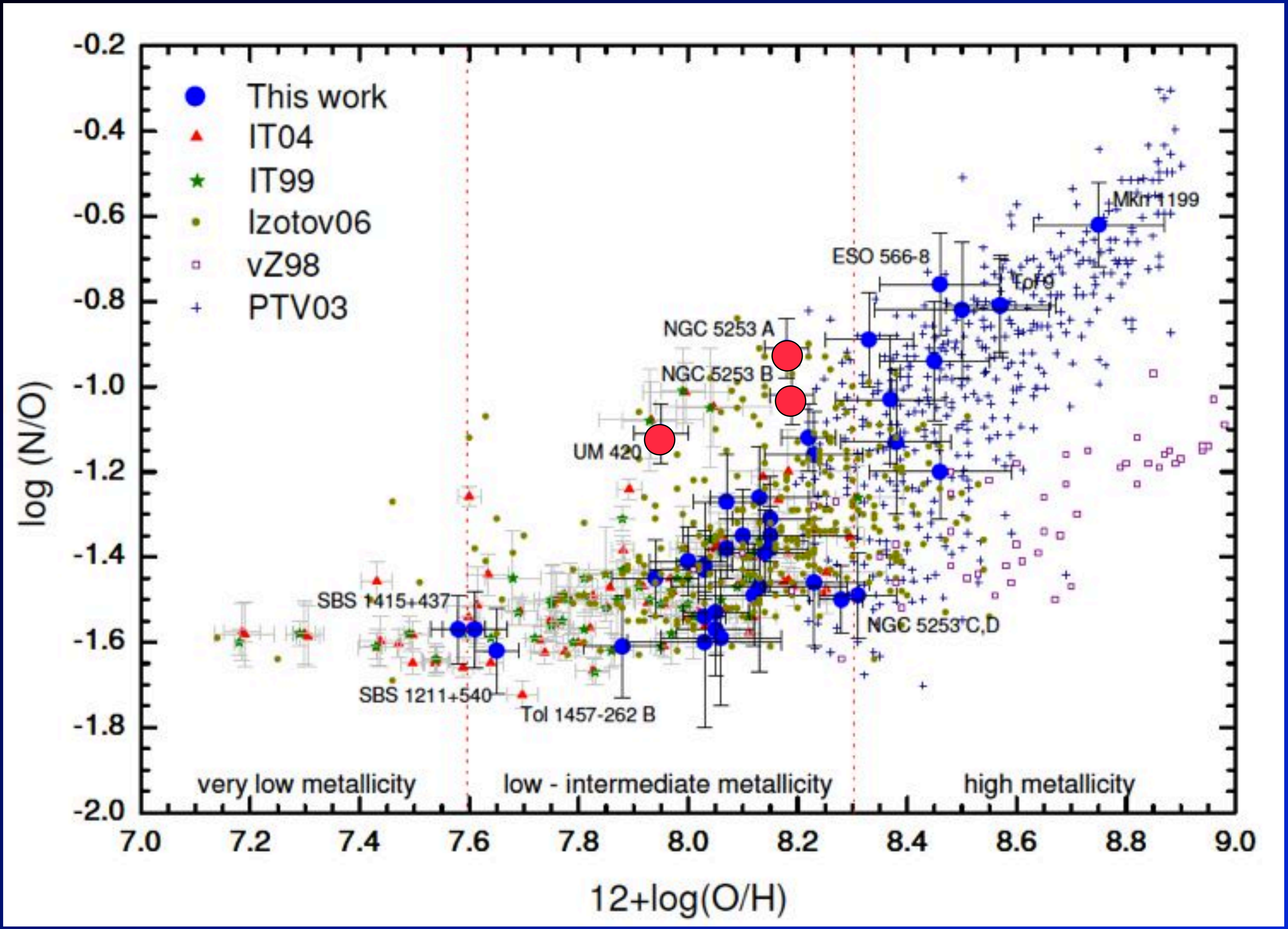

– Constant for 12+log O/H < 7.6 *Primary production* Izotov & Thuan (1999) However see Henry et al. 2000, Pilyugin et al. 2003, Mollá et al. 2006, Berg et al. 2012

– Dispersion for 7.6 < 12+log O/H < 8.3 *Delay in N production & loss via galactic winds* (e.g. Kobulnicky & Skillman 1999)

– Increases for 12+log O/H > 8.3 Metalicity-dependence of N in both massive and intermediate-mass stars *Secondary production* (e.g. Pilyugin et al. 2003)

– Some objects with very high N/O ratio. Chemical pollution by winds of WR stars?

López-Sánchez & Esteban, 2010b, A&A, 517, 85

Kobulnicky et al. 1997; Izotov et al 2006; Pérez-Montero & Contini 2009

Example: Evolution of the N/O ratio with the O/H in WR galaxies

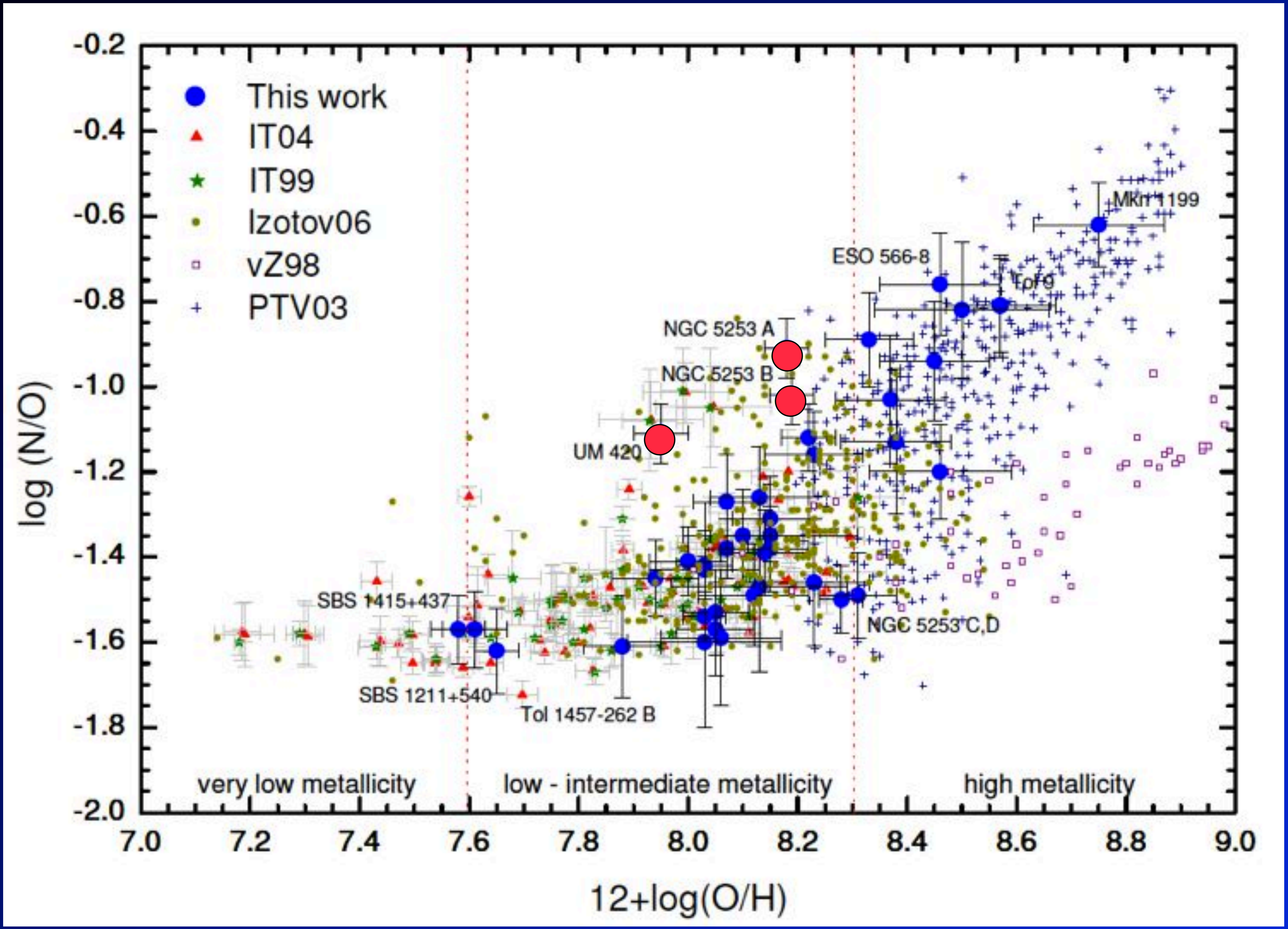

- Constant for 12+log O/H < 7.6 *Primary production* Izotov & Thuan (1999) However see Henry et al. 2000, Pilyugin et al. 2003, Mollá et al. 2006, Berg et al. 2012
- Dispersion for 7.6 < 12+log O/H < 8.3 *Delay in N production & loss via galactic winds* (e.g. Kobulnicky & Skillman 1999)
- Increases for 12+log O/H > 8.3 Metalicity-dependence of N in both massive and intermediate-mass stars *Secondary production* (e.g. Pilyugin et al. 2003)
- Some objects with very high N/O ratio. Chemical pollution by winds of WR stars?

López-Sánchez & Esteban, 2010b, A&A, 517, 85

Kobulnicky et al. 1997; Izotov et al 2006; Pérez-Montero & Contini 2009

- Important to consider Star Formation Histories, in agreement with predictions by theoretical models (e.g., Mollá et al. 2006)

Example: Multiwavelength analysis of WR galaxies

- Optical / NIR data complemented with X-ray, UV, IR and radio data
  - SFRs, neutral gas mass, baryonic mass, dust mass, neutral gas morphology & kinematics
  - An unique (*although small*) database of SF galaxies: **López-Sánchez 2010, A&A, 521, 63**

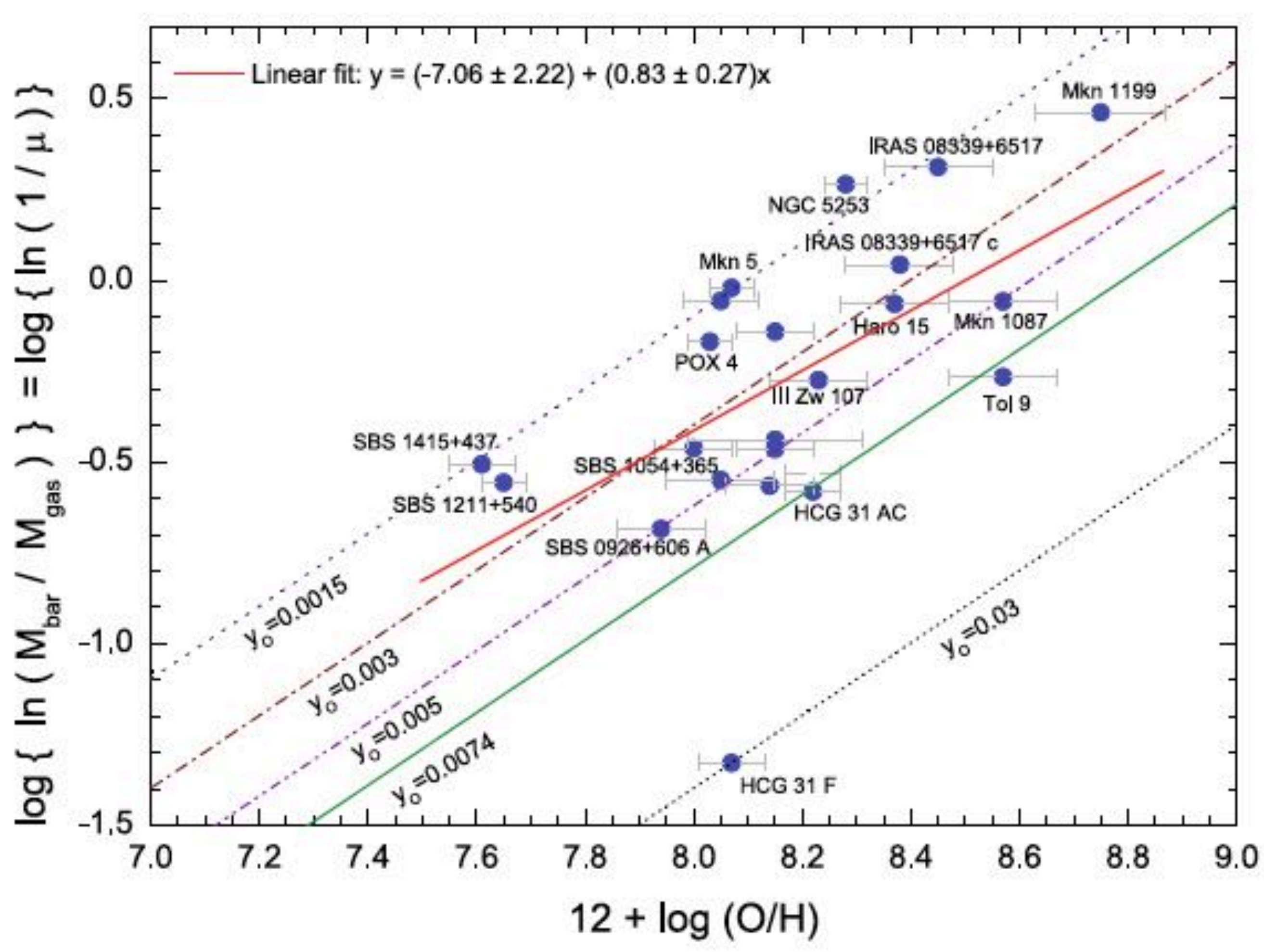

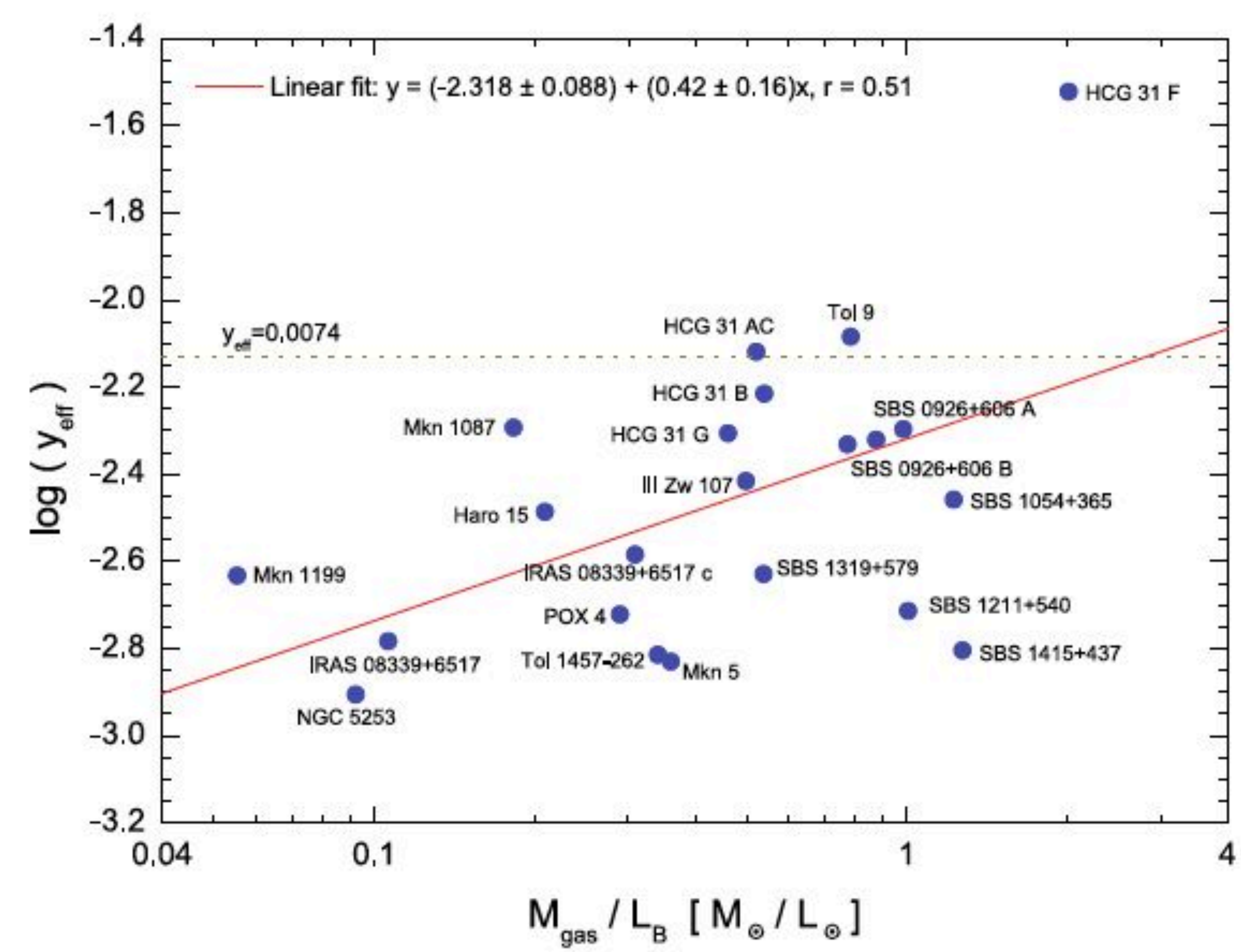

- **E.g., Observational data compared with predictions given by a closed-box model:**

$y_O = 0.0074$: theoretical yield of O expected for stars with rotation following Meynet & Maeder (2002) models

The data are not well reproduced by such simple model → **inflows + outflows of gas**

Deriving oxygen abundances using strong-line methods

Use the bright emission lines in the integrated spectrum of a galaxy to derive O/H

- See López-Sánchez (2006), Kewley & Ellison (2008), López-Sánchez & Esteban (2010b)

1. Calibrations of the **bright emission lines** using objects for which the Te is known
   - Edmunds & Pagel (1984), McCall et al. (1995), Zaritsky et al. (1994) : ***R23***
   - Pilyugin method: Pilyugin (2001a,b), Pilyugin & Thuan (2005), Pilyugin et al. (2010): ***R23, P***
   - Denicoló et al. (2002), Pagel & Pettini (2004): ***N2, O3N2***
   - Vílchez & Esteban (1996), Pérez-Montero & Díaz (2005): ***S23***
2. Use calibrations based on **photoionization models**
   - McGaugh (1991): ***R23, y***
   - Kewley & Dopita (2002) and Kobulnicky & Kewley (2004): ***R23, q* (derived from *y*)**

- High and low metallicity branches if using *R23* !
- Uncertainties of **~ 0.10 dex or higher**
- Please be **CAREFUL**: these are "recipes" which are only valid for the kind of SF galaxies used to get the calibration (Stansiska 2010) !
  - Galaxies with different parameters (starburst / quiescent, ionization parameter, interactions...) may have different calibrations! (López-Sánchez & Esteban 2010b)

$$R_3 = \frac{I([\mathrm{O\,III}])\lambda 4959 + I([\mathrm{O\,III}])\lambda 5007}{\mathrm{H}\beta},$$

$$R_2 = \frac{I([\mathrm{O\,II}])\lambda 3727}{\mathrm{H}\beta},$$

$$R_{23} = R_3 + R_2,$$

$$P = \frac{R_3}{R_{23}},$$

$$y = \log\frac{R_3}{R_2} = \log\frac{1}{P^{-1}-1}.$$

$$N_2 \equiv \log\frac{I([\mathrm{N\,II}])\lambda 6583}{\mathrm{H}\alpha},$$

$$\mathrm{O_3N_2} \equiv \log\frac{[\mathrm{O\,III}]\,\lambda 5007/\mathrm{H}\beta}{[\mathrm{N\,II}]\,\lambda 6583/\mathrm{H}\alpha}.$$

Strong-line calibrations using *R23*

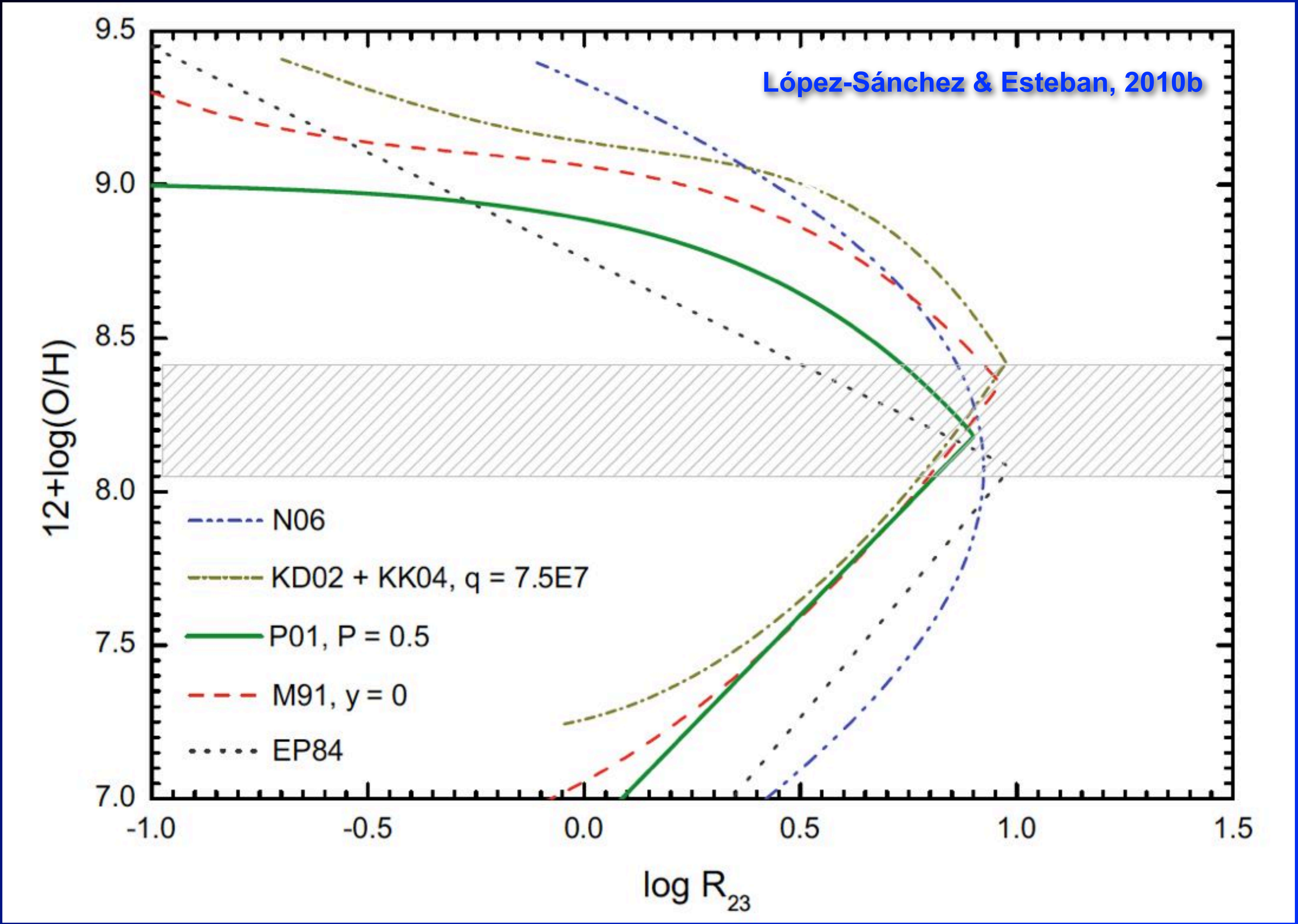

Comparing Te-based O/H with those derived using strong-line methods

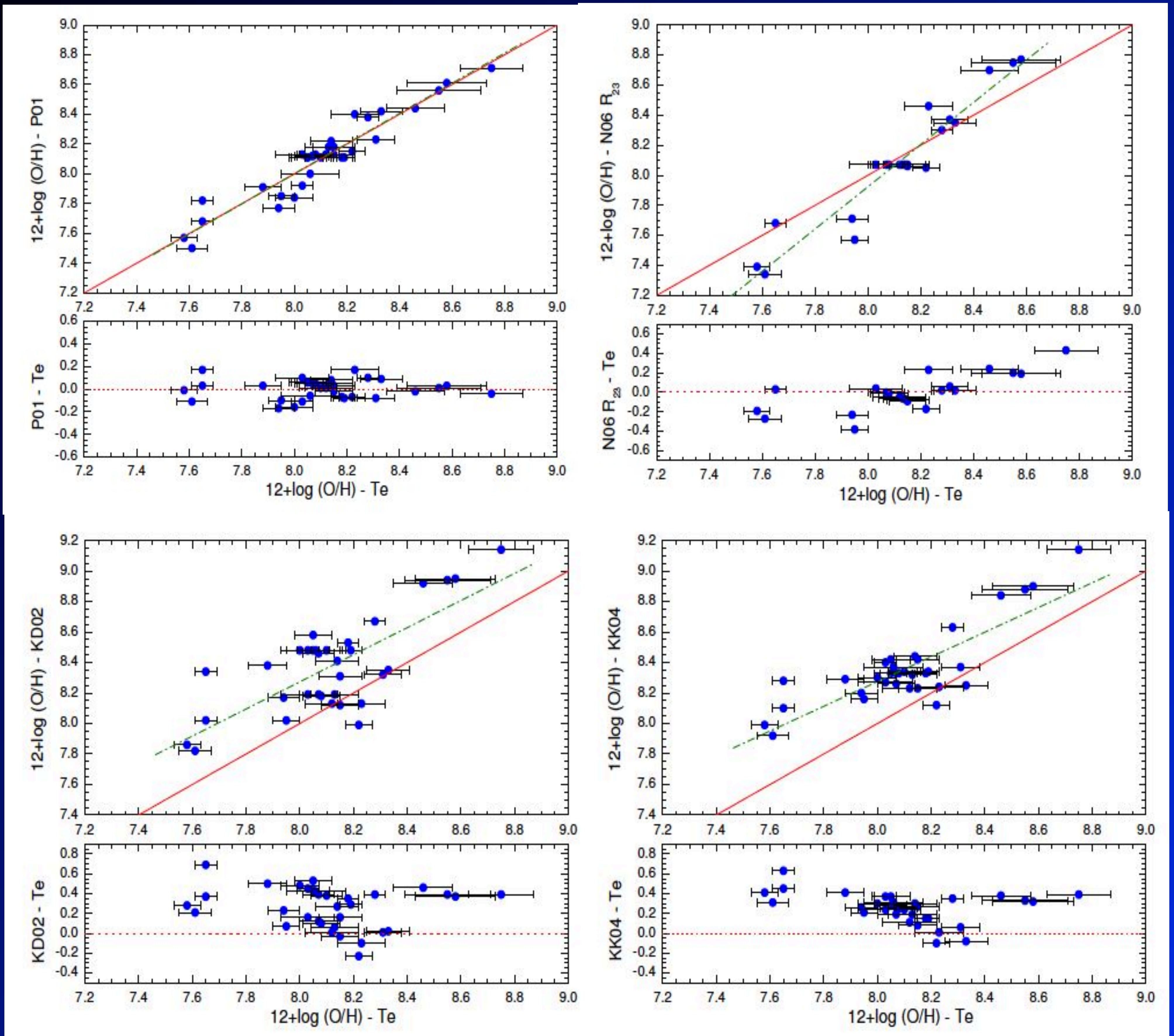

López-Sánchez 2006 PhD
López-Sánchez & Esteban, 2010b

- Pilyugin (2001) and Pilyugin & Thuan (2005) give the best results

- Calibrations based on photoionization models (e.g., Kewley & Dopita 2002; Kobulnicky & Kewley 2004) overestimate O/H in 0.2-0.4 dex !!

- Please, do NOT use empirical calibrations which consider hundreds of thousands galaxies with very different properties!!! (Nagao et al 2006)

see also:
Yin et al. (2007)
Kewley & Ellison (2008)
Stasinska (2010)
Moustakas et al. (2010)
Rosales-Ortega (2011)

O/H - M_{star} using different strong-line calibrators

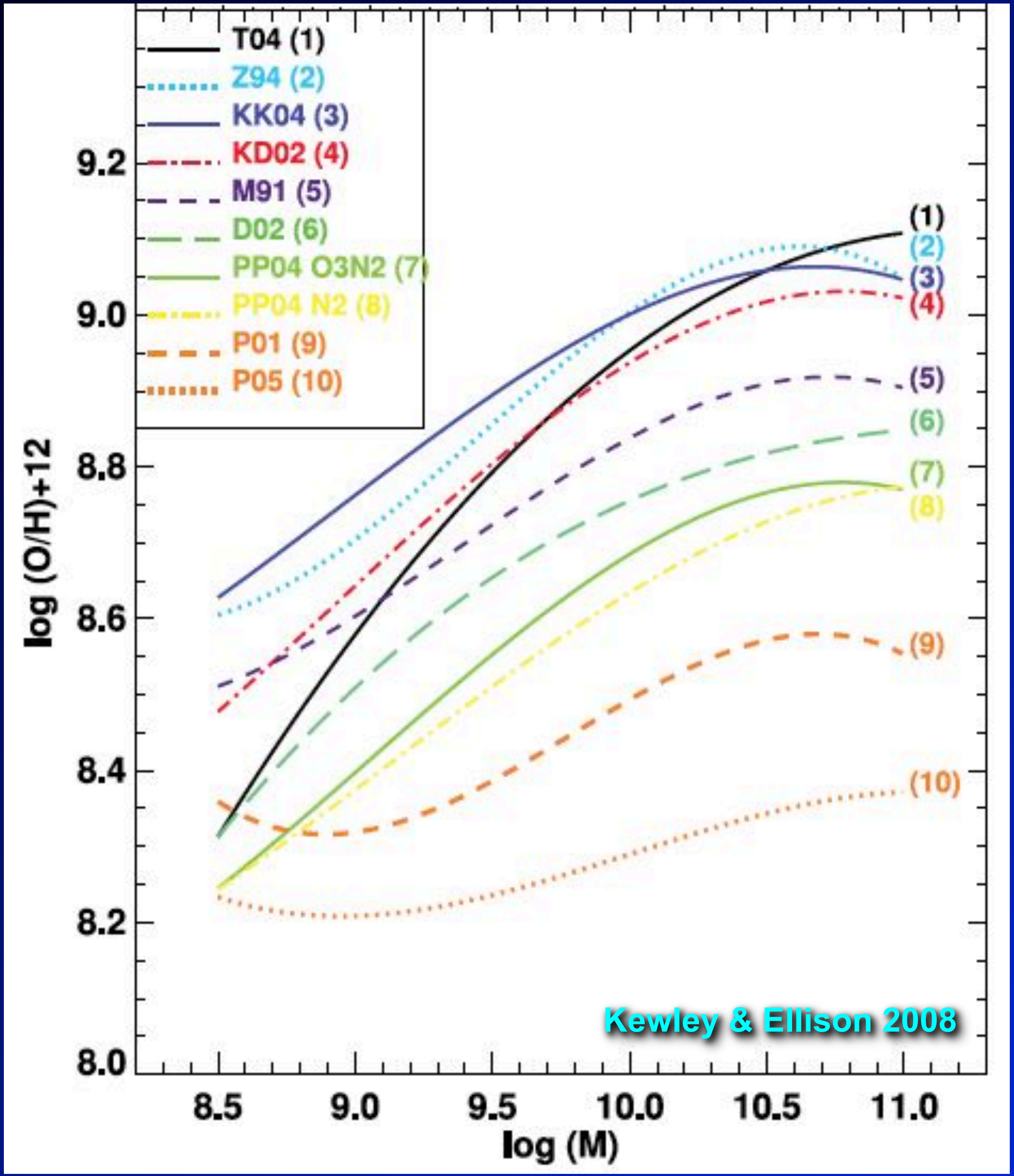

- Kewley & Ellison 2008
  - Used SDSS data of 27,730 star-forming galaxies
  - Only HIGH metallicity
  - HUGE differences depending on the calibration used!
  - Large galaxy surveys (SDSS, GAMA) are using T04-based and KD02-based O/H, which are based on photoionization models

O/H - M_{star} using different strong-line calibrators

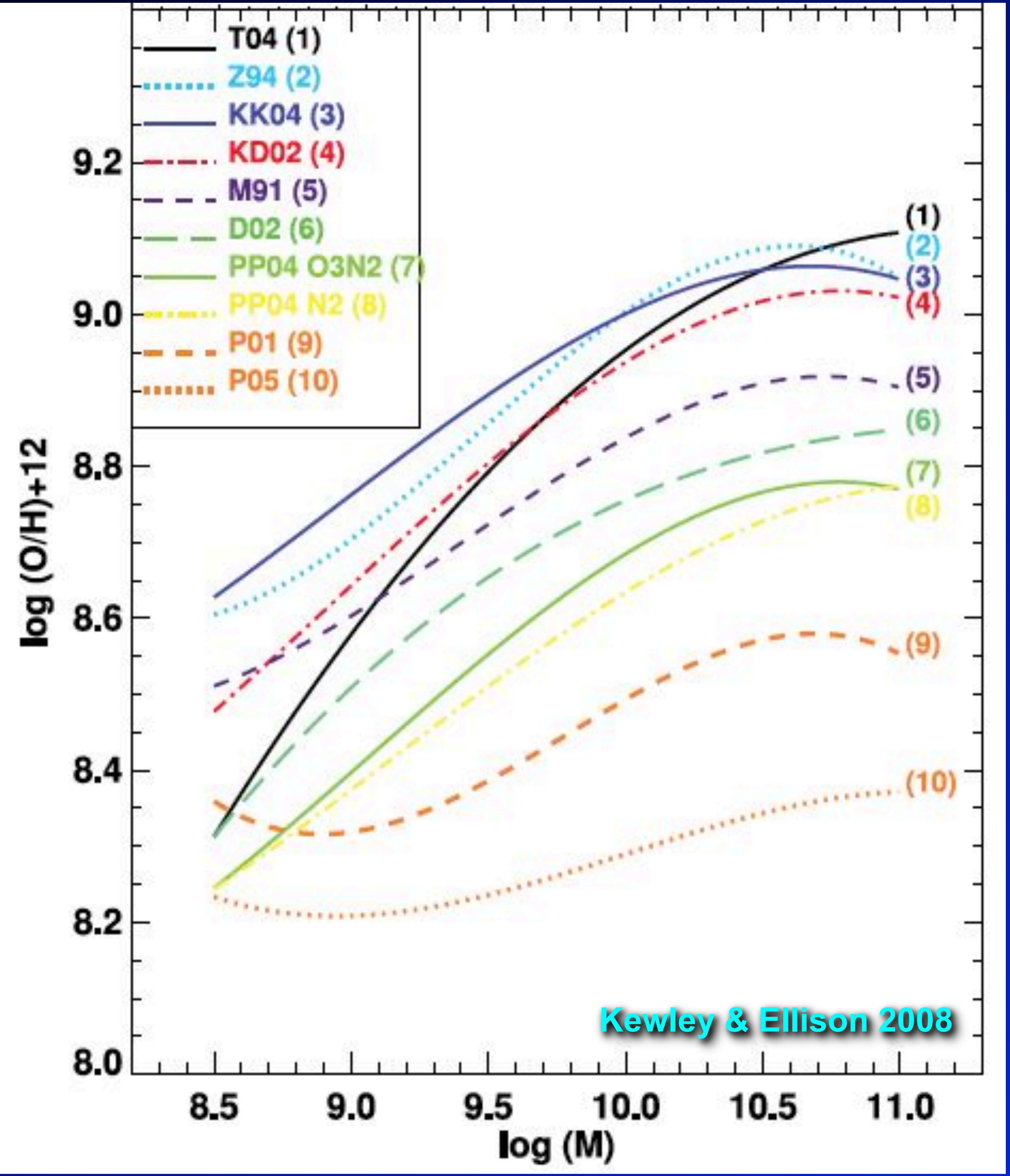

- **Kewley & Ellison 2008**
  - **Used SDSS data of 27,730** star-forming galaxies
  - Only HIGH metallicity
  - **HUGE differences** depending on the calibration used!
  - **Large galaxy surveys (SDSS, GAMA) are using T04-based and KD02-based O/H, which are based on photoionization models**

- **Kudritzki+ (2012):**

  Stellar O abundances of nearby galaxies (LG+beyond) **agree with results given by PP04 calibrations** (N2, O3N2)

– *Cif. from* ***Norbert Przybilla*** *talk*

- See also: **Urbaneja et al (2005, 2008), Bresolin et al. (2009, 2011)**

Metallicity gradients in M 33 using stars and HII regions

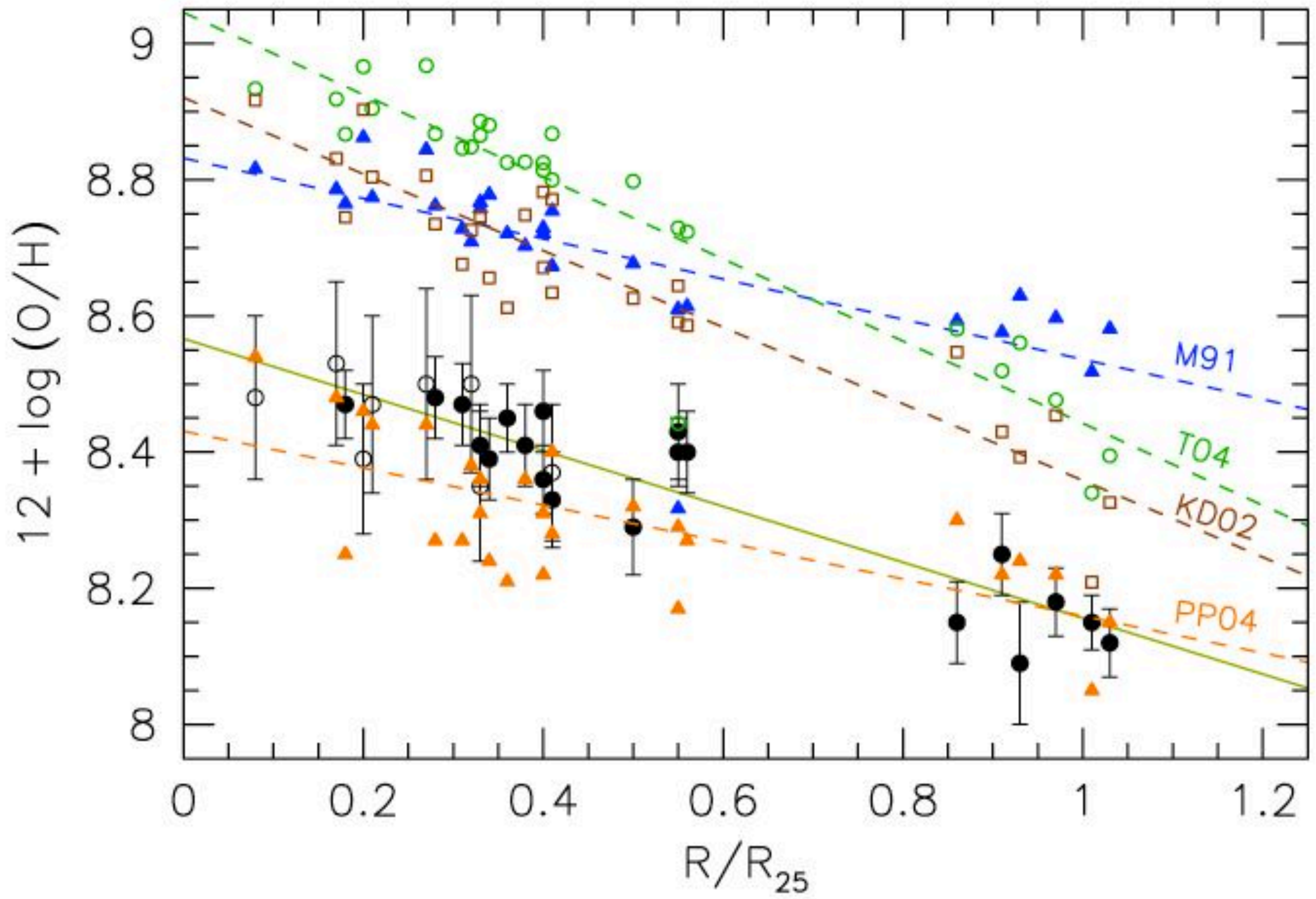

Figure 12. Galactocentric distribution of the abundance values obtained from different strong-line methods and calibrations: R_{23} (McGaugh 1991: M91, blue triangles; Tremonti et al. 2004: T04, green circles), [N II]/[O II] (Kewley & Dopita 2002: KD02, open squares), and N2 (Pettini & Pagel 2004: PP04, orange triangles). Linear least-squares fits are shown by the dashed lines, and labeled with the appropriate reference. The direct abundances determined from our work are shown by the full and open circle symbols, and the corresponding linear fit is shown by the continuous line (same as in Figure 10).

- **Bresolin, Gieren, Kudritzki, Pietrzynski, Urbaneja, Carraro 2009, ApJ 700, 309**
- Oxygen abundances derived using calibrations based on **photoionization models** are **~0.3 dex higher** than those derived using the Te method
- In this case, **stellar abundances** agree very well with **gas-phase abundances** derived from the **Te method**!

Metallicity gradient in NGC 628 using PINGS & CALIFA data

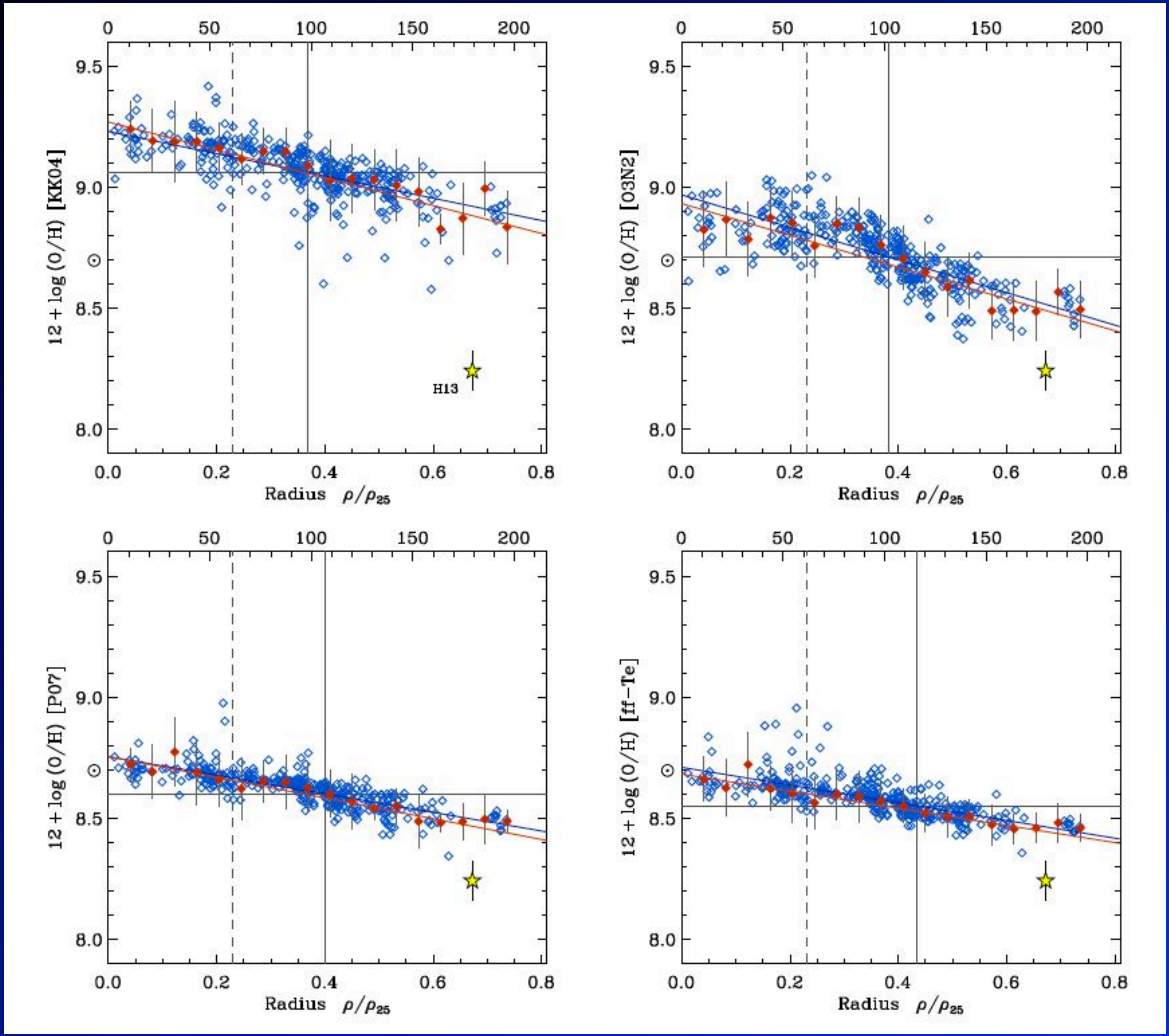

Rosales-Ortega et al. 2011
Sánchez et al. 2012 (sub,)

Metallicity gradient in NGC 628 using PINGS & CALIFA data

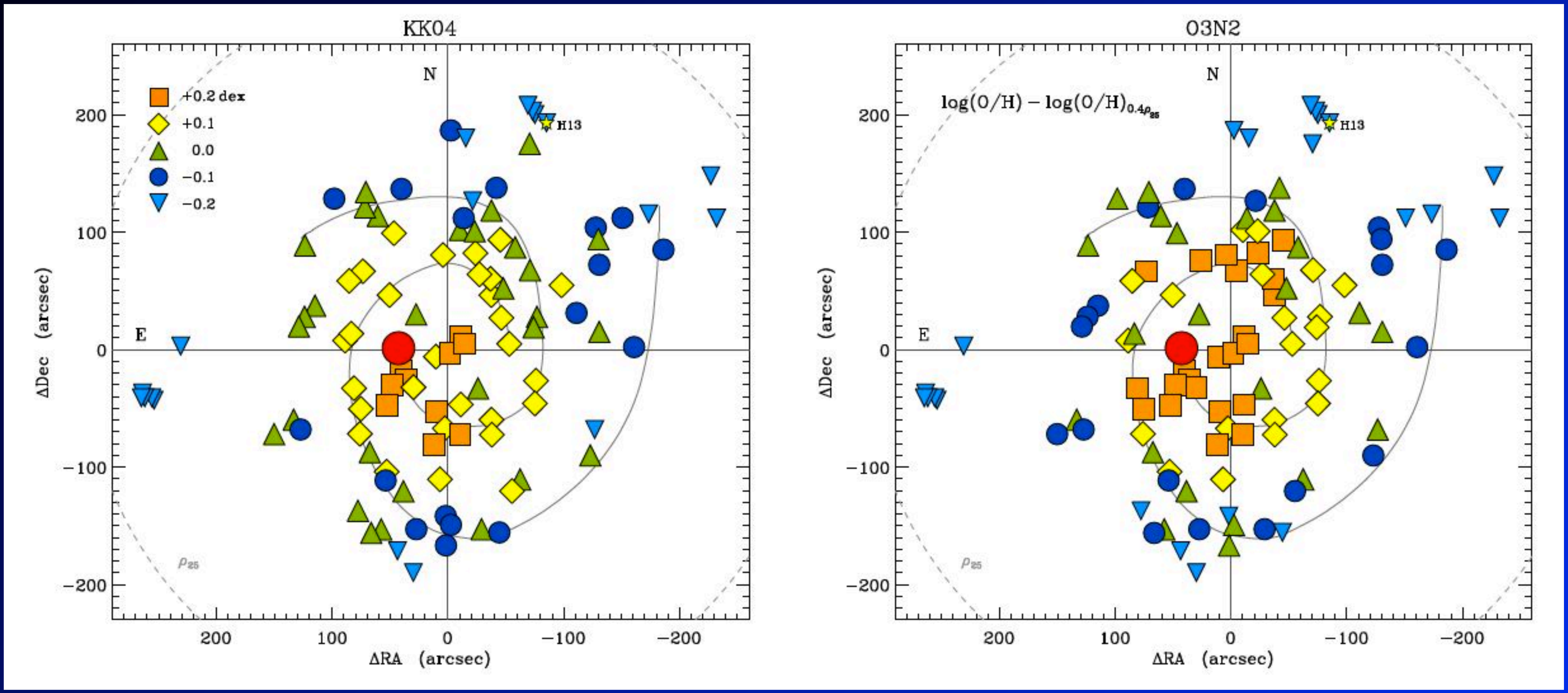

There is something else than a gradient !!

2D variations

See Fabian Rosales-Ortega talk.

Rosales-Ortega et al. 2011

Oxygen abundance maps using empirical calibrations

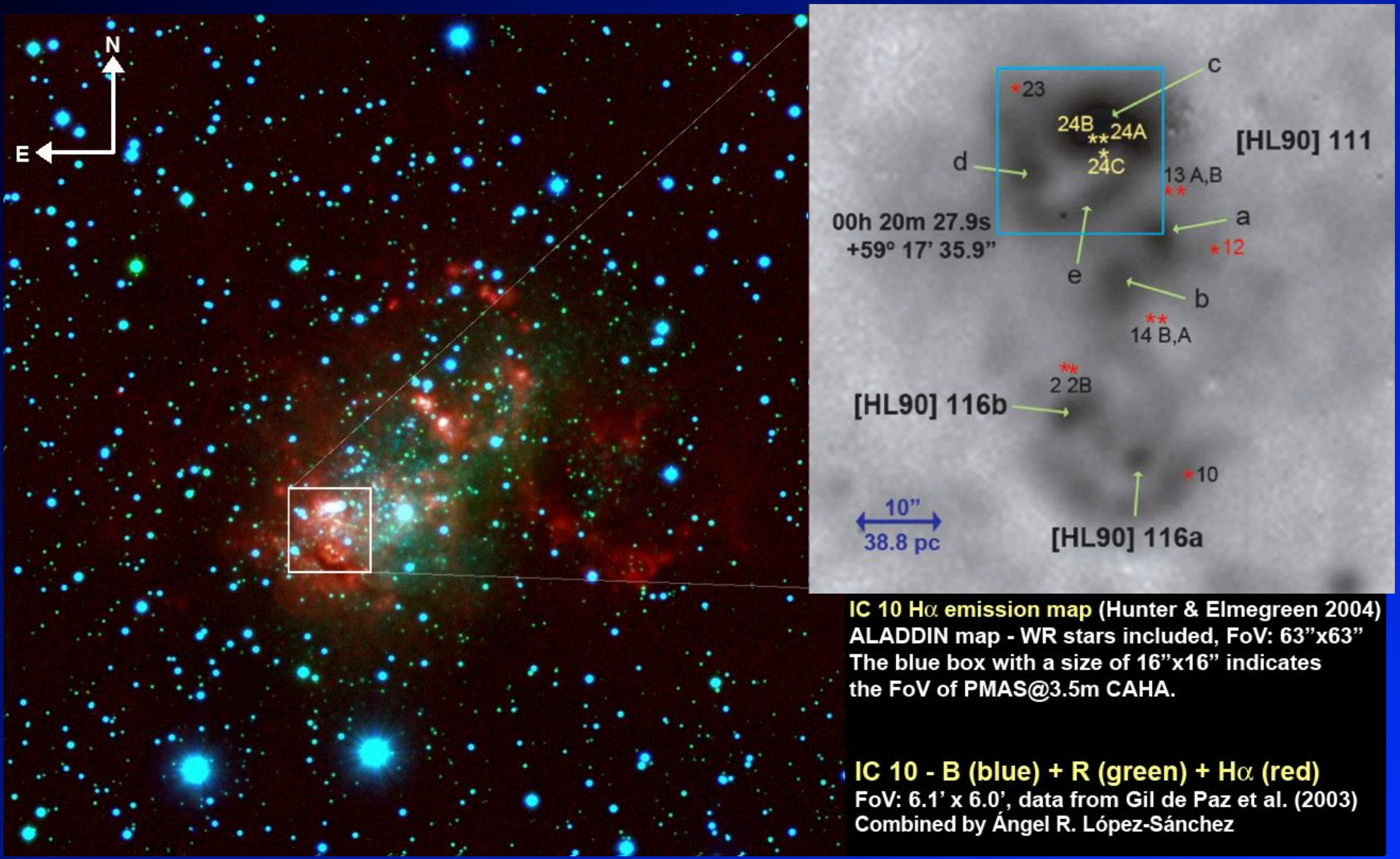

IC 10 Hα emission map (Hunter & Elmegreen 2004)
ALADDIN map - WR stars included, FoV: 63"x63"
The blue box with a size of 16"x16" indicates the FoV of PMAS@3.5m CAHA.

IC 10 - B (blue) + R (green) + Hα (red)
FoV: 6.1' x 6.0', data from Gil de Paz et al. (2003)
Combined by Ángel R. López-Sánchez

López-Sánchez et al. 2011, MNRAS, 411, 2076

Oxygen abundance maps using empirical calibrations

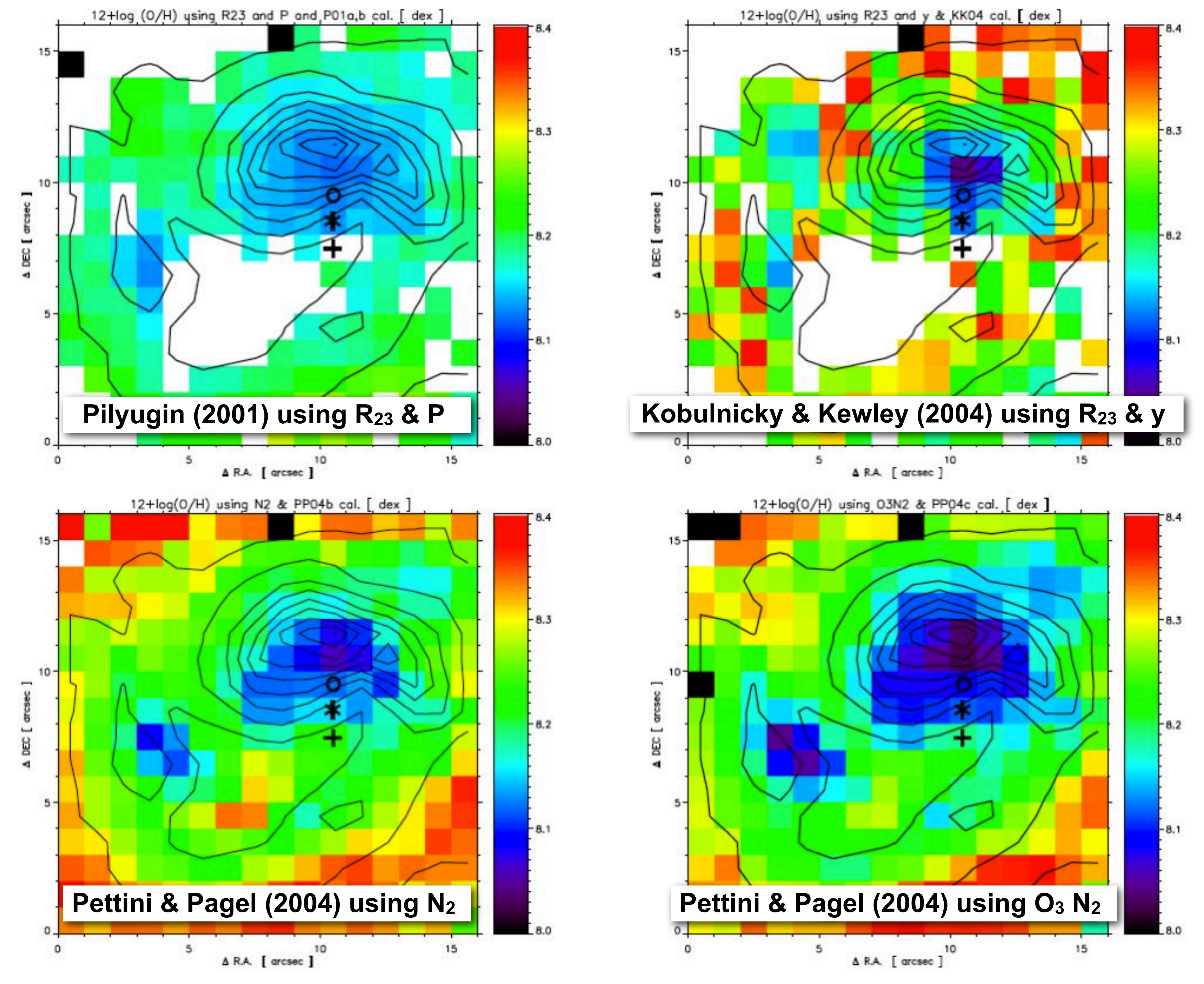

- The **ionization structure** plays an important role !
  - Very evident when using N2 and O_3N_2
- Results from **integrated spectra** are closer to those derived from the Te method.
- Analysis of star-forming galaxies using 2D spectroscopy needs **observations deep enough to detect the faint auroral lines** (James et al. 2009, 2010, Pérez-Montero+2011).
- Oxygen abundance maps obtained using empirical calibrations **may show features that are not related with the actual metallicity** distribution of a star-forming galaxy but with the ionization structure within its giant H II regions.
- See L-S et al. 2011

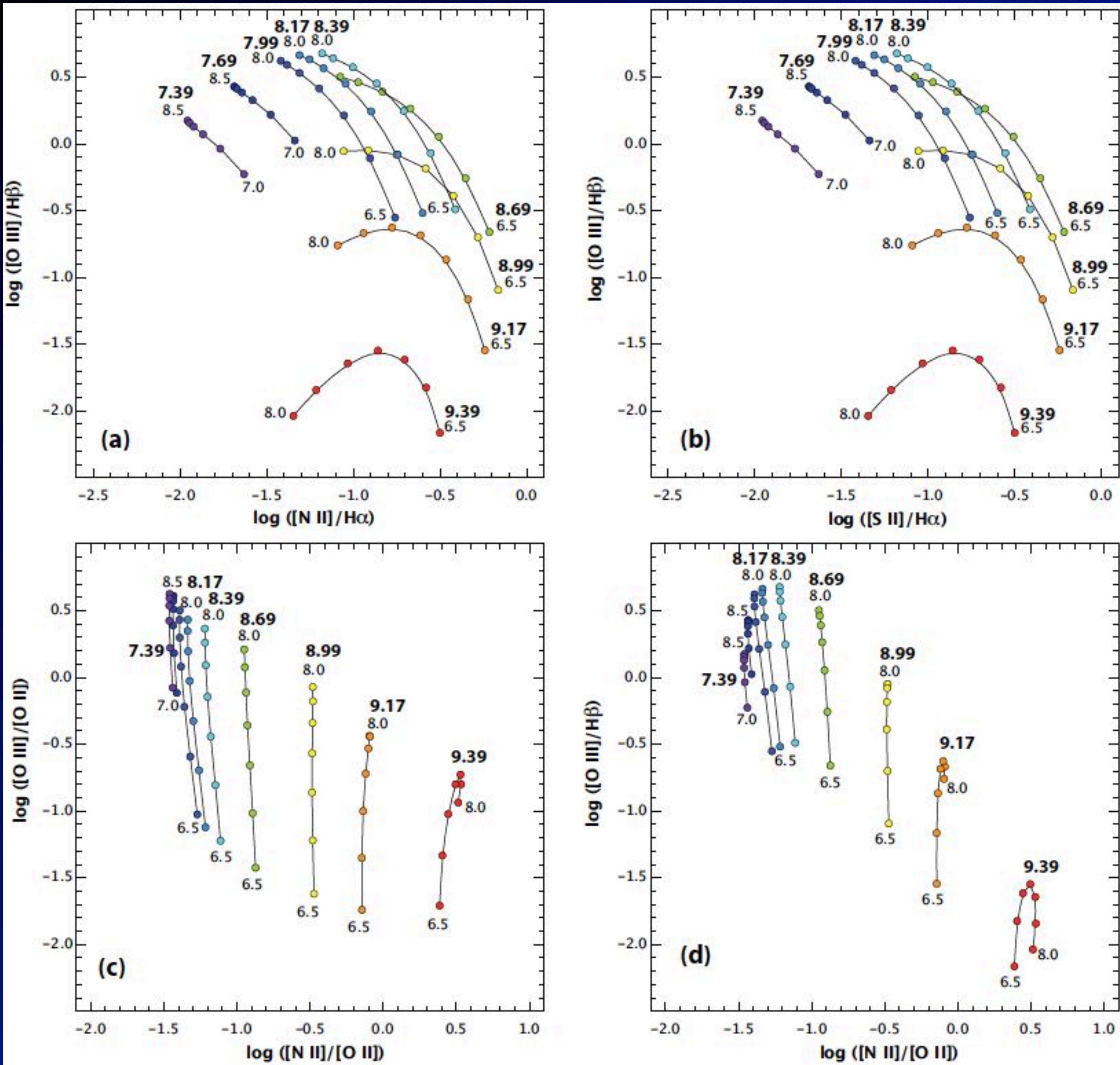

Doble-Blind test models

López-Sánchez, Dopita, Kewley et al. 2012, MNRAS, in press

- Theoretical model HII region grid given from Dopita to L-S for analysis:
- **O/H & q BOTH UNKNOWN !!**
  - Use observation techniques to derive both !!
- Mappings III (Sutherland & Dopita 1993)
- Chemical abundances fitted to SDSS data (Kewley et al. 2006)
- Starburst 99 code (Leitherer + 1999)

Doble-Blind test models: Electron Temperatures

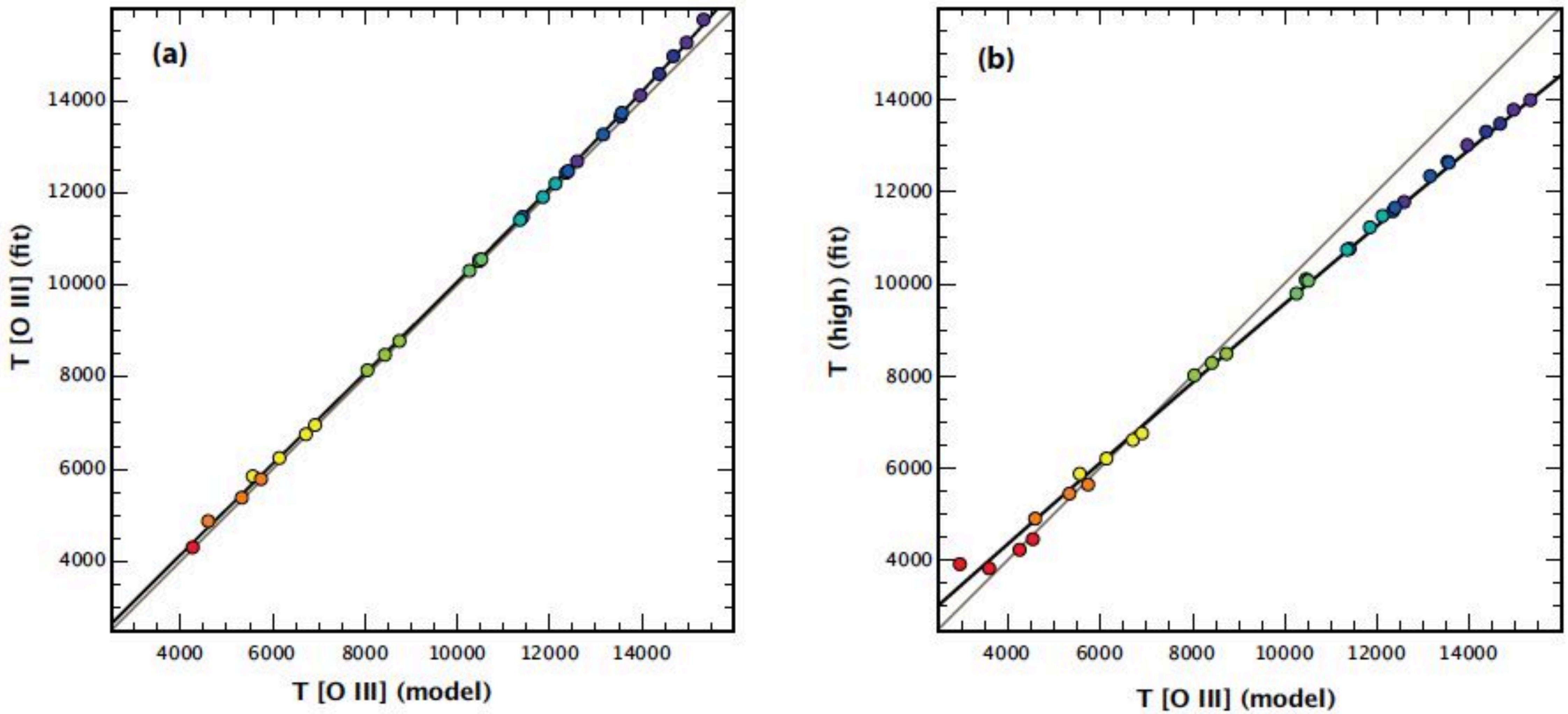

Figure 3. Comparison between the T_e[O III] given by the model (x-axis) and the temperature derived by analysis of the model spectra. The left hand panel directly compares the [O III] temperature from the model and the derived [O III] temperature, while the right -hand panel compares the fitted temperature drawn from the mean of the [O III] , [S III] and [Ar III] temperatures with the [O III] temperature from the model. The empirical fits we have derived are shown as a solid line for both panels. As in figure 2, the points are color coded according to the input abundance set.

López-Sánchez, Dopita, Kewley et al. 2012, MNRAS, in press

Doble-Blind test models: Chemical Abundances using T_{high} & T_{low}

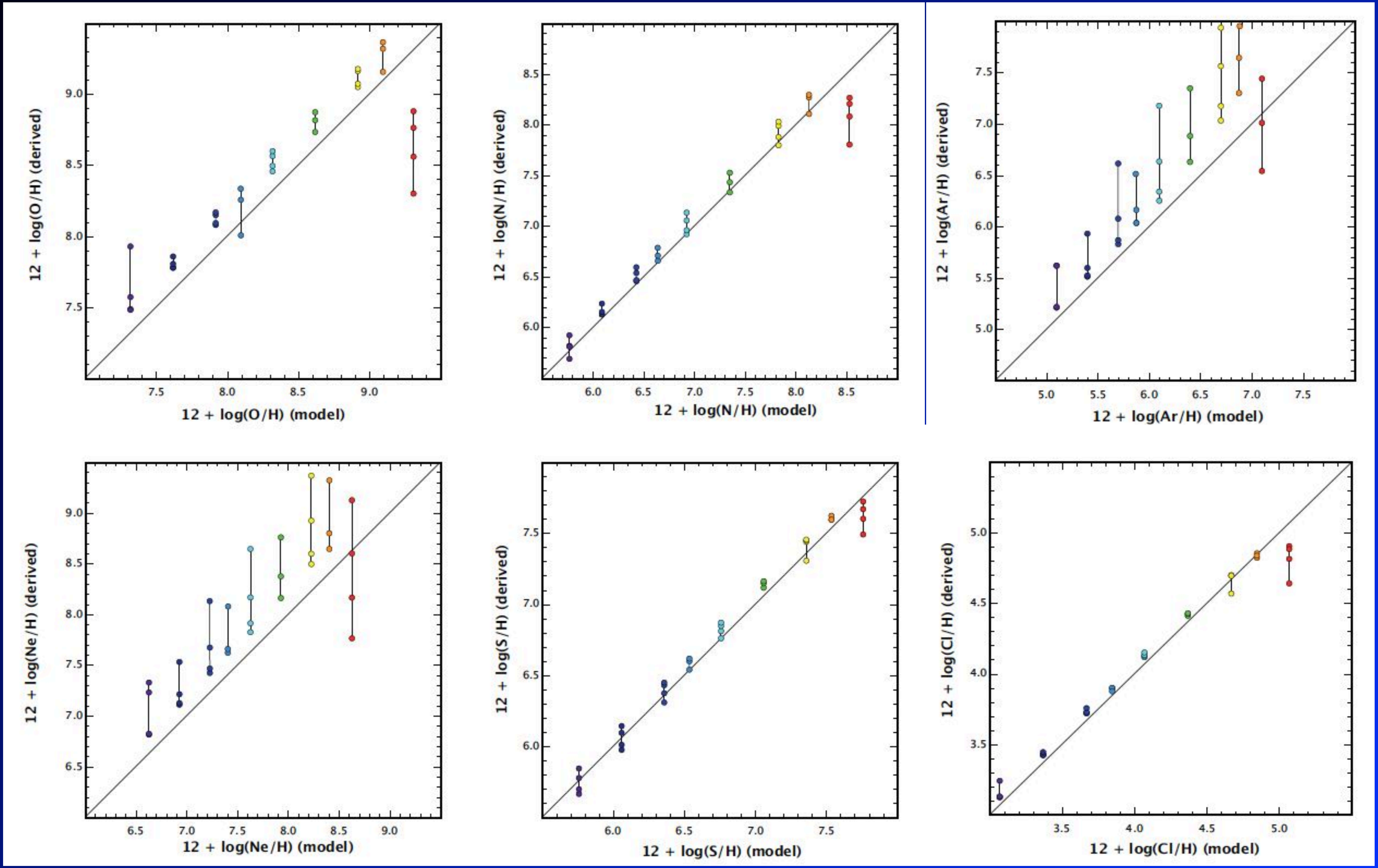

López-Sánchez, Dopita, Kewley et al. 2012, MNRAS, in press

Doble-Blind test models: Chemical Abundances using T[O III] & T[O II]

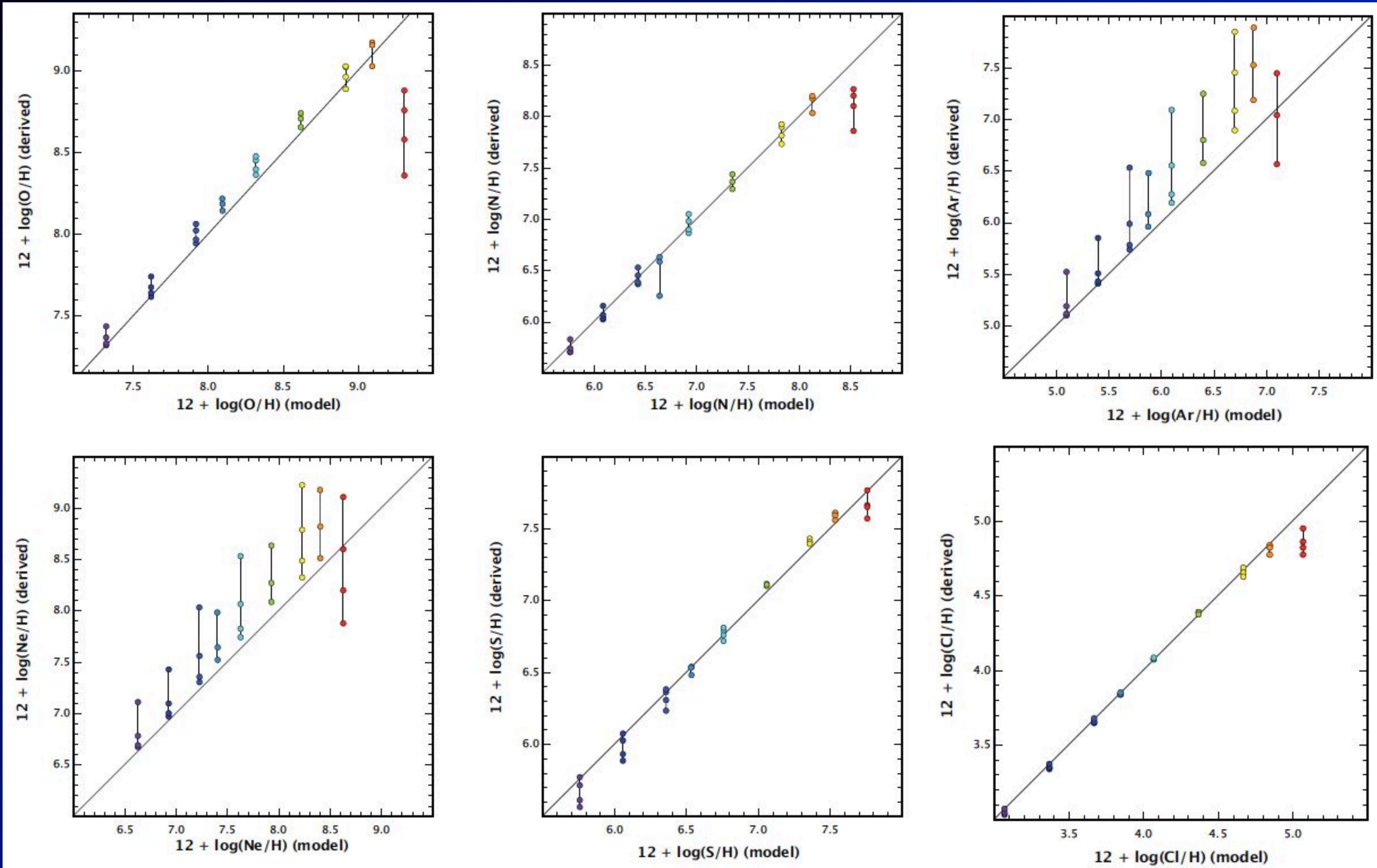

López-Sánchez, Dopita, Kewley et al. 2012, MNRAS, in press

Doble-Blind test models: Chemical Abundances using T[O III] & T[O II]

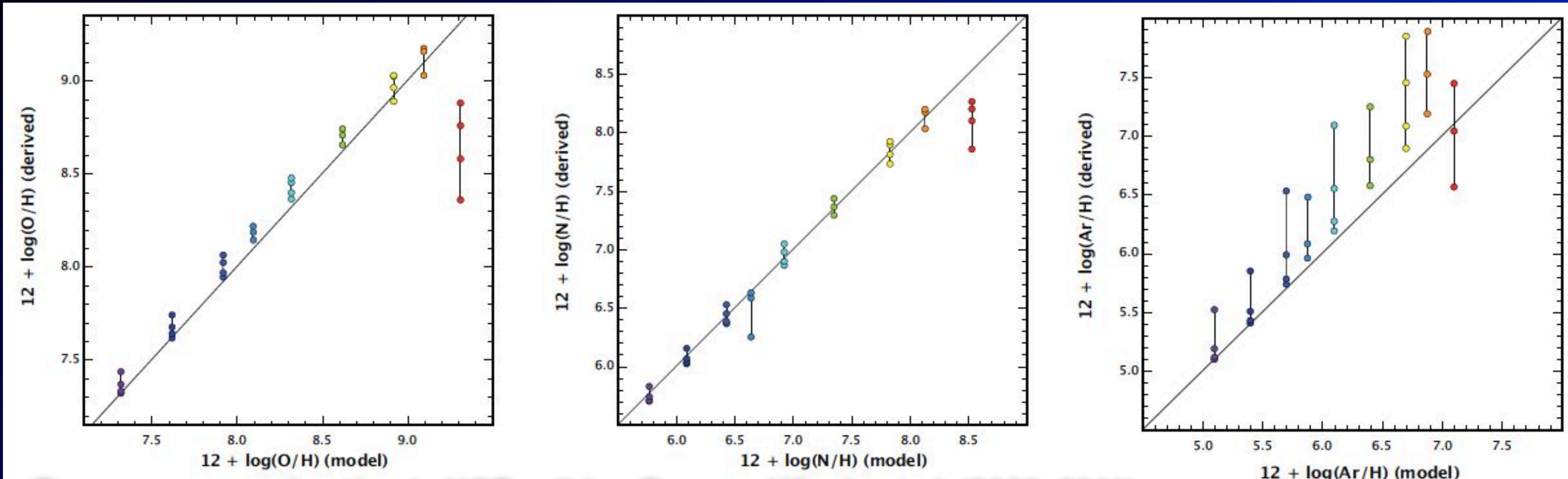

Two-zone approximation is NOT valid → E.g. see Hägele et al. (2008, 2011)

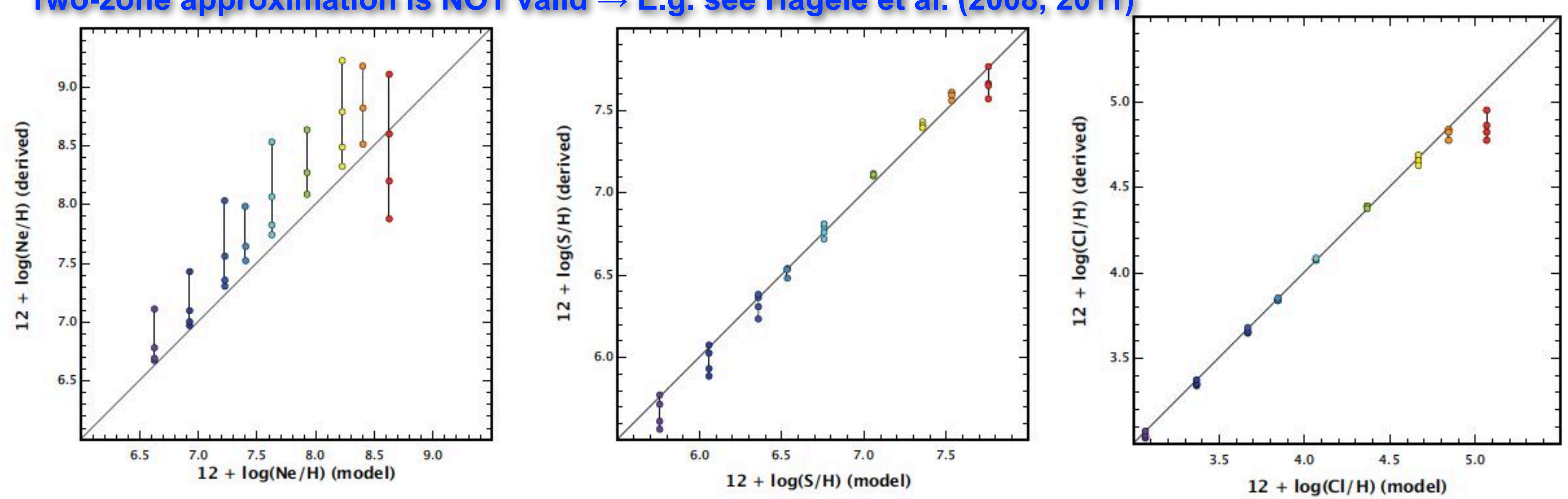

López-Sánchez, Dopita, Kewley et al. 2012, MNRAS, in press

Comparison with strong-line calibrations

$$N_2 \equiv \log \frac{I([\mathrm{N\,II}])\lambda 6583}{\mathrm{H}\alpha},$$

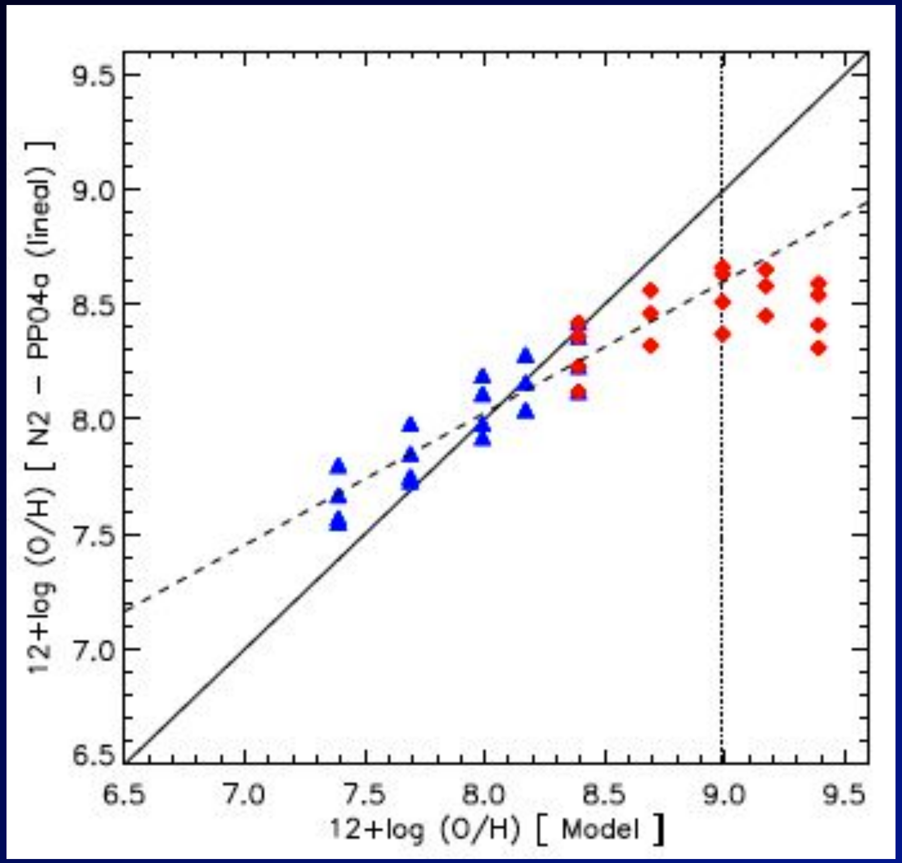

- Pagel & Pettini (2004)
- Dispersion **~ 0.25 dex**
- Not valid for **12+log(O/H) ≥ 8.7 - 9.0**
- **BE CAREFUL High Mstar!**
  - Yin et al. (2007) sugested ≥ 8.5
  - **Morales-Luis et al. 2011**: NOT valid for < 7.6 !!

Comparison with strong-line calibrations

$$N_2 \equiv \log \frac{I([\text{N II}])\lambda 6583}{\text{H}\alpha},$$

$$S_{23} = \frac{I([\text{S II}])\lambda\lambda 6717,31 + I([\text{S III}])\lambda\lambda 9076,9532}{\text{H}\beta},$$

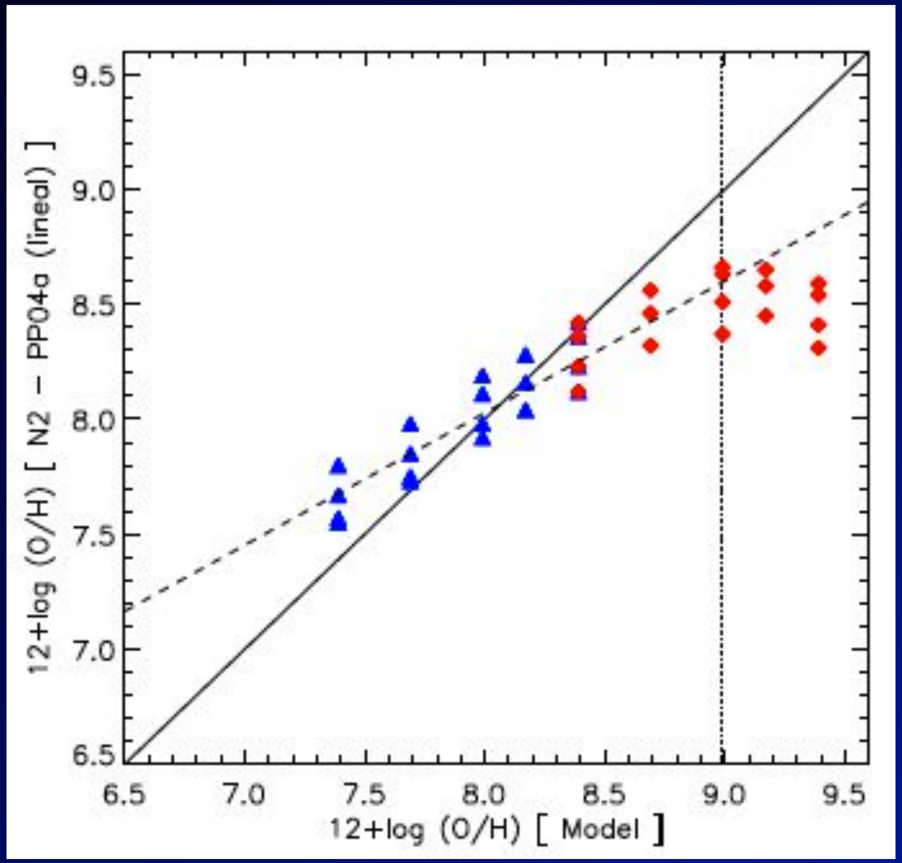

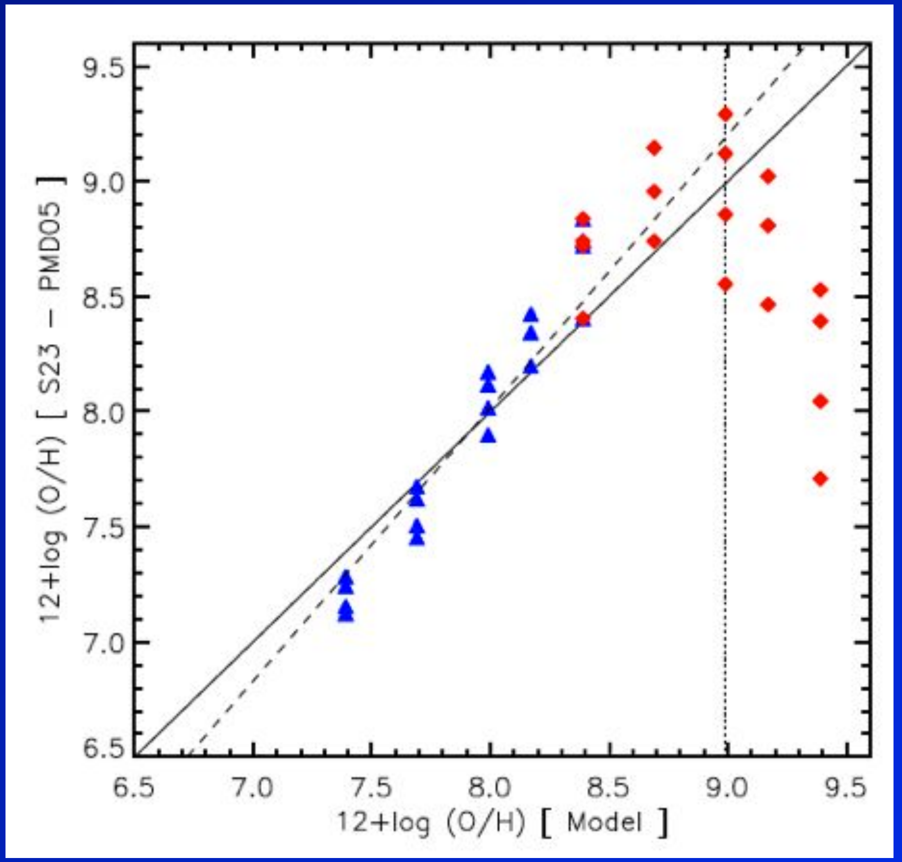

- Pagel & Pettini (2004)
- Dispersion **~ 0.25 dex**
- Not valid for
  12+log(O/H) ≥ 8.7 - 9.0
- **BE CAREFUL High Mstar!**
  - Yin et al. (2007) sugested ≥ 8.5
  - **Morales-Luis et al. 2011**:
    NOT valid for < 7.6 !!

- Pérez-Montero & Díaz (2005)
- Dispersion **~ 0.24 dex**
- Not valid for
  12+log(O/H) ≤ 9.0

Comparison with strong-line calibrations

$$N_2 \equiv \log \frac{I([\mathrm{N\,II}])\lambda 6583}{\mathrm{H}\alpha},$$

$$\mathrm{O_3N_2} \equiv \log \frac{[\mathrm{O\,III}]\ \lambda 5007/\mathrm{H}\beta}{[\mathrm{N\,II}]\ \lambda 6583/\mathrm{H}\alpha}.$$

$$S_{23} = \frac{I([\mathrm{S\,II}])\lambda\lambda 6717,31 + I([\mathrm{S\,III}])\lambda\lambda 9076,9532}{\mathrm{H}\beta},$$

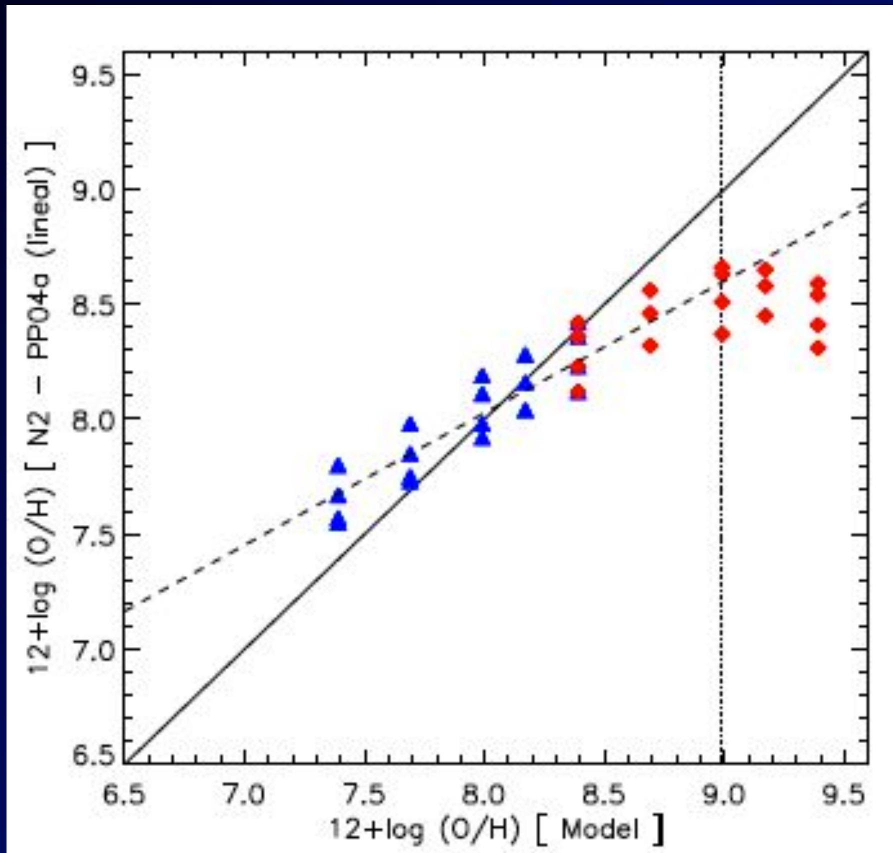

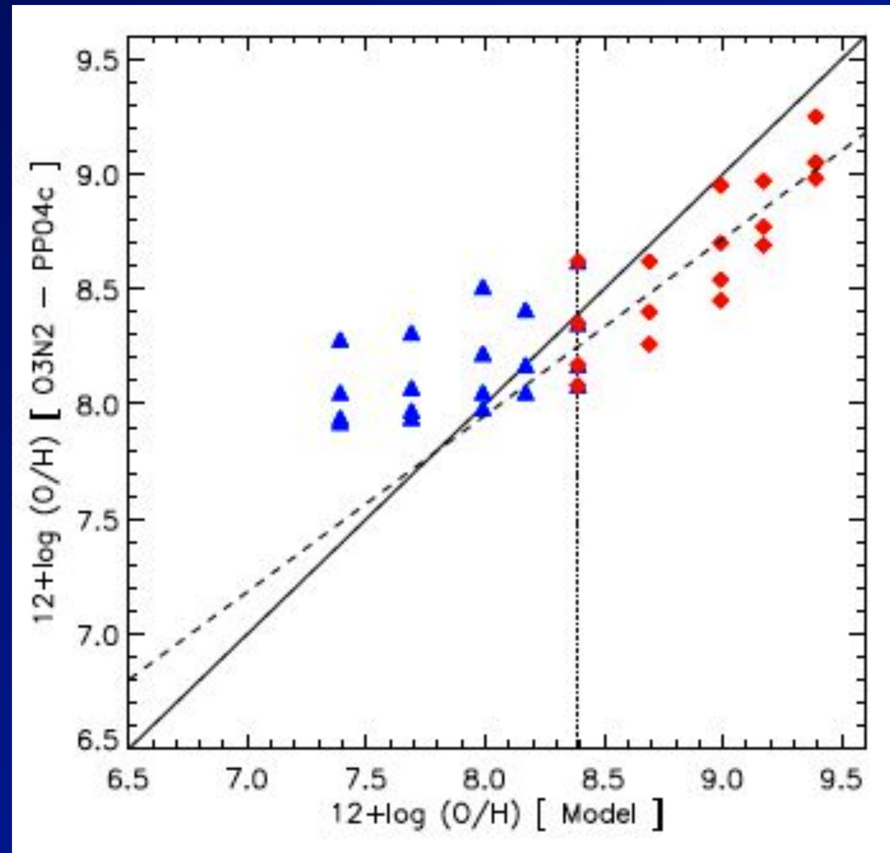

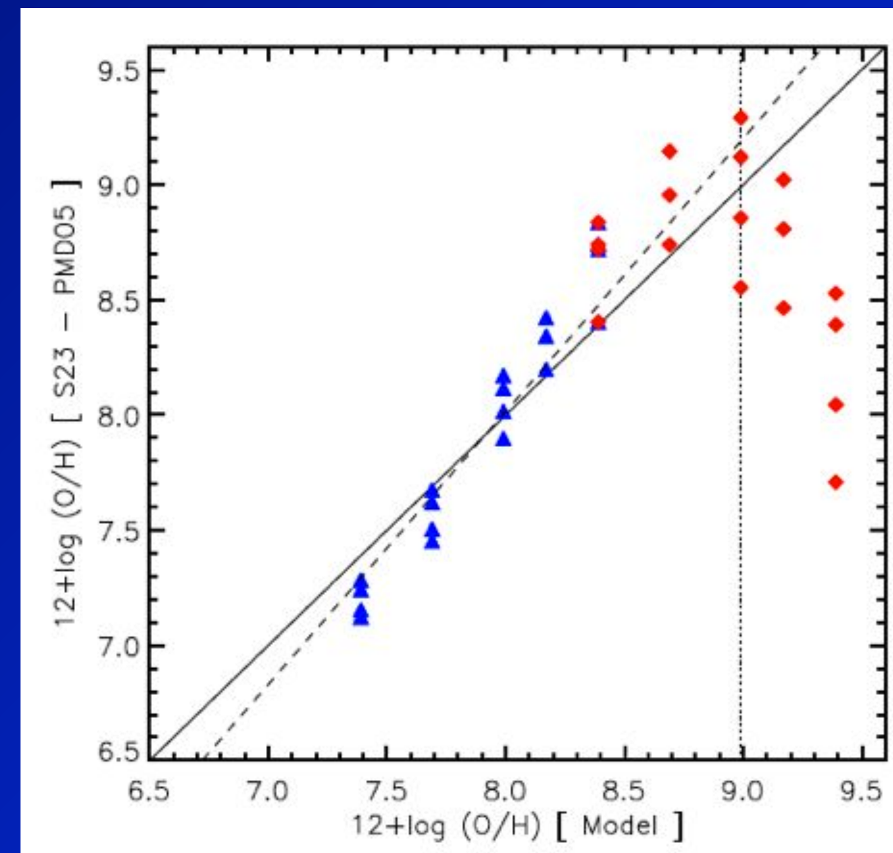

- Pagel & Pettini (2004)
- Dispersion ~ **0.25 dex**
- Not valid for **12+log(O/H) ≥ 8.7 - 9.0**
- **BE CAREFUL High Mstar!**
  - Yin et al. (2007) sugested ≥ 8.5
  - **Morales-Luis et al. 2011**: NOT valid for < 7.6 !!

- Pagel & Pettini (2004)
- Dispersion ~ **0.25 dex**
- **Seem to understimate O/H!**
- Not valid for **12+log(O/H) ≤ 8.3 - 8.5**
  - Pérez-Montero & Contini (2009) suggested ≤ 8.0

- Pérez-Montero & Díaz (2005)
- Dispersion ~ **0.24 dex**
- Not valid for **12+log(O/H) ≤ 9.0**

O/H derived from O3N2 in SN and GRB host galaxies

Sanders et al. 2012

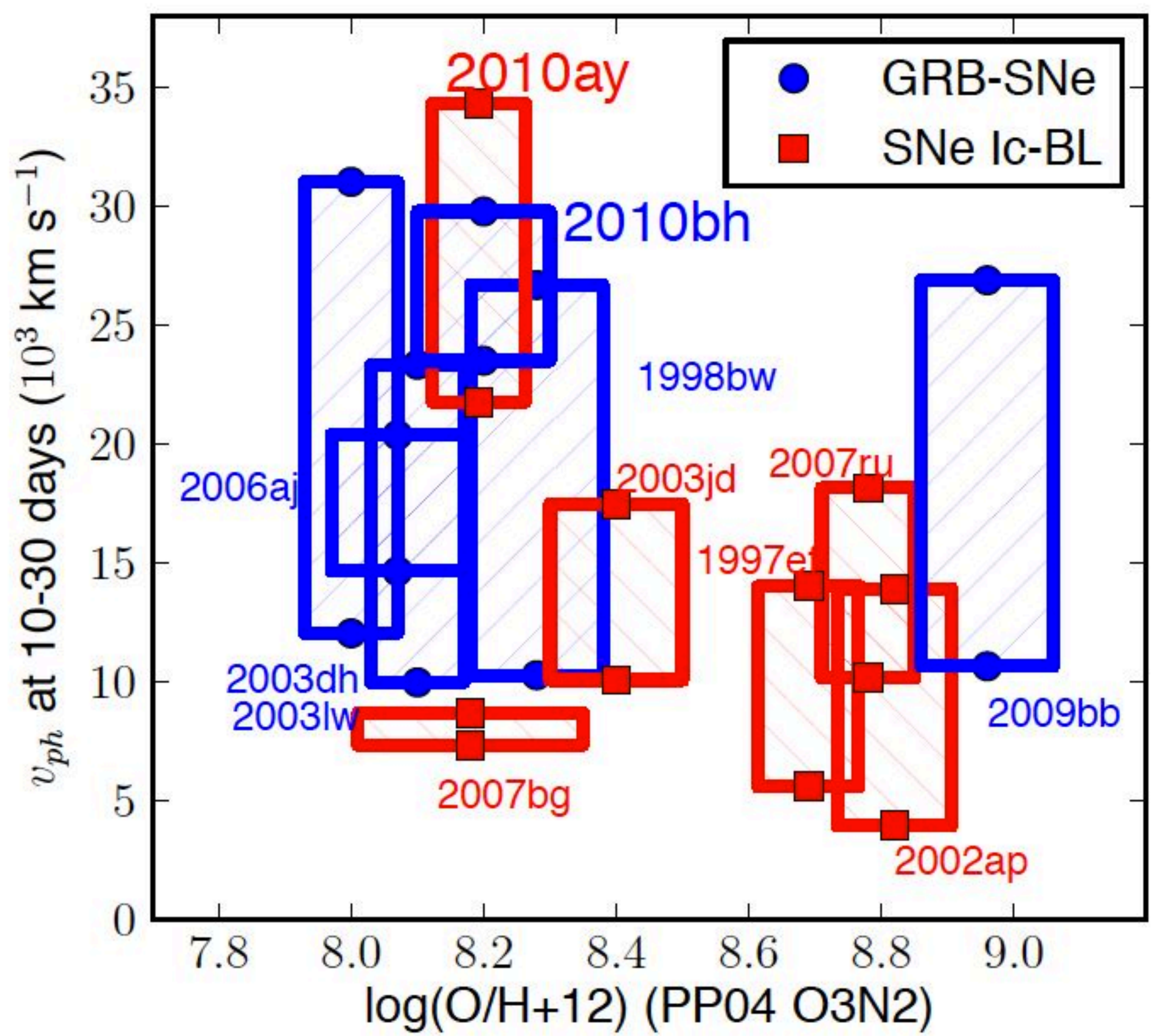

FIG. 10.— SN photspheric velocity, as traced by the Si II λ6355Å feature, versus host galaxy oxygen abundance for SN 2010ay and other Ic-BL (red) and SNe-GRB (blue) from the literature (as in Figure 5). The range of velocities hatched for each object comes from the velocity at 10 days and at 30 days after explosion, according to the power law fits presented in Figure 5. The oxygen abundance measurements using the PP04 O3N2 diagnostic are from Levesque et al. (2010a) (GRB-SNe), Sahu et al. (2009) (SN2007ru), Young et al. (2010) (SN 2007bg), and Modjaz et al. (2010a) (other SNe Ic-BL). The range of oxygen abundance hatched reflects the error bars quoted in the literature (when stated) plus the ~ 0.07 dex systematic error of the PP04 O3N2 diagnostic (Kewley & Ellison 2008).

O/H derived from O3N2 in SN and GRB host galaxies

Sanders et al. 2012

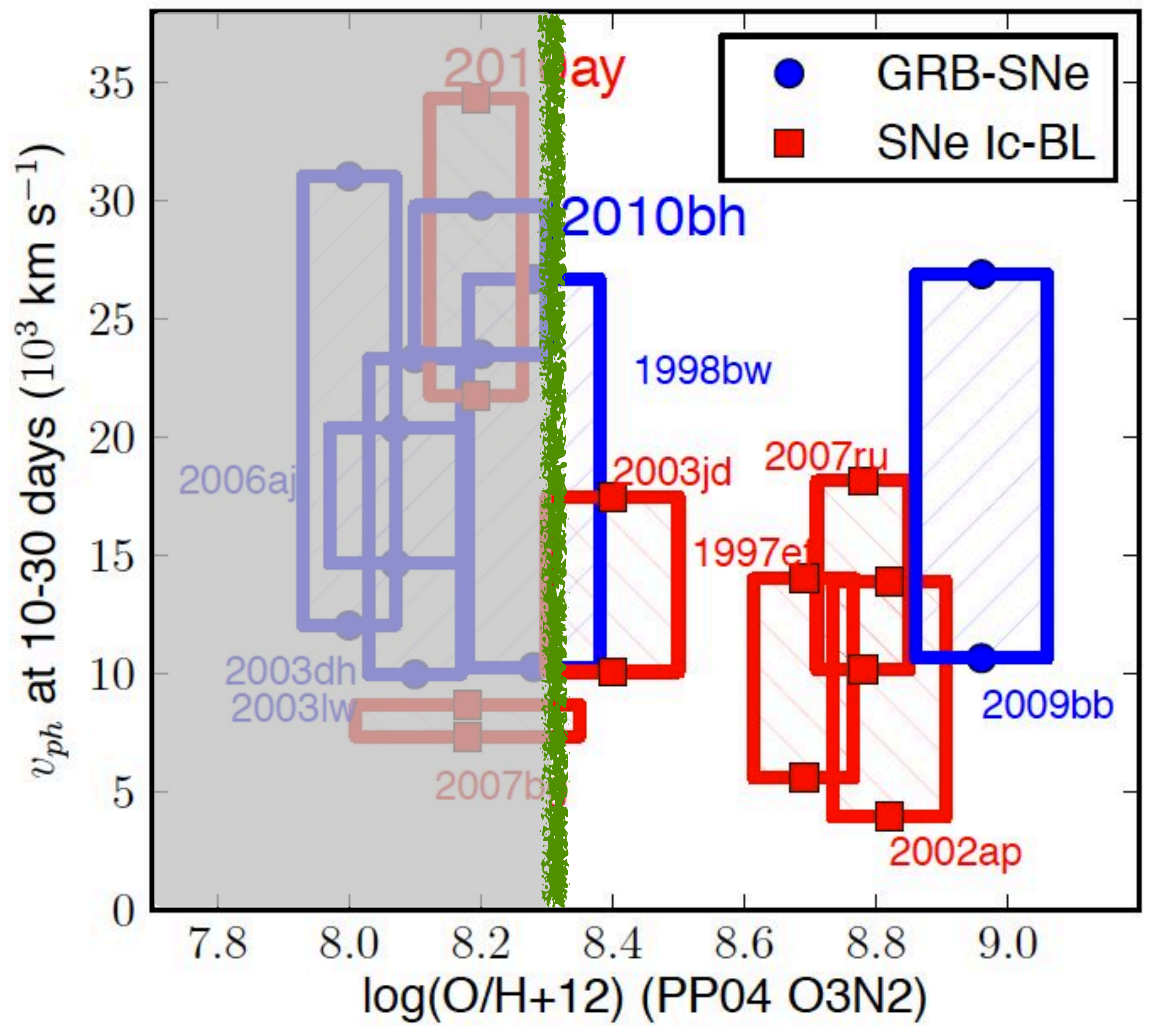

FIG. 10.— SN photspheric velocity, as traced by the Si II λ6355Å feature, versus host galaxy oxygen abundance for SN 2010ay and other Ic-BL (red) and SNe-GRB (blue) from the literature (as in Figure 5). The range of velocities hatched for each object comes from the velocity at 10 days and at 30 days after explosion, according to the power law fits presented in Figure 5. The oxygen abundance measurements using the PP04 O3N2 diagnostic are from Levesque et al. (2010a) (GRB-SNe), Sahu et al. (2009) (SN2007ru), Young et al. (2010) (SN 2007bg), and Modjaz et al. (2010a) (other SNe Ic-BL). The range of oxygen abundance hatched reflects the error bars quoted in the literature (when stated) plus the ∼ 0.07 dex systematic error of the PP04 O3N2 diagnostic (Kewley & Ellison 2008).

Comparison with strong-line calibrations

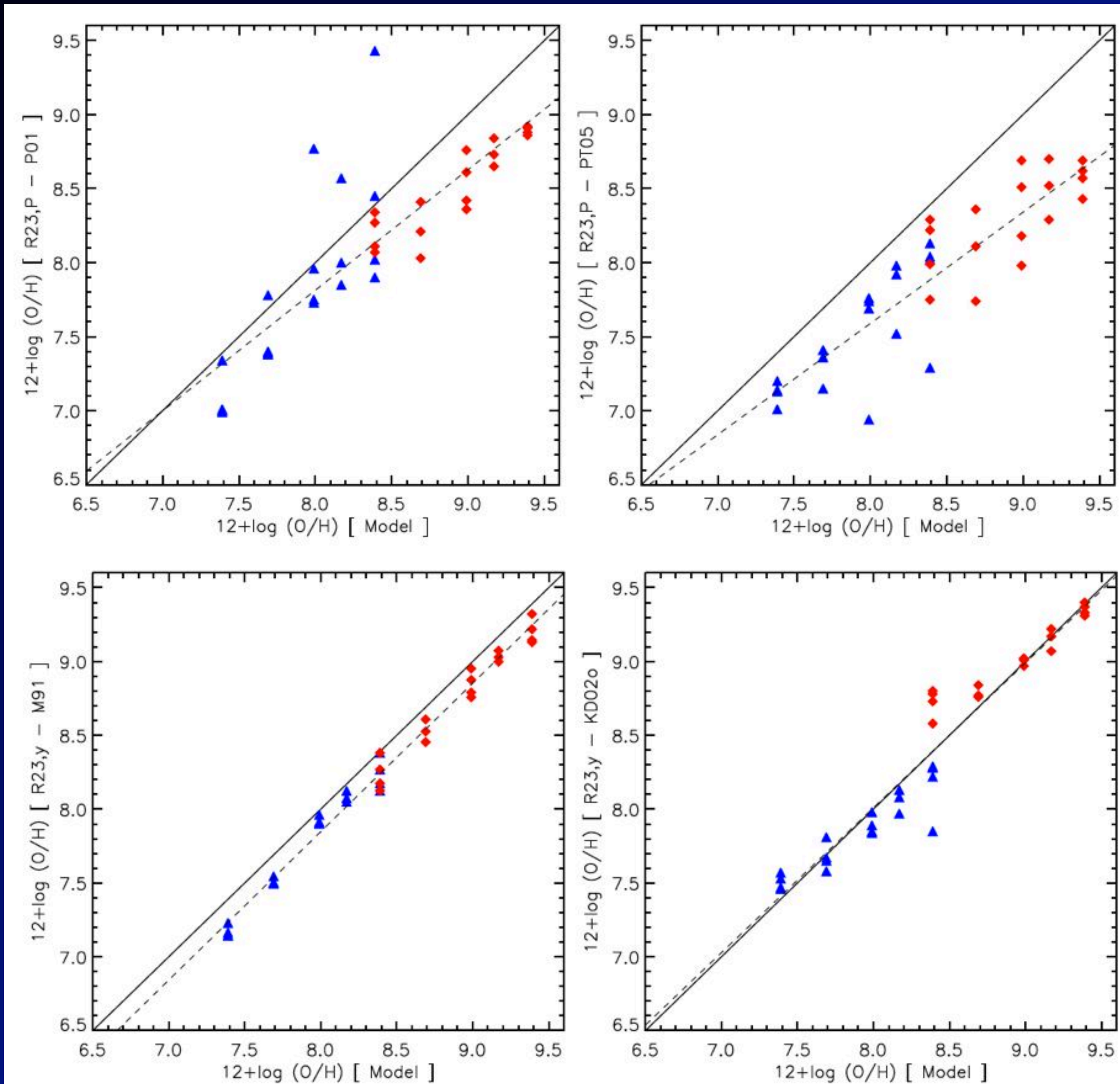

Calibrations based on photoionization models (KD02) work well but calibrations based on direct estimation of Te (P01, PT05) underestimate the oxygen abundances in 0.2-0.4 dex !!

But Te-derived O/H agree with the O/H consider by the models!!

López-Sánchez, Dopita, Kewley, Zahid, Nicholls & Scharwächter 2012 MNRAS, in press

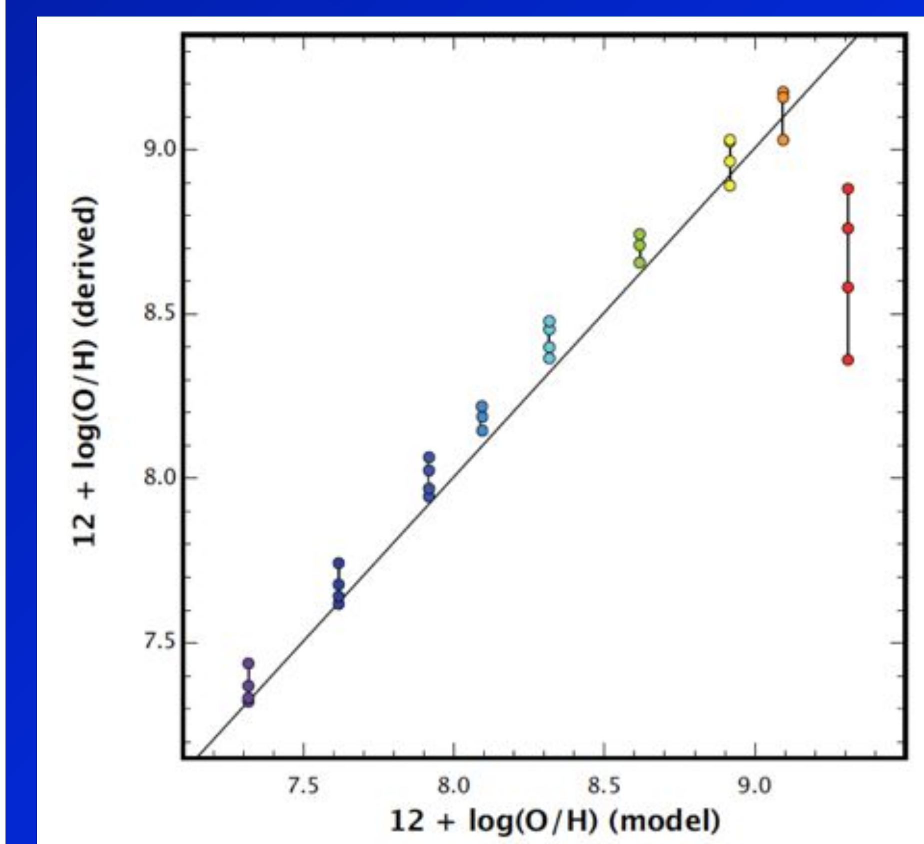

Deriving O/H from Te using photoionization model spectra

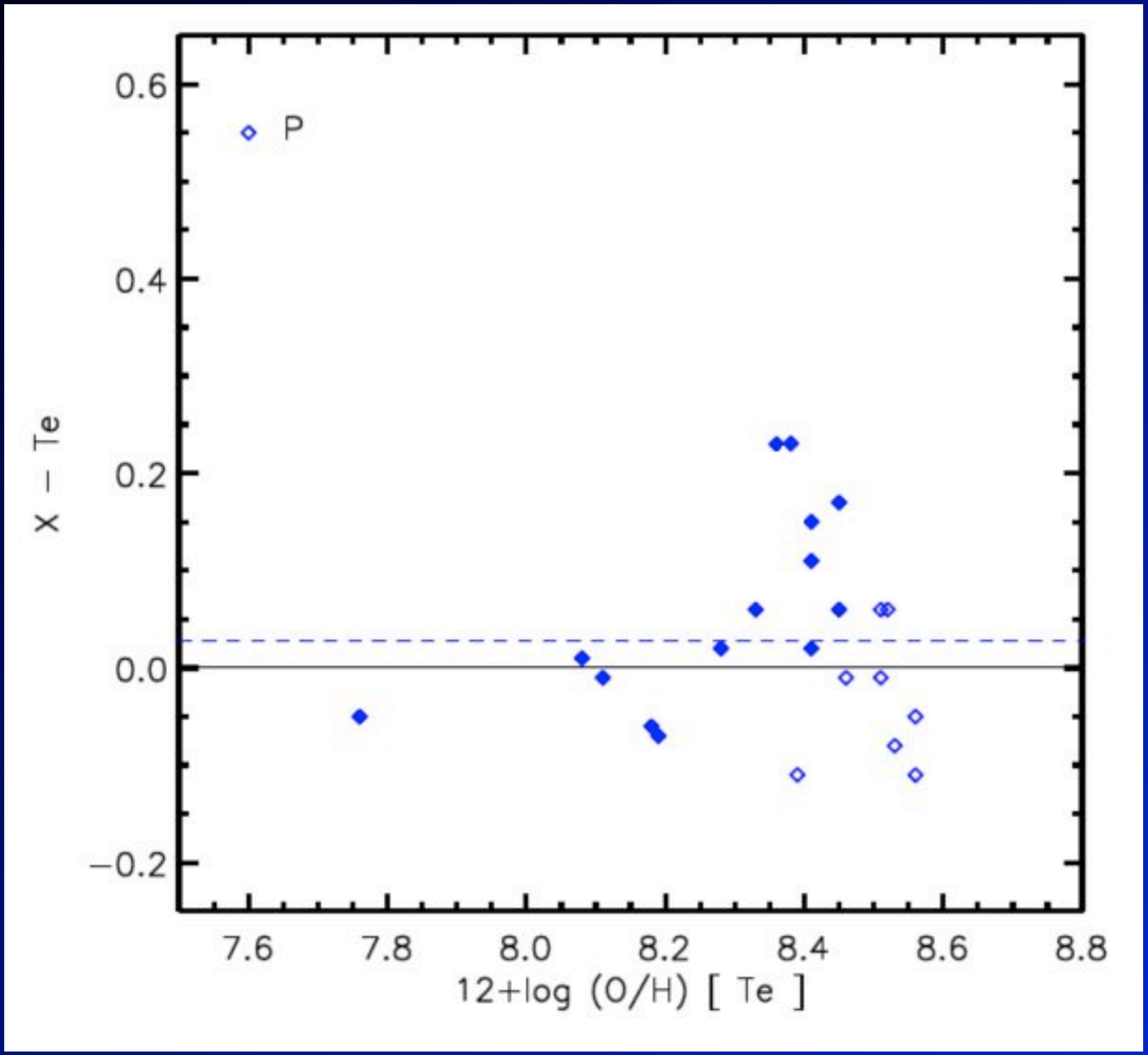

We compiled ALL existing HII regions with oxygen Recombination Lines (RL)

- Te-based empirical calibrations (Pilyugin+) agree with Te-method

López-Sánchez, Dopita, Kewley, Zahid, Nicholls & Scharwächter 2012 MNRAS, in press

Deriving O/H from Te using photoionization model spectra

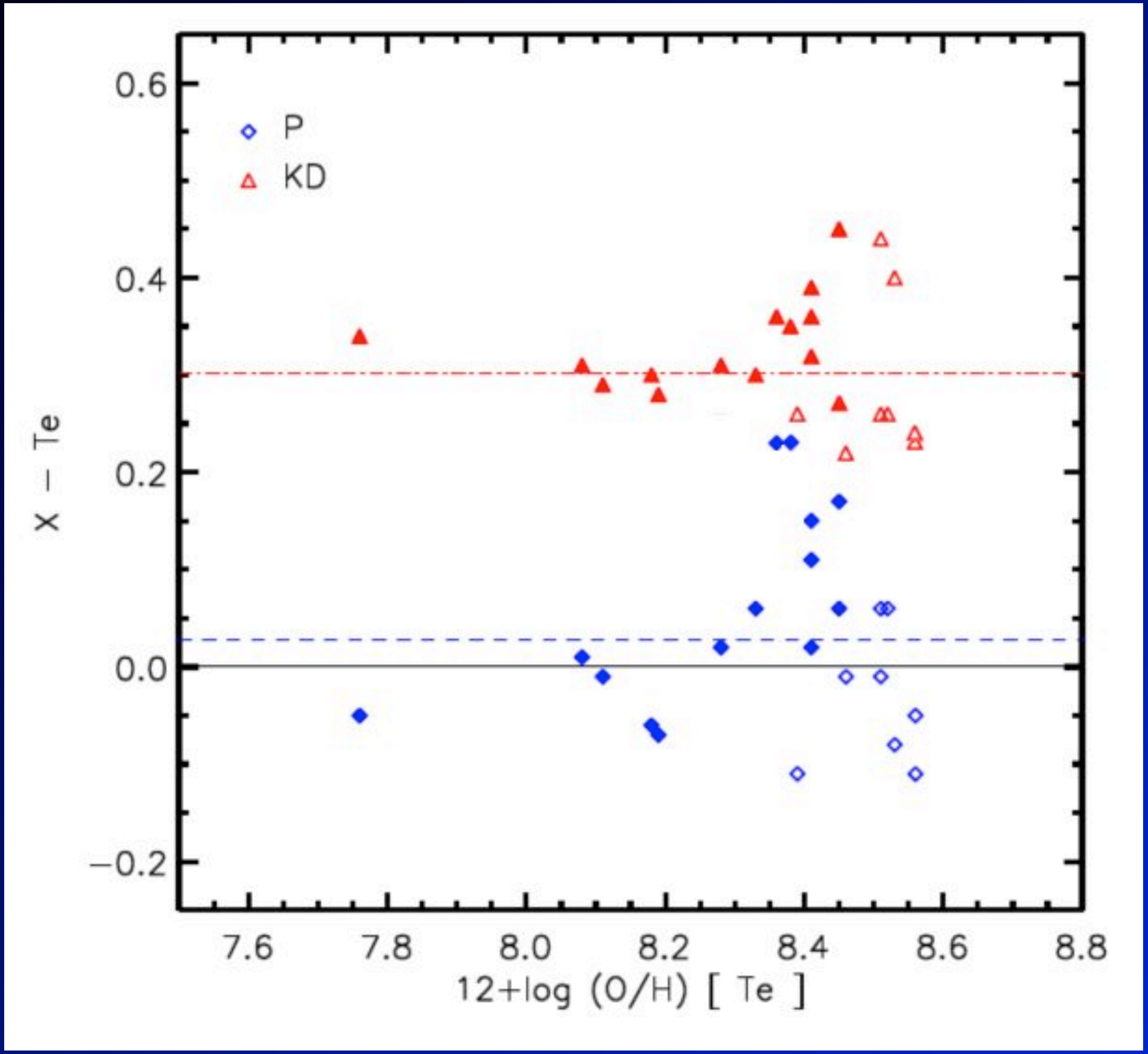

We compiled ALL existing HII regions with oxygen Recombination Lines (RL)

- Te-based empirical calibrations (Pilyugin+) agree with Te-method

- O/H based on photoionization models (Kewley & Dopita 2002) are ~0.3 dex HIGHER than Te-based O/H

López-Sánchez, Dopita, Kewley, Zahid, Nicholls & Scharwächter 2012 MNRAS, in press

Deriving O/H from Te using photoionization model spectra

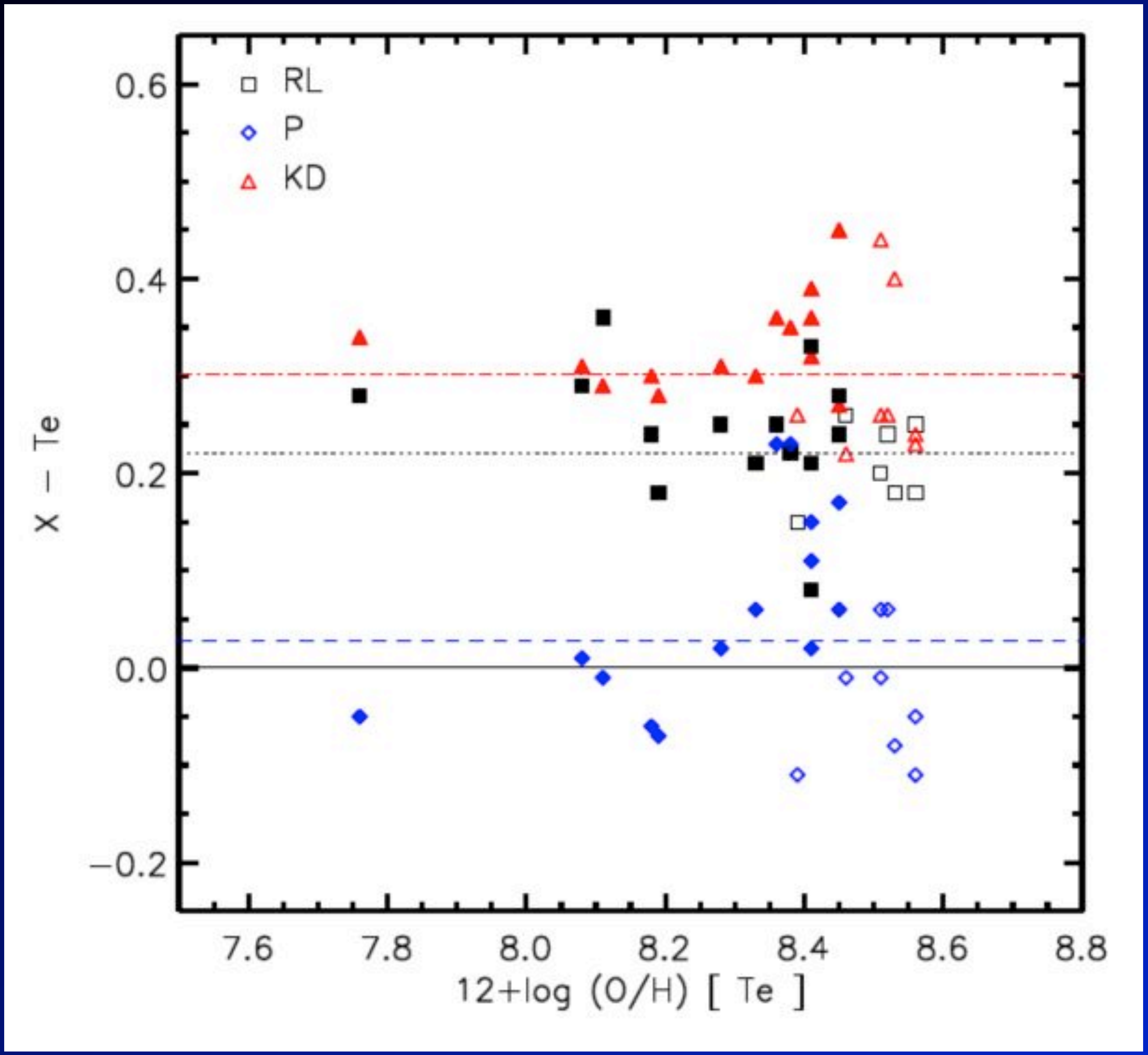

We compiled ALL existing HII regions with oxygen Recombination Lines (RL)

- Te-based empirical calibrations (Pilyugin+) agree with Te-method
- O/H based on photoionization models (Kewley & Dopita 2002) are ~0.3 dex HIGHER than Te-based O/H
- RL-based abundances are 0.2 - 0.4 dex higher than Te-method (García-Rojas & Esteban 2006, 2007, Esteban et al. 2004, 2009, López-Sánchez et al. 2007, Mesa-Delgado et al. 2009)

López-Sánchez, Dopita, Kewley, Zahid, Nicholls & Scharwächter 2012 MNRAS, in press

Deriving O/H from Te using photoionization model spectra

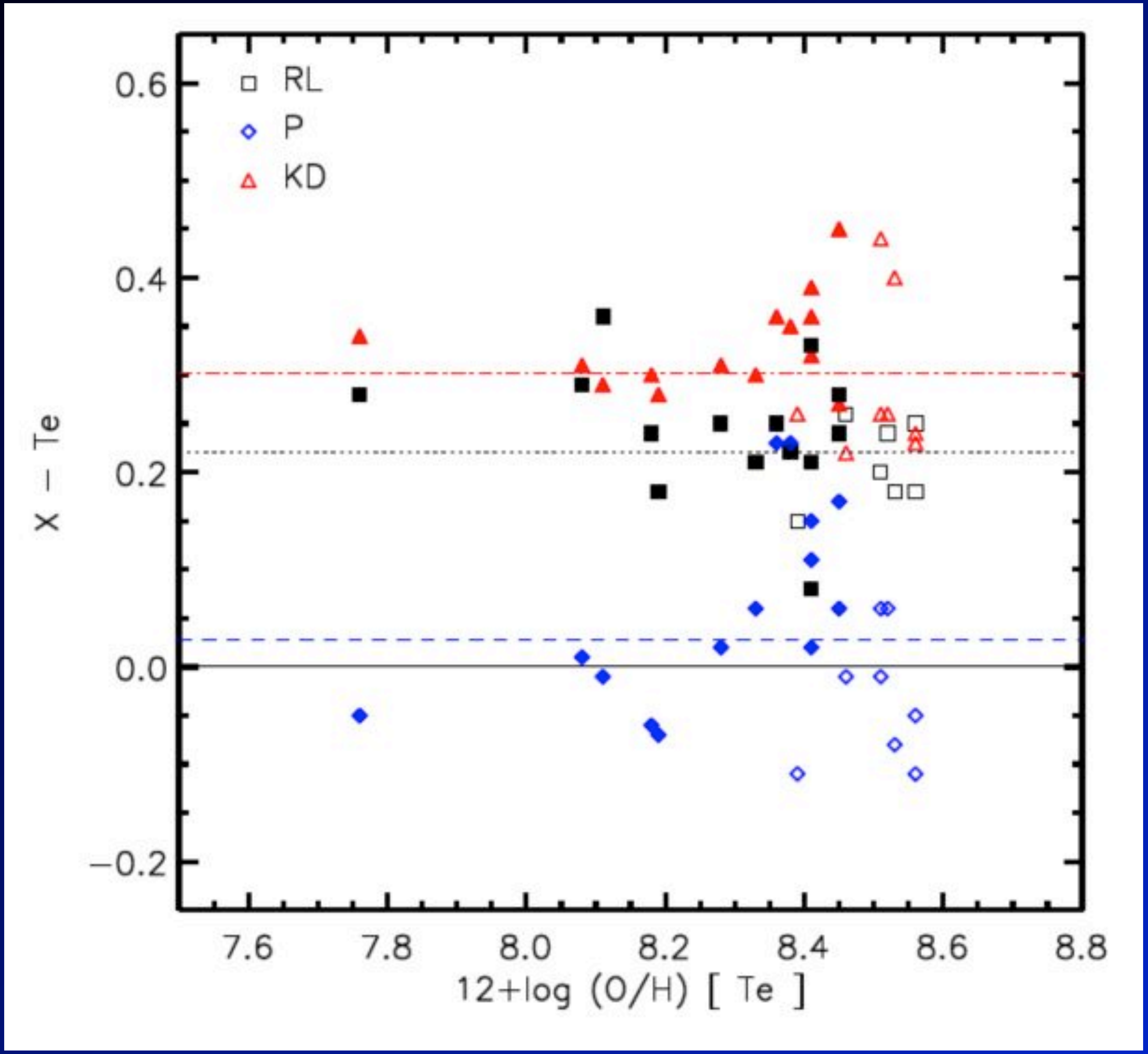

We compiled ALL existing HII regions with oxygen Recombination Lines (RL)

- Te-based empirical calibrations (Pilyugin+) agree with Te-method
- O/H based on photoionization models (Kewley & Dopita 2002) are ~0.3 dex HIGHER than Te-based O/H
- RL-based abundances are 0.2 - 0.4 dex higher than Te-method (García-Rojas & Esteban 2006, 2007, Esteban et al. 2004, 2009, López-Sánchez et al. 2007, Mesa-Delgado et al. 2009)
- RL and calibrations based on photoionization models (Kewley & Dopita 2002) agree well !!

López-Sánchez, Dopita, Kewley, Zahid, Nicholls & Scharwächter 2012 MNRAS, in press

Deriving O/H from Te using photoionization model spectra

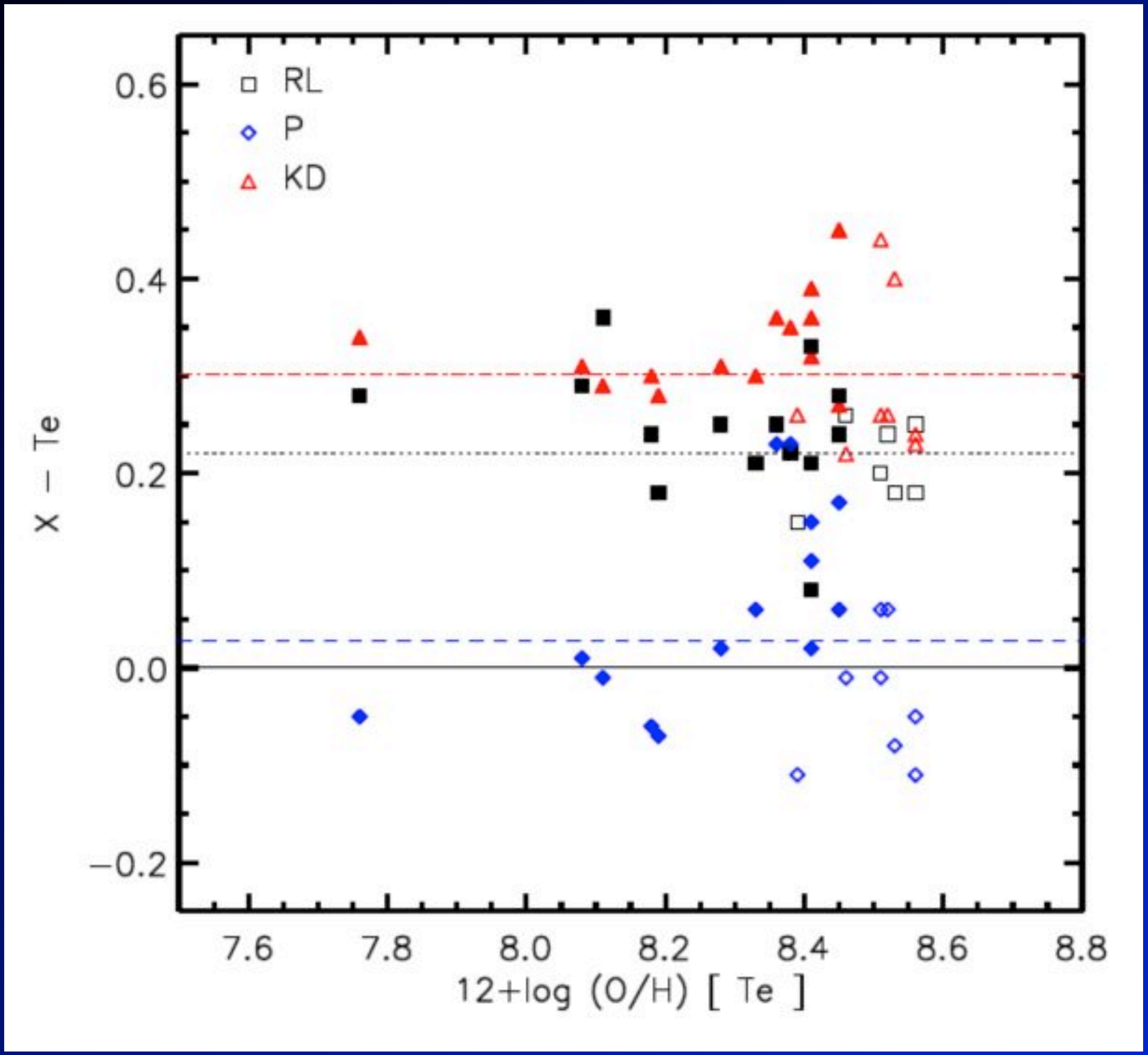

We compiled ALL existing HII regions with oxygen Recombination Lines (RL)

- Te-based empirical calibrations (Pilyugin+) agree with Te-method

- O/H based on photoionization models (Kewley & Dopita 2002) are ~0.3 dex HIGHER than Te-based O/H

- RL-based abundances are 0.2 - 0.4 dex higher than Te-method
(García-Rojas & Esteban 2006, 2007, Esteban et al. 2004, 2009, López-Sánchez et al. 2007, Mesa-Delgado et al. 2009)

- RL and calibrations based on photoionization models (Kewley & Dopita 2002) agree well !!

Temperature Fluctuations?
(Peimbert 1967)

López-Sánchez, Dopita, Kewley, Zahid, Nicholls & Scharwächter 2012 MNRAS, in press

Deriving O/H from Te using photoionization model spectra

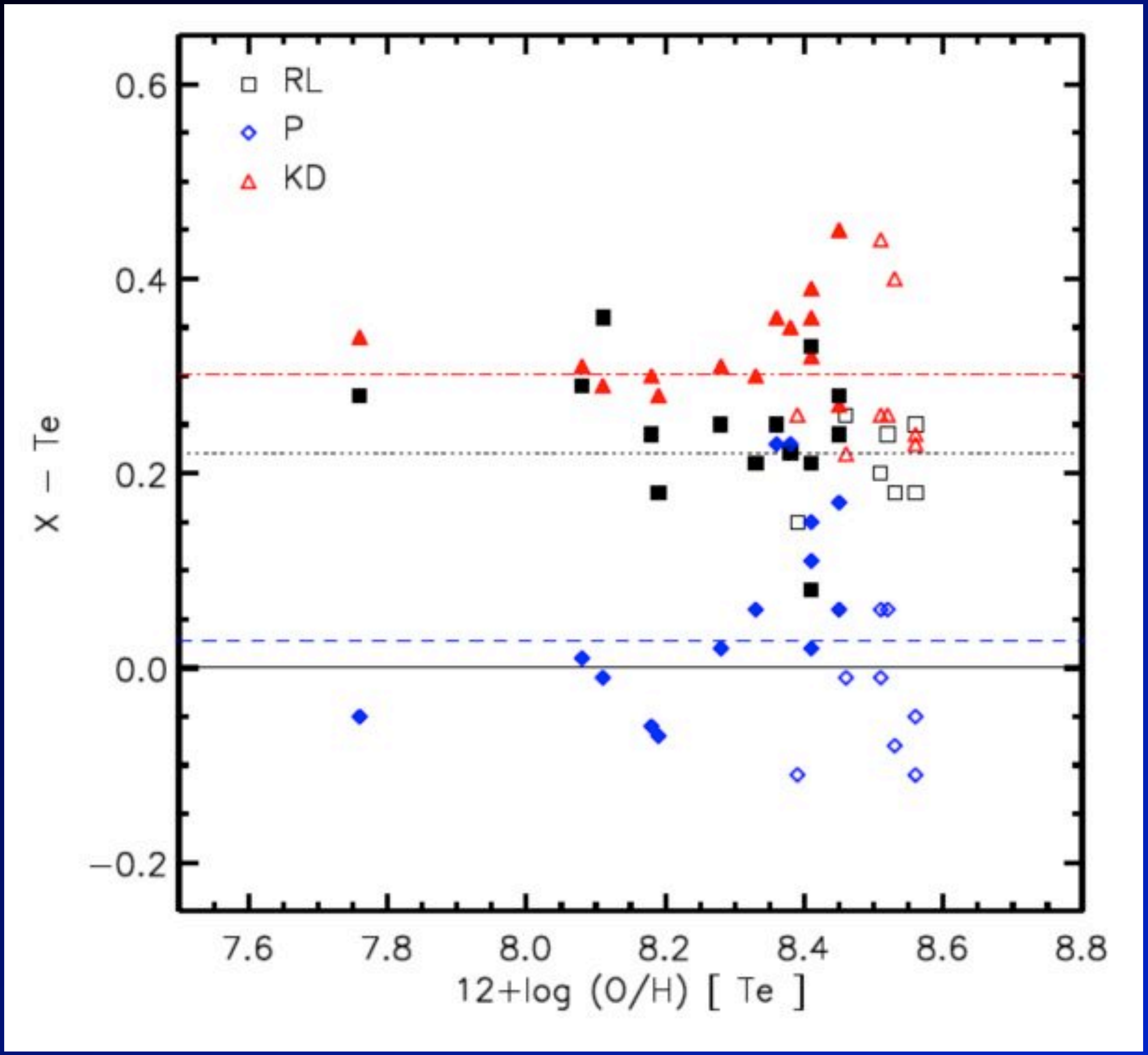

We compiled ALL existing HII regions with oxygen Recombination Lines (RL)

- Te-based empirical calibrations (Pilyugin+) agree with Te-method
- O/H based on photoionization models (Kewley & Dopita 2002) are ~0.3 dex HIGHER than Te-based O/H
- RL-based abundances are 0.2 - 0.4 dex higher than Te-method (García-Rojas & Esteban 2006, 2007, Esteban et al. 2004, 2009, López-Sánchez et al. 2007, Mesa-Delgado et al. 2009)
- RL and calibrations based on photoionization models (Kewley & Dopita 2002) agree well !!

Temperature Fluctuations?
(Peimbert 1967)

- KD02 models DO NOT account for small-scale temperature fluctuations

López-Sánchez, Dopita, Kewley, Zahid, Nicholls & Scharwächter 2012 MNRAS, in press

Deriving O/H from Te using photoionization model spectra

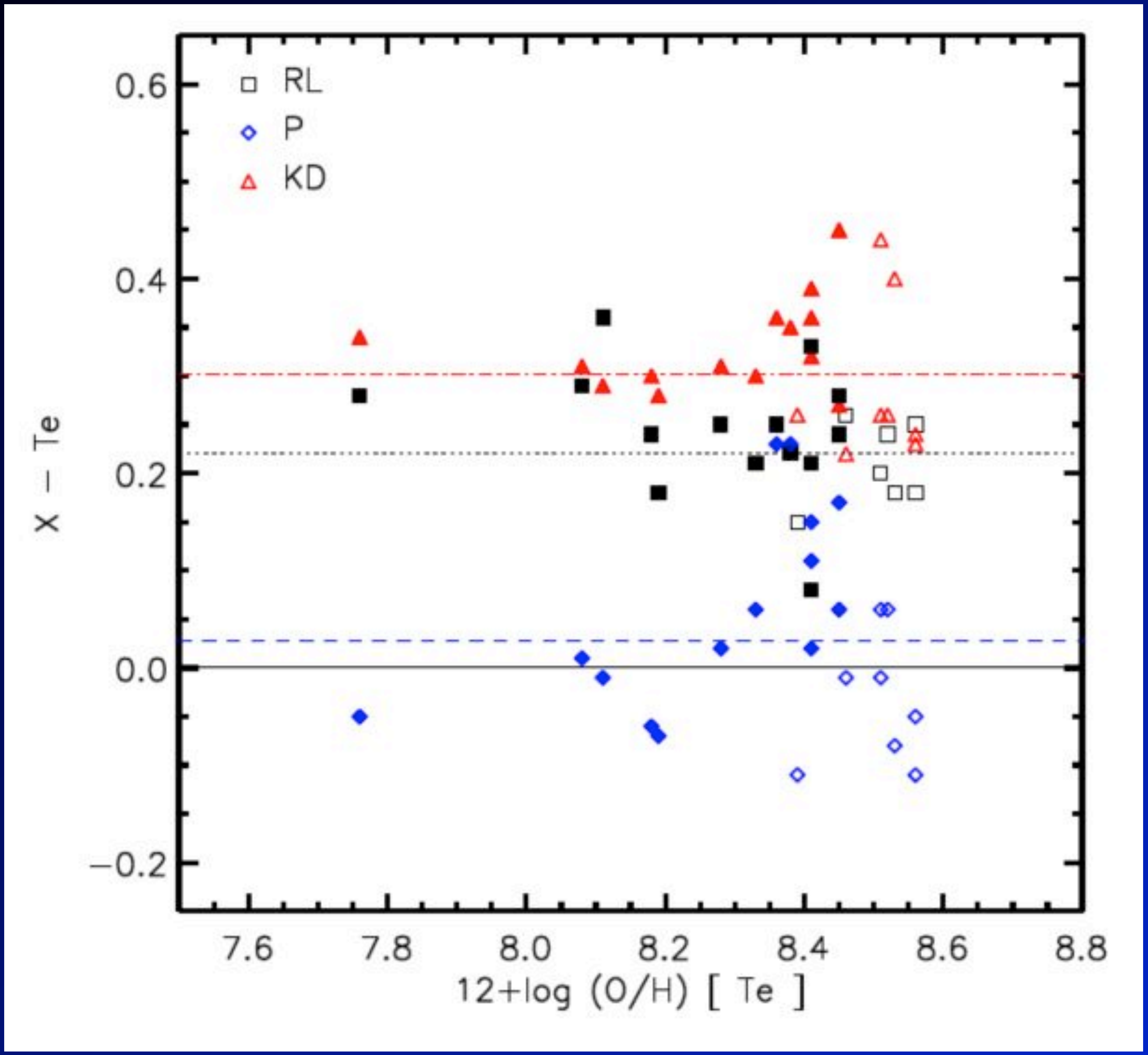

We compiled ALL existing HII regions with oxygen Recombination Lines (RL)

- Te-based empirical calibrations (Pilyugin+) agree with Te-method

- O/H based on photoionization models (Kewley & Dopita 2002) are ~0.3 dex HIGHER than Te-based O/H

- RL-based abundances are 0.2 - 0.4 dex higher than Te-method (García-Rojas & Esteban 2006, 2007, Esteban et al. 2004, 2009, López-Sánchez et al. 2007, Mesa-Delgado et al. 2009)

- RL and calibrations based on photoionization models (Kewley & Dopita 2002) agree well !!

Temperature Fluctuations?
(Peimbert 1967)

- KD02 models DO NOT account for small-scale temperature fluctuations

Temp fluctuations mainly affect auroral [O III] λ4363: Te decreases → O/H increases

López-Sánchez, Dopita, Kewley, Zahid, Nicholls & Scharwächter 2012 MNRAS, in press

Deriving O/H from Te using photoionization model spectra

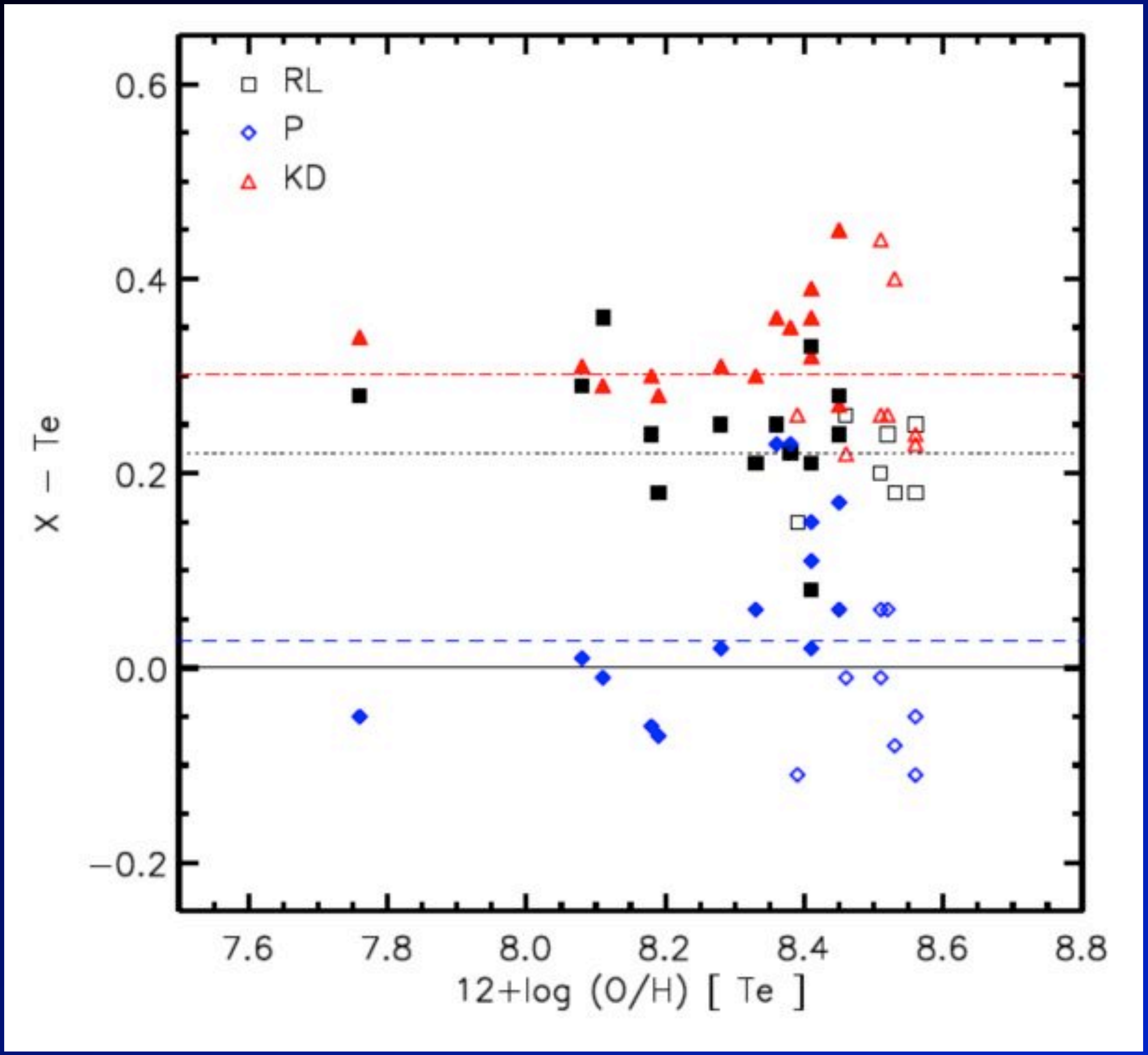

We compiled ALL existing HII regions with oxygen Recombination Lines (RL)

- Te-based empirical calibrations (Pilyugin+) agree with Te-method
- O/H based on photoionization models (Kewley & Dopita 2002) are ~0.3 dex HIGHER than Te-based O/H
- RL-based abundances are 0.2 - 0.4 dex higher than Te-method (García-Rojas & Esteban 2006, 2007, Esteban et al. 2004, 2009, López-Sánchez et al. 2007, Mesa-Delgado et al. 2009)
- RL and calibrations based on photoionization models (Kewley & Dopita 2002) agree well !!

Temperature Fluctuations?
(Peimbert 1967)

- KD02 models DO NOT account for small-scale temperature fluctuations

Temp fluctuations mainly affect auroral [O III] λ4363: Te decreases → O/H increases

- Photoionization codes have difficulty reproducing the observed line-strengths of the auroral lines (Stasinska & Schaerer 1999; Jamet et al. 2005).

López-Sánchez, Dopita, Kewley, Zahid, Nicholls & Scharwächter 2012 MNRAS, in press

Deriving O/H from Te using photoionization model spectra

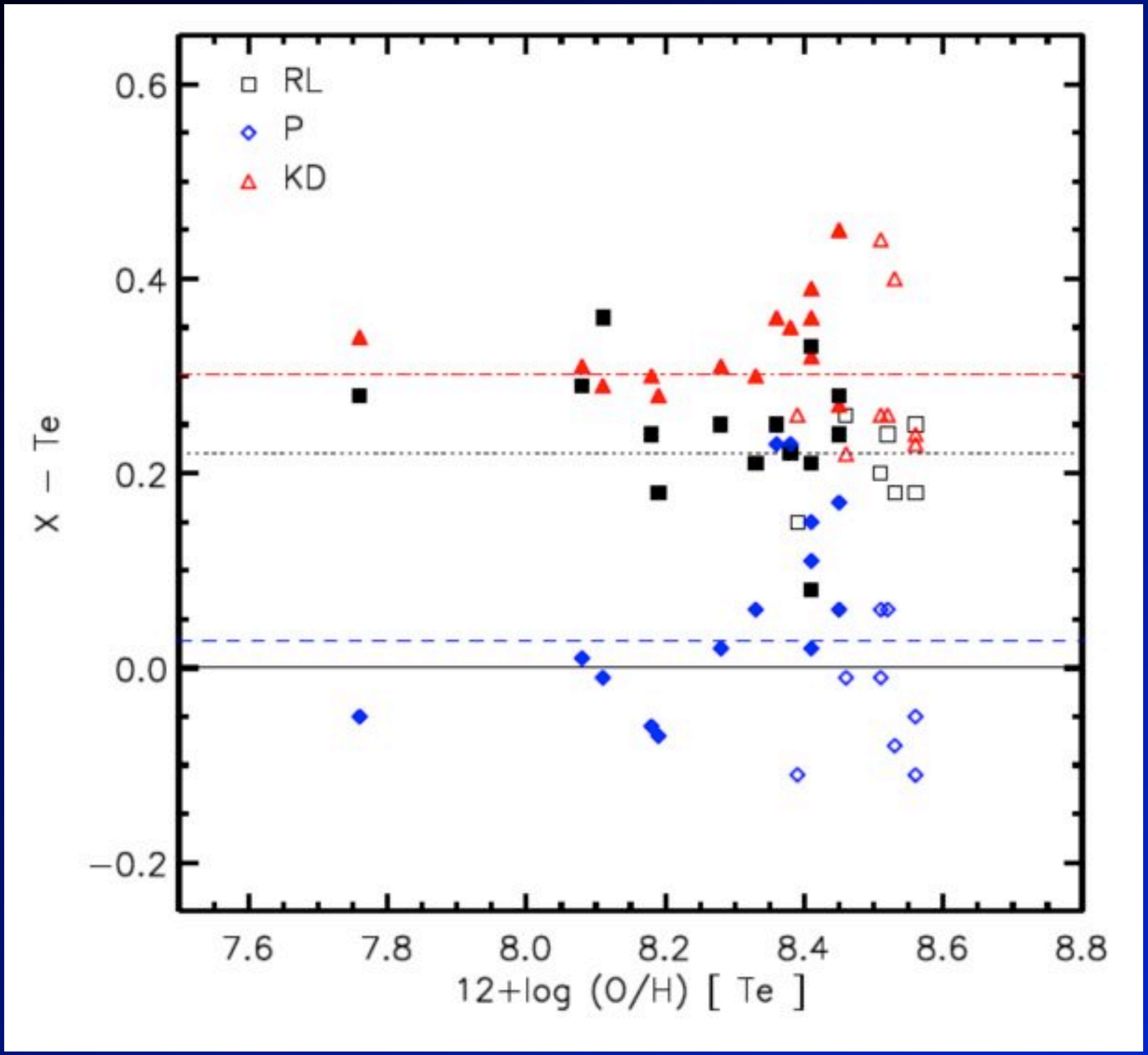

We compiled ALL existing HII regions with oxygen Recombination Lines (RL)

- Te-based empirical calibrations (Pilyugin+) agree with Te-method
- O/H based on photoionization models (Kewley & Dopita 2002) are ~0.3 dex HIGHER than Te-based O/H
- RL-based abundances are 0.2 - 0.4 dex higher than Te-method (García-Rojas & Esteban 2006, 2007, Esteban et al. 2004, 2009, López-Sánchez et al. 2007, Mesa-Delgado et al. 2009)
- RL and calibrations based on photoionization models (Kewley & Dopita 2002) agree well !!

Temperature Fluctuations?
(Peimbert 1967)

- KD02 models DO NOT account for small-scale temperature fluctuations

Temp fluctuations mainly affect auroral [O III] λ4363: Te decreases → O/H increases

- Photoionization codes have difficulty reproducing the observed line-strengths of the auroral lines (Stasinska & Schaerer 1999; Jamet et al. 2005).

López-Sánchez, Dopita, Kewley, Zahid, Nicholls & Scharwächter 2012 MNRAS, in press

Using tailored photoionization models

- *"Photoionization modeling is sometimes more efficient than direct method as it can take into account coherently and simultaneously all the observables of a given object, as well as aperture, dust, N-components, 3D effects"* cif. **Christophe Morisset**
- Tailored photoionization models of individual HII regions (e.g. **Castellanos et al. 2002, Garnett et al 2004, Morisset et al.**) and HII galaxies (e.g. **Pérez-Montero et al. 2010, Dors et al. 2011**) *sometimes* provide results similar to those derived from the Te method.
- Test different hypothesis to explain Te fluctuations (**Roy Matadamas** talk)

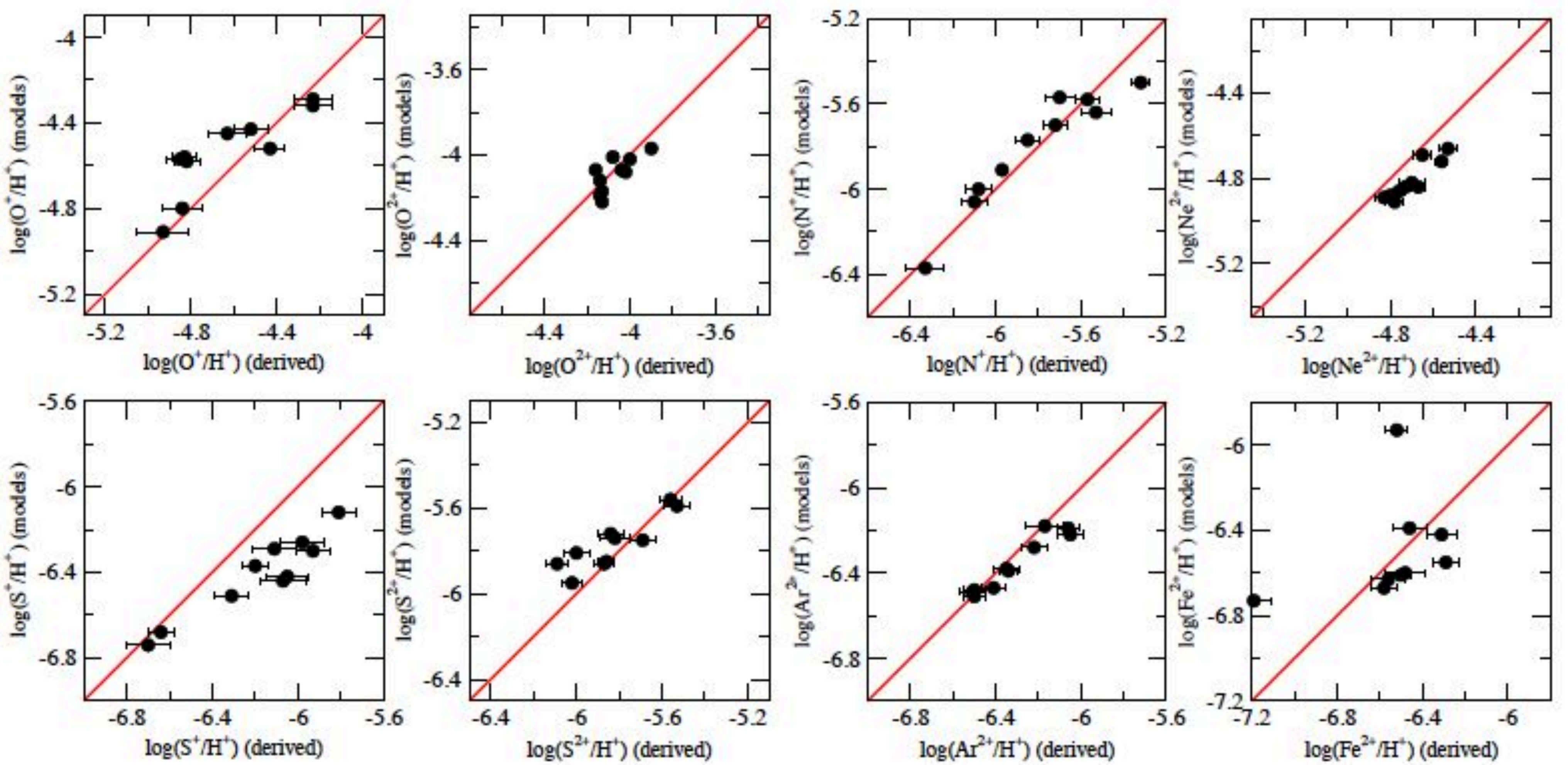

Figure 10. Comparison between ionic abundances as derived from the observations using the direct method and the predictions of tailor-made photoionization models.

Pérez-Montero et al. 2010

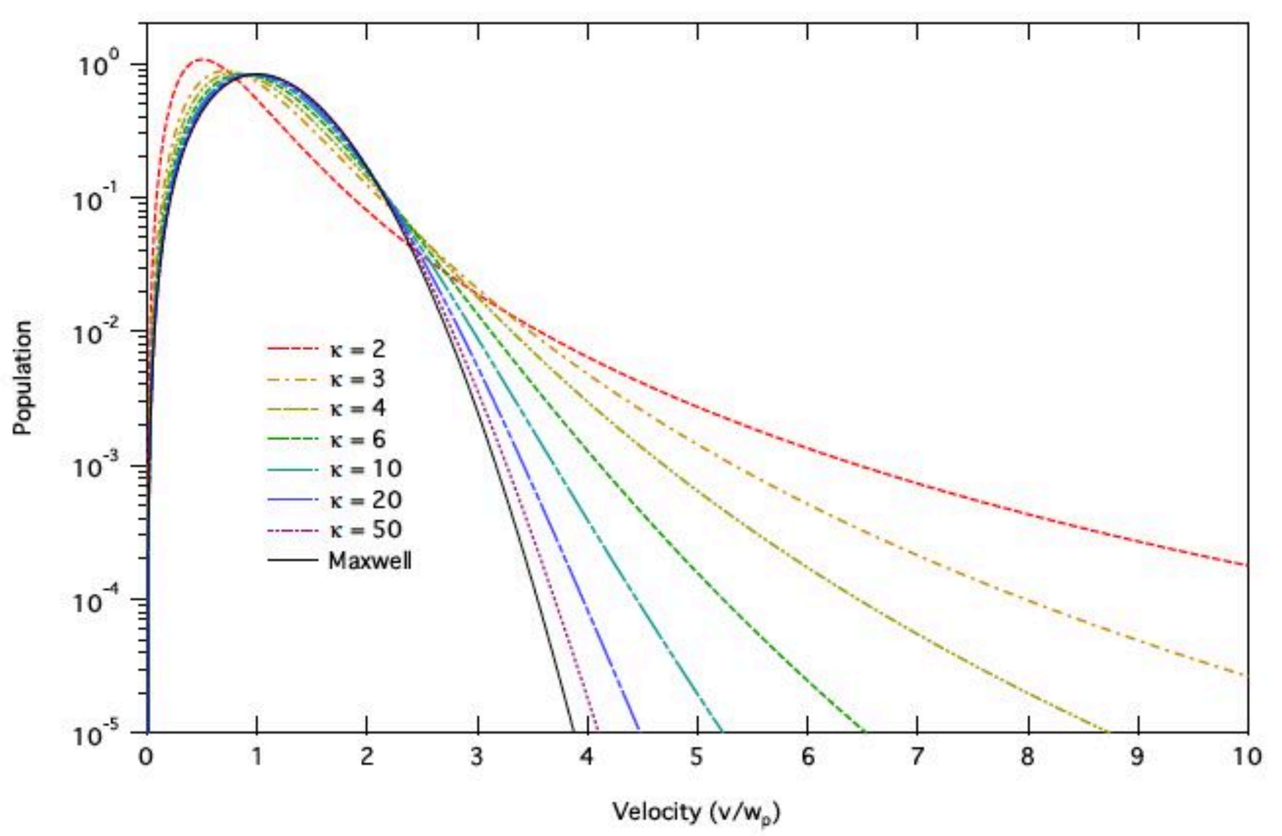

FIG. 1.— κ– velocity distributions (log scale) for κ from 2 to 50, with Maxwell-Boltzmann distribution.

Te fluctuations
Any other mechanism?

- Nicholls, Dopita & Sutherland, 2012, ApJ, accepted , arXiv : 1204.3880
- They explore the possibility that electrons in H II regions and PNe depart from a Maxwell-Boltzmann equilibrium energy distribution.
- They adopt a non-equilibrium κ-distribution for the electron energies, as found in other astrophysical plasmas

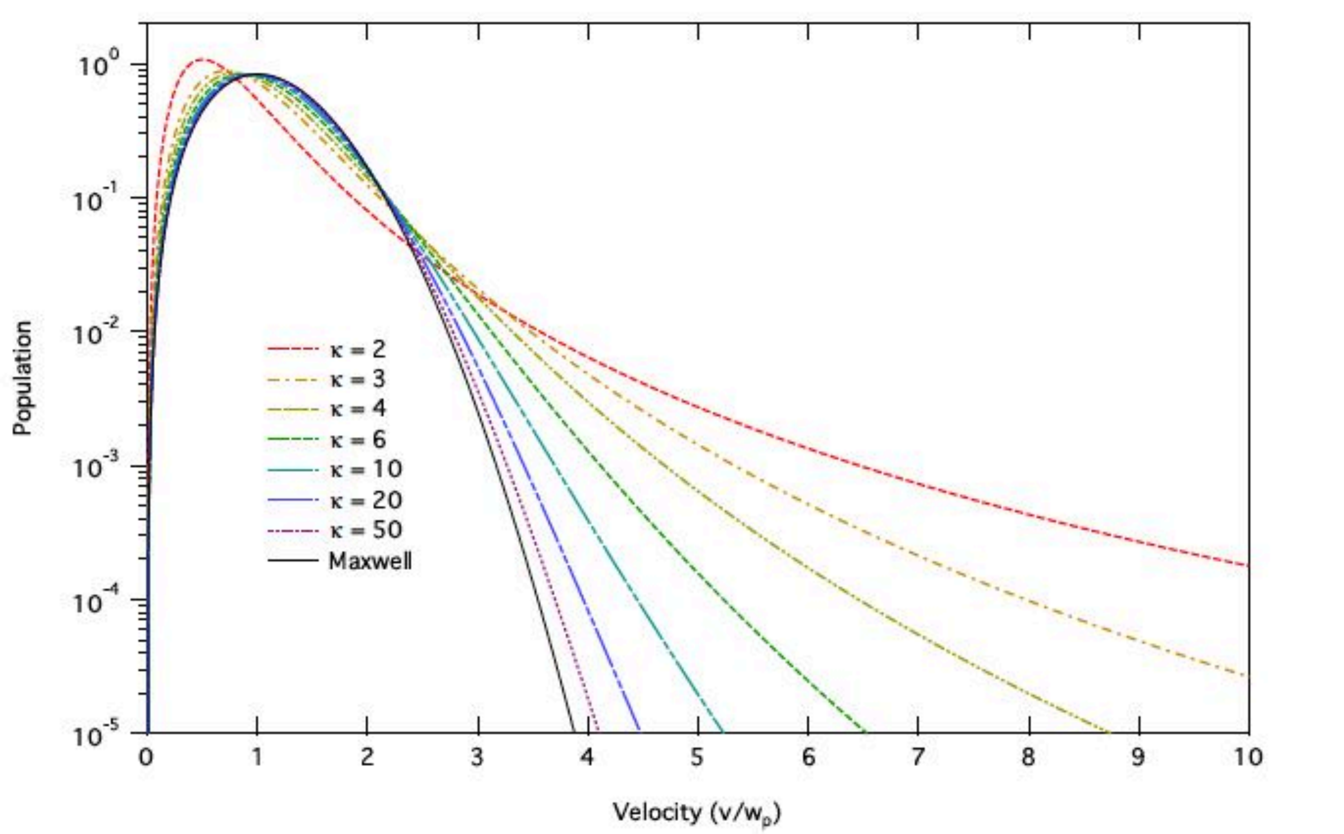

FIG. 1.— κ– velocity distributions (log scale) for κ from 2 to 50, with Maxwell-Boltzmann distribution.

Te fluctuations
Any other mechanism?

- Nicholls, Dopita & Sutherland, 2012, ApJ, accepted , arXiv : 1204.3880
- They explore the possibility that electrons in H II regions and PNe depart from a Maxwell-Boltzmann equilibrium energy distribution.
- They adopt a non-equilibrium κ-distribution for the electron energies, as found in other astrophysical plasmas

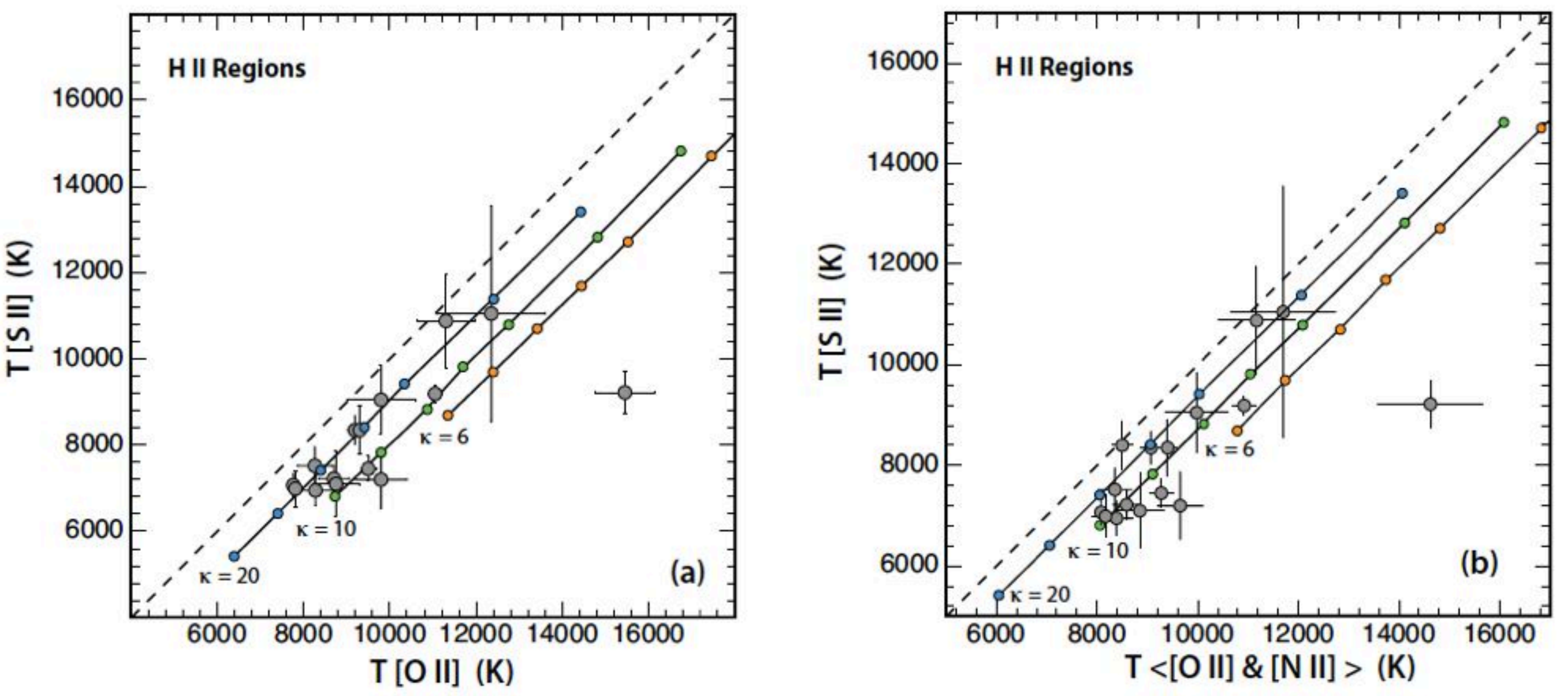

- This assumption is able to explain the temperature and metallicity discrepancies in H II regions and PNe arising from the different measurement techniques.

ADF maps in HH202 (Orion Nebula) !

Mesa-Delgado et al. (2009)

"H II regions are COMPLEX"

cif. from
Adal Mesa-Delgado talk

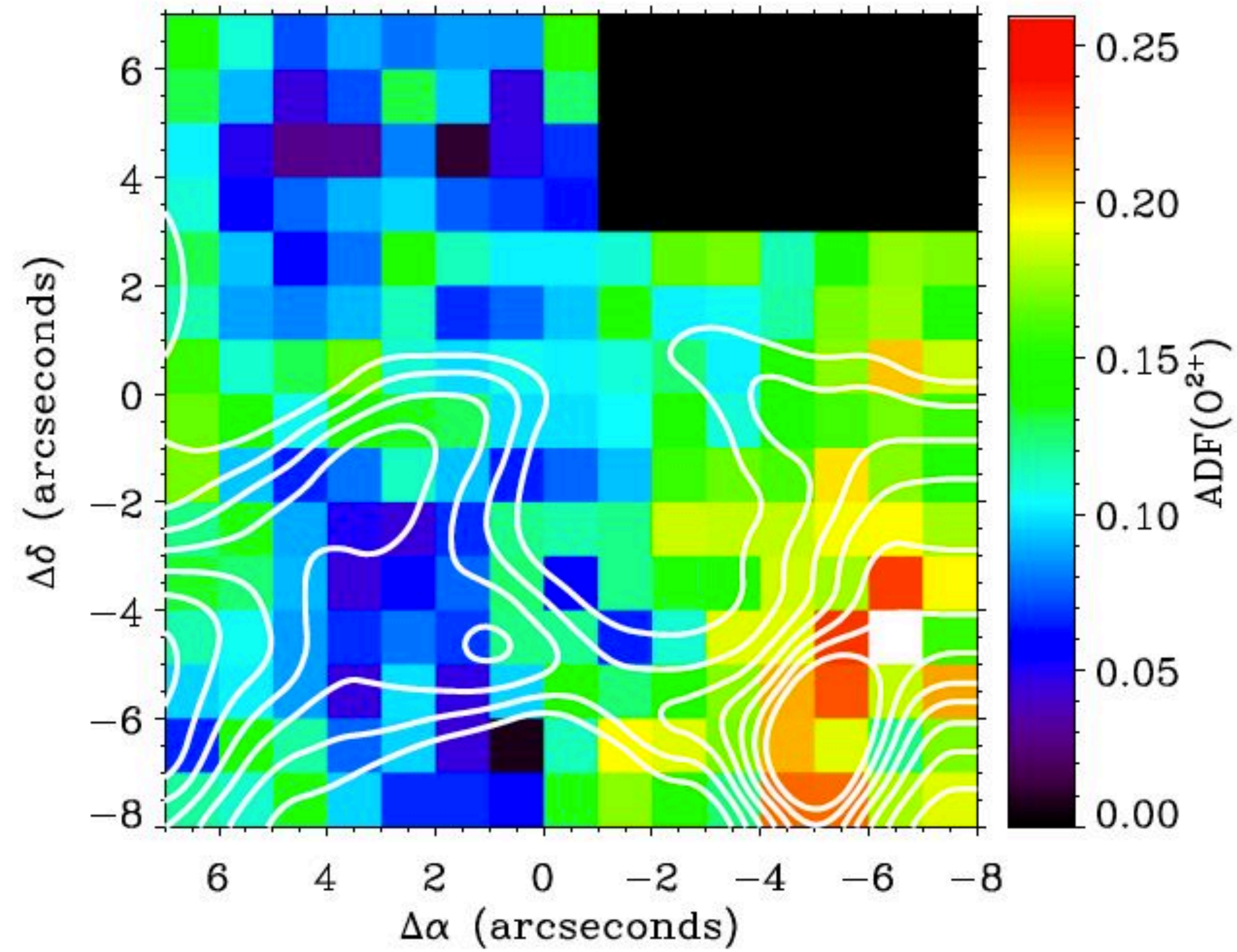

Figure 9. ADF(O^{2+}) map with Hα contours overplotted. The black rectangle on the northwest corner corresponds to an area masked due to the bad determination of the O^{2+} abundance from RLs.

Summary & Conclusions

Summary & Conclusions

- **Well-studied database of ~30 strong star-forming galaxies with good measurements of Te, O/H, N/O, SFR, M_{star}, M_{gas}, M_{dust}, SFH ...**
  - Good to compare with models / other data from extragalactic HII regions
  - **López-Sánchez & Esteban 2010b, López-Sánchez 2010**

Summary & Conclusions

- **Well-studied database of ~30 strong star-forming galaxies with good measurements of Te, O/H, N/O, SFR, M_{star}, M_{gas}, M_{dust}, SFH …**
  - Good to compare with models / other data from extragalactic HII regions
  - **López-Sánchez & Esteban 2010b, López-Sánchez 2010**
- **Strong-line methods have biases**
  - Check you **CAN** use the empirical calibration you want to use
    - N2 is **NOT** valid for high-metallicity (8.7 - 8.9), O3N2 is **NOT** valid for low-metallicity (8.3 - 8.4)
  - Estimate the **ionization degree** of the gas
    - Calibrations tend to give lower O/H when increasing ionization degree (L-S+ 2011)
  - Use **several calibrations** (and parameters) to confirm your **trends**

Summary & Conclusions

- **Well-studied database of ~30 strong star-forming galaxies with good measurements of Te, O/H, N/O, SFR, M_{star}, M_{gas}, M_{dust}, SFH ...**
  – Good to compare with models / other data from extragalactic HII regions
  – **López-Sánchez & Esteban 2010b, López-Sánchez 2010**
- **Strong-line methods have biases**
  – Check you **CAN** use the empirical calibration you want to use
    - N2 is **NOT** valid for high-metallicity (8.7 - 8.9), O3N2 is **NOT** valid for low-metallicity (8.3 - 8.4)
  – Estimate the **ionization degree** of the gas
    - Calibrations tend to give lower O/H when increasing ionization degree (L-S+ 2011)
  – Use **several calibrations** (and parameters) to confirm your **trends**
- **Empirically, abundances derived using the P-method agrees better than those derived using the KD-method when comparing with Te-based O/H**
  – KD-method systematically overestimates Te-method is 0.2 - 0.4 dex

Summary & Conclusions

- **Well-studied database of ~30 strong star-forming galaxies with good measurements of Te, O/H, N/O, SFR, M_{star}, M_{gas}, M_{dust}, SFH ...**
  - Good to compare with models / other data from extragalactic HII regions
  - **López-Sánchez & Esteban 2010b, López-Sánchez 2010**
- **Strong-line methods have biases**
  - Check you **CAN** use the empirical calibration you want to use
    - N2 is **NOT** valid for high-metallicity (8.7 - 8.9), O3N2 is **NOT** valid for low-metallicity (8.3 - 8.4)
  - Estimate the **ionization degree** of the gas
    - Calibrations tend to give lower O/H when increasing ionization degree (L-S+ 2011)
  - Use **several calibrations** (and parameters) to confirm your **trends**
- **Empirically, abundances derived using the P-method agrees better than those derived using the KD-method when comparing with Te-based O/H**
  - KD-method systematically overestimates Te-method is 0.2 - 0.4 dex
- **But abundances derived using KD-method agree with the abundances derived using the RL !!!**
  - RL-based O/H agree much better than Te-based O/H with stellar abundances in Local Neighbourhood, but NOT in other nearby galaxies (P-method agrees best)
  - If RL are giving the "good" abundances values, the KD-method is providing good abundances values

Summary & Conclusions

- **Well-studied database of ~30 strong star-forming galaxies with good measurements of Te, O/H, N/O, SFR, M_{star}, M_{gas}, M_{dust}, SFH ...**
  - Good to compare with models / other data from extragalactic HII regions
  - **López-Sánchez & Esteban 2010b, López-Sánchez 2010**
- **Strong-line methods have biases**
  - Check you **CAN** use the empirical calibration you want to use
    - N2 is **NOT** valid for high-metallicity (8.7 - 8.9), O3N2 is **NOT** valid for low-metallicity (8.3 - 8.4)
  - Estimate the **ionization degree** of the gas
    - Calibrations tend to give lower O/H when increasing ionization degree (L-S+ 2011)
  - Use **several calibrations** (and parameters) to confirm your **trends**
- **Empirically, abundances derived using the P-method agrees better than those derived using the KD-method when comparing with Te-based O/H**
  - KD-method systematically overestimates Te-method is 0.2 - 0.4 dex
- **But abundances derived using KD-method agree with the abundances derived using the RL !!!**
  - RL-based O/H agree much better than Te-based O/H with stellar abundances in Local Neighbourhood, but NOT in other nearby galaxies (P-method agrees best)
  - If RL are giving the "good" abundances values, the KD-method is providing good abundances values
- **WHAT DO WE TRUST?**

Summary & Conclusions

- Assuming KD abundances are the “good ones”, these two diagnostic diagrams can help to dissentangle q and O/H in extragalactic HII regions
  - But more work in the underlying physics of phot. models is needed (e.g., **κ-distribution)**

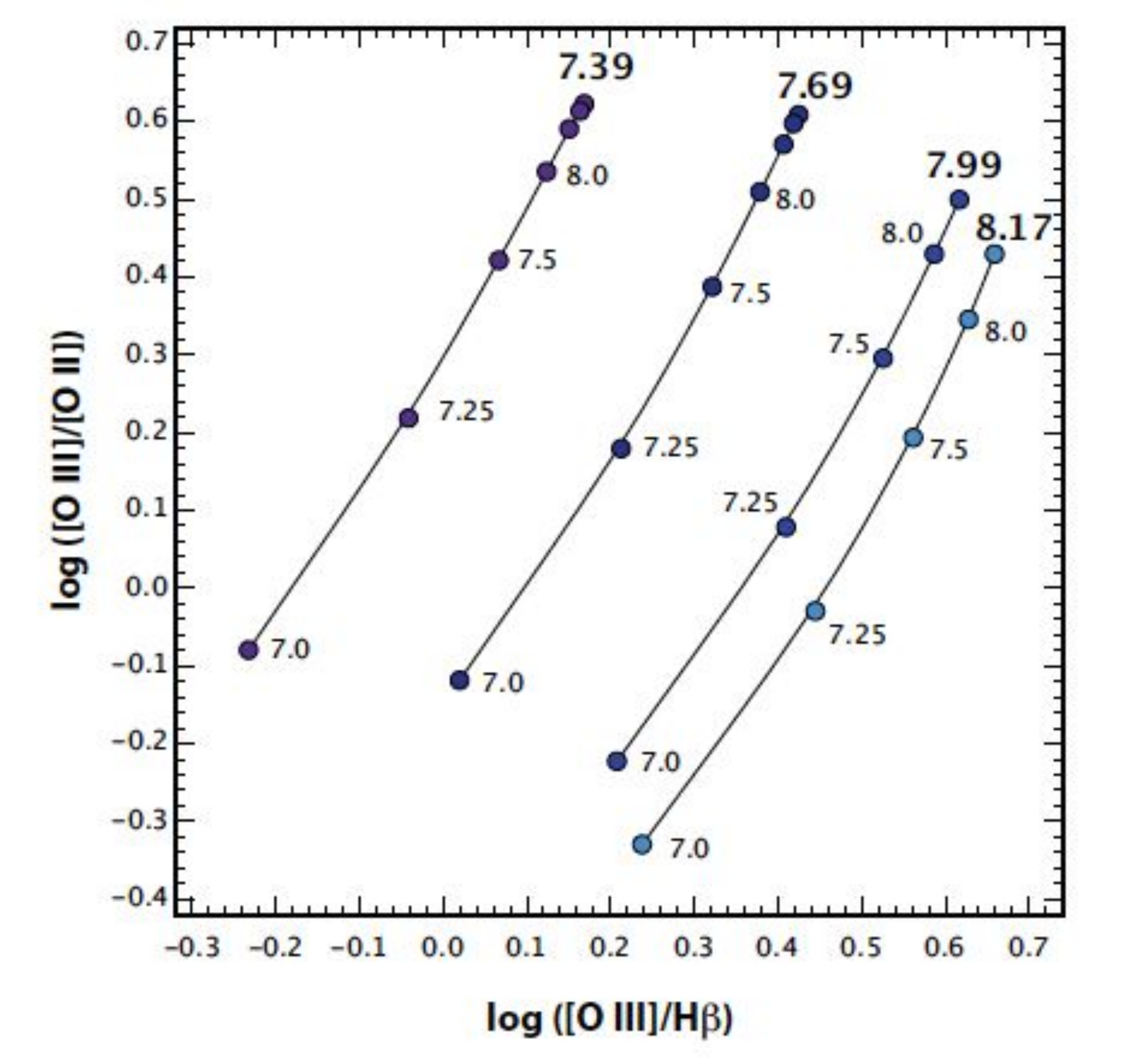

Low Metallicities

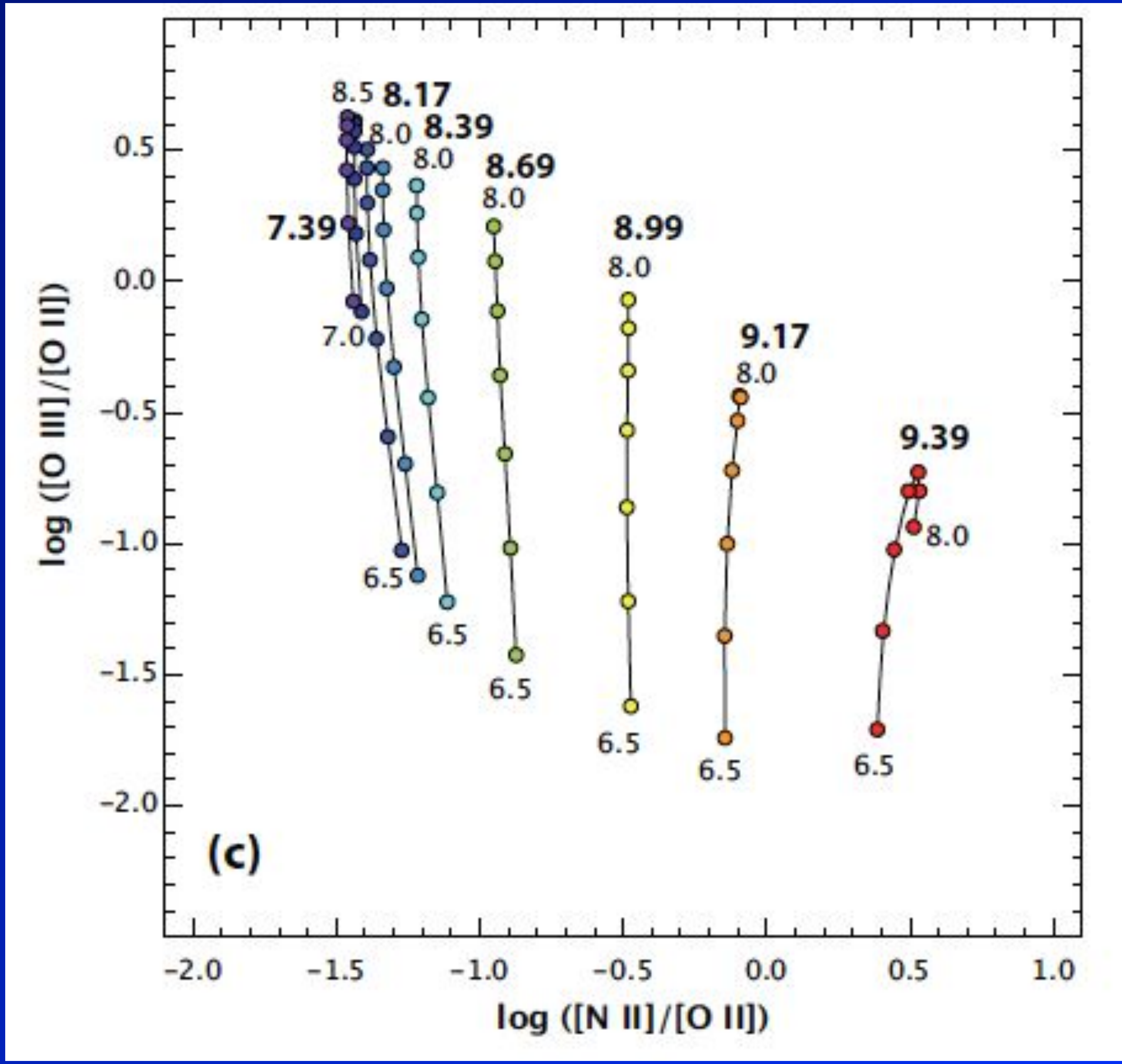

High Metallicities

López-Sánchez, Dopita, Kewley, Zahid, Nicholls & Scharwächter 2012 MNRAS, in press